National Library of Canada
Bibliothèque nationale du Canada

Canadian Theses Service
Services des thèses canadiennes

Ottawa, Canada
K1A 0N4

CANADIAN THESES

THÈSES CANADIENNES

NOTICE

The quality of this microfiche is heavily dependent upon the quality of the original thesis submitted for microfilming. Every effort has been made to ensure the highest quality of reproduction possible.

If pages are missing, contact the university which granted the degree.

Some pages may have indistinct print especially if the original pages were typed with a poor typewriter ribbon or if the university sent us an inferior photocopy.

Previously copyrighted materials (journal articles, published tests, etc.) are not filmed.

Reproduction in full or in part of this film is governed by the Canadian Copyright Act, R.S.C. 1970, c. C-30.

AVIS

La qualité de cette microfiche dépend grandement de la qualité de la thèse soumise au microfilmage. Nous avons tout fait pour assurer une qualité supérieure de reproduction.

S'il manque des pages, veuillez communiquer avec l'université qui a conféré le grade.

La qualité d'impression de certaines pages peut laisser à désirer, surtout si les pages originales ont été dactylographiées à l'aide d'un ruban usé ou si l'université nous a fait parvenir une photocopie de qualité inférieure.

Les documents qui font déjà l'objet d'un droit d'auteur (articles de revue, examens publiés, etc.) ne sont pas microfilmés.

La reproduction, même partielle, de ce microfilm est soumise à la Loi canadienne sur le droit d'auteur, SRC 1970, c. C-30.

THIS DISSERTATION HAS BEEN MICROFILMED EXACTLY AS RECEIVED

LA THÈSE A ÉTÉ MICROFILMÉE TELLE QUE NOUS L'AVONS REÇUE

NL-339 (r. 86/06)

Canada

THE UNIVERSITY OF ALBERTA

INTERNAL HYDRAULIC JUMPS

by

RICHARD L. POWLEY

A THESIS

SUBMITTED TO THE FACULTY OF GRADUATE STUDIES AND RESEARCH

IN PARTIAL FULFILMENT OF THE REQUIREMENTS FOR THE DEGREE

OF MASTER OF SCIENCE

DEPARTMENT OF CIVIL ENGINEERING

EDMONTON, ALBERTA

SPRING, 1987

Permission has been granted to the National Library of Canada to microfilm this thesis and to lend or sell copies of the film.

L'autorisation à été accordée à la Bibliothèque nationale du Canada de microfilmer cette thèse et de prêter ou de vendre des exemplaires du film.

The author (copyright owner) has reserved other publication rights, and neither the thesis nor extensive extracts from it may be printed or otherwise reproduced without his/her written permission.

L'auteur (titulaire du droit d'auteur) se réserve les autres droits de publication; ni la thèse ni de longs extraits de celle-ci ne doivent être imprimés ou autrement reproduits sans son autorisation écrite.

ISBN 0-315-37789-5

THE UNIVERSITY OF ALBERTA

RELEASE FORM

NAME OF AUTHOR RICHARD L. POWLEY

TITLE OF THESIS INTERNAL HYDRAULIC JUMPS

DEGREE FOR WHICH THESIS WAS PRESENTED MASTER OF SCIENCE

YEAR THIS DEGREE GRANTED SPRING, 1987

Permission is hereby granted to THE UNIVERSITY OF ALBERTA LIBRARY to reproduce single copies of this thesis and to lend or sell such copies for private, scholarly or scientific research purposes only.

The author reserves other publication rights, and neither the thesis nor extensive extracts from it may be printed or otherwise reproduced without the author's written permission.

(SIGNED) R. Powley

PERMANENT ADDRESS:

11167-62 AVENUE

EDMONTON, ALBERTA

T6H 1N3

DATED APRIL 3 1987

THE UNIVERSITY OF ALBERTA

FACULTY OF GRADUATE STUDIES AND RESEARCH

The undersigned certify that they have read, and recommend to the Faculty of Graduate Studies and Research, for acceptance, a thesis entitled INTERNAL HYDRAULIC JUMPS submitted by RICHARD L. POWLEY in partial fulfilment of the requirements for the degree of MASTER OF SCIENCE in CIVIL ENGINEERING.

.....

Supervisor

.....

.....

Date 13 Mar 87

ABSTRACT

One of the most important and interesting phenomena associated with stratified flow is the internal hydraulic jump. While a great deal of knowledge of this subject has been gained in the brief history of its study, a complete understanding of internal hydraulic jumps is far from being realized.

Internal hydraulic jumps are, in many ways, analagous to open channel hydraulic jumps. With this in mind, this thesis attempts to analyse a number of internal hydraulic jump types in a manner similar to the corresponding open channel phenomena. In doing this, a review of the literature on open channel jumps, general stratified flow and internal hydraulic jumps is summarized, and this is followed by a section in which the theory behind the present analyses is outlined. The results of experiments are then presented in support of the theory, and theoretical limitations are discussed.

ACKNOWLEDGEMENTS

The Author would like to thank Dr. N. Rajaratnam for his support, inspiration and guidance in this study. The assistance of S. Lovell and L. Flint-Petersen in setting up and maintaining the experimental apparatus is also greatly appreciated. Financial support for this study was provided by the Natural Sciences and Engineering Research Council through grants to Dr. N. Rajaratnam. This support is gratefully acknowledged. The Author is also grateful to his employer, Agriculture Canada, P.F.R.A. for granting a leave of absence to enable him to pursue graduate study full time.

Table of Contents

Chapter		Page
1.	PART ONE: LITERATURE REVIEW	1
	1.1 INTRODUCTION	1
	1.2 FREE SURFACE HYDRAULIC JUMPS	2
	1.2.1 The Classical Hydraulic Jump	2
	1.2.2 The Submerged Hydraulic Jump	4
	1.2.3 The Sloping Hydraulic Jump	6
	1.3 INTERNAL HYDRAULIC JUMPS	8
	1.4 SUMMARY	16
2.	PART TWO: THEORETICAL DEVELOPMENT	17
	2.1 GENERAL STRATIFIED FLOW	17
	2.2 THE FREE INTERNAL JUMP	26
	2.3 THE SUBMERGED INTERNAL JUMP	30
	2.4 THE SLOPING INTERNAL JUMP	34
3.	PART THREE: EXPERIMENTS	39
	3.1 INTRODUCTION	39
	3.2 APPARATUS	39
	3.2.1 Flume	39
	3.2.2 Cold Water Supply	41
	3.2.3 Hot Water Supply	43
	3.2.4 Thermometer	43
	3.2.5 Photographic Equipment	43
	3.2.6 Modifications	44
	3.2.6.1 Free Internal Jump	44
	3.2.6.2 Sloping Internal Jump	44
	3.3 EXPERIMENTAL PROCEDURE	45
4.	PART FOUR:ANALYSIS AND DISCUSSION OF RESULTS	52

4.1 THE FREE INTERNAL JUMP 52
4.2 THE SUBMERGED INTERNAL JUMP 64
4.3 THE SLOPING INTERNAL JUMP 83
5. PART FIVE: CONCLUSIONS 98
5.1 THE FREE INTERNAL JUMP 98
5.2 THE SUBMERGED INTERNAL JUMP 98
5.3 THE SLOPING INTERNAL JUMP 99
5.4 LIMITATIONS OF THE PRESENT ANALYSIS 99
6. REFERENCES 101
7. APPENDIX A 105

LIST OF TABLES

Table Page

A1 Free Internal Jump Data.....105

A2 Submerged Internal Jump Data.....106

A3 Sloping Internal Jump Data.....107

LIST OF FIGURES

Figure Page

1. The Classical Hydraulic Jump.....3
2. The Submerged Hydraulic Jump.....3
3. The Sloping Hydraulic Jump.....3
4. The Internal Hydraulic Jump.....9
5. Density Jump.....12
6. Stratified Flow.....18
7. The Free Internal Jump.....27
8. The Submerged Internal Jump.....31
9. The Sloping Internal Jump.....35
10. Schematic Diagram of Test Apparatus.....40
11. Rotameter Calibration Chart.....42
12. Nondimensional Profiles of Free Internal Jump - y_o=0.007m 53
13. Nondimensional Profiles of Free Internal Jump - y_o=0.012m 54
14. Nondimensional Profiles of Free Internal Jump - y_o=0.0195m 55
15. Ordinary Free Internal Jump - Theoretical vs. Experimental Sequent Depth Ratio.....56
16. Ordinary Free Internal Jump - Sequent Depth Ratio vs. Densimetric Froude Number.....57
17. Plan View of Free Internal Jump.....58

Figure Page

18. Entrainment at Toe of Jump.....61
19. Ordinary Free Internal Jump - Roller Length vs. Densimetric Froude Number.....63
20. Ordinary Free Internal Jump - Normalized Jump Profiles.....65
21. Ordinary Free Internal Jump - Nondimensional Energy Loss in Jump - Theoretical vs. Experimental.....66
22. Nondimensional Profiles of Submerged Internal Jumps - y_o= 0.007m.....67
23. Nondimensional Profiles of Submerged Internal Jumps - y_o= 0.007m.....68
24. Nondimensional Profiles of Submerged Internal Jumps - y_o= 0.007m.....69
25. Nondimensional Profiles of Submerged Internal Jumps - y_o= 0.007m.....70
26. Nondimensional Profiles of Submerged Internal Jumps - y_o= 0.007m.....71
27. Nondimensional Profiles of Submerged Internal Jumps - y_o= 0.007m.....72
28. Nondimensional Profiles of Submerged Internal Jumps - y_o= 0.007m.....73
29. Nondimensional Profiles of Submerged Internal Jumps - y_o= 0.007m.....74
30. Nondimensional Profiles of Submerged Internal Jumps - y_o= 0.007m.....75

Figure Page

31. Submerged Internal Jump - Experimental vs. Theoretical Inlet Depth Factor - ψ.....76

32. Submerged Internal Jump - Experimental vs. Theoretical Nondimensional Energy Loss.....78

33. Submerged Internal Jump - Growth of Roller Length with Submergence 79

34. Submerged Internal Jump - Growth of Jump Length with Submergence 80

35. Sloping Internal Jump - Dimensionless Profiles - Bed Slope=1:18.5 84

36. Sloping Internal Jump - Dimensionless Profiles - Bed Slope=1:10 85

37. Sloping Internal Jump - Dimensionless Profiles - Bed Slope=1:6.67 86

38. Sloping Internal Jump - Theoretical vs. Experimental Sequent Depth Ratio.....87

39. Sloping Internal Jump - Sequent Depth Ratio vs. G_{o_*} ..88

40. Sloping Internal Jump - Theoretical vs. Experimental Jump Length 90

41. Sloping Internal Jump - Theoretical vs. Experimental Nondimensional Energy Loss.....91

42. Coordinates and Length Scales for Normalization of Sloping Jump Profiles.....92

Figure Page

43. Sloping Internal Jump - Normalized Profiles α=3.10 deg. 94

44. Sloping Internal Jump - Normalized Profiles α=5.71 deg. 95

45. Sloping Internal Jump - Normalized Profiles α=8.53 deg. 96

46. Internal Hydraulic Jump - Normalized Profiles.....97

LIST OF PLATES

Plate — Page

1.Free Internal Jump - $F_* \simeq 4.0$ 48

2.Free Internal Jump - $F_* \simeq 7.9$ 48

3.Submerged Internal Jump - $F_* \simeq 3.8$, $S \simeq 0.80$ 49

4.Submerged Internal Jump - $F_* \simeq 11.4$, $S \simeq 0.92$ 49

5.Sloping Internal Jump - $F_* \simeq 6.1$, $\alpha = 3.10$ deg 50

6.Sloping Internal Jump - $F_* \simeq 4.4$, $\alpha = 5.71$ deg 50

7.Downstream depth control 51

LIST OF SYMBOLS

E - specific energy

F - Froude number

F_* - densimetric Froude number

G_* - function of densimetric Froude number and slope

h - vertical height above a datum

L_{RJ} - length of roller of free internal jump

L_{SJ} - length of submerged internal jump

L_{RSJ} - length of roller in submerged internal jump

L_{SLJ} - length of sloping internal jump

L'_{SLJ} - length of sloping internal jump as measured along bed

p - mean pressure at a point

q - discharge intensity

S - submergence factor

S_o - bed slope

U - mean flow velocity in x direction

u - point velocity in x direction

v - point velocity in y direction

y_o - depth of flow at section 0

y'_{SLJ} - depth of flow at end of roller of sloping internal jump as measured normal to the bed

ρ - density of heavier fluid

ρ_a - density of lighter fluid

ν - kinematic viscosity of heavier fluid

τ - total shear stress

α - angle of inclination of channel bed with horizontal

ψ - inlet depth factor

ϕ - sequent depth ratio

Γ - function of slope α

Other symbols used are defined in the text.

1. PART ONE: LITERATURE REVIEW

1.1 INTRODUCTION

Fluid motion which arises due to the effect of gravity on density variations within a fluid field are called stratified flows. Many naturally occurring stratified flows are ones involving two fluids of differing density but with the density difference being rather small. Such flows can be treated as Boussinesq-type flows or as flows involving a fluid field of uniform density but variable specific weight. In such a situation, fluid motion can be treated as that which would arise in a reduced gravitational field given by $g'=g\Delta\rho/\rho$ where g is the acceleration due to gravity, $\Delta\rho$ is the density difference between the two fluids and ρ is the characteristic density of the fluid field.

Stratified flows occur widely in nature, both in the atmosphere and in water bodies. The movement of cold fronts, flows of gases in mines, density currents in lakes and oceans, thermal discharges into lakes, flow conditions at marine estuaries, and exchange flows in navigation locks are all examples of every-day situations involving stratified flow.

A great deal of theoretical work on internal motion was done prior to 1900 but this work concentrated mainly on internal wave motion. It wasn't until the 1950's, however, that research activity in the field of stratified flow began to rapidly expand to encompass a wide range of stratified

flow phenomena. One such phenomenon that began to receive research attention in the 1950's was the occurrence of hydraulic jumps in stratified flows, or internal hydraulic jumps.

Internal hydraulic jumps are, in many ways, analagous to the better known free surface hydraulic jump. Indeed, in a rigorous sense, all free surface flows are stratified flows with water, the heavier fluid, being overlain by air, the lighter fluid. However, in this case the density difference between the two fluids is so great that the situation reduces to the case of a homogeneous fluid flowing in a normal gravitational field. Nevertheless, it is useful to gain an understanding of the free surface hydraulic jump phenomenon before attempting an analysis of internal jumps.

1.2 FREE SURFACE HYDRAULIC JUMPS

1.2.1 The Classical Hydraulic Jump

The case where the flow of water in a smooth, wide, horizontal rectangular channel undergoes a rapid transition from supercritical to subcritical conditions is known as the classical hydraulic jump. As shown in Figure 1, the water surface at the toe of the jump or supercritical section begins an abrupt rise to a section of subcritical flow beyond which it is essentially level. The region between the supercritical and subcritical sections is quite violent and is characterized by a region near the surface where the flow

FIGURE 1 – THE CLASSICAL HYDRAULIC JUMP

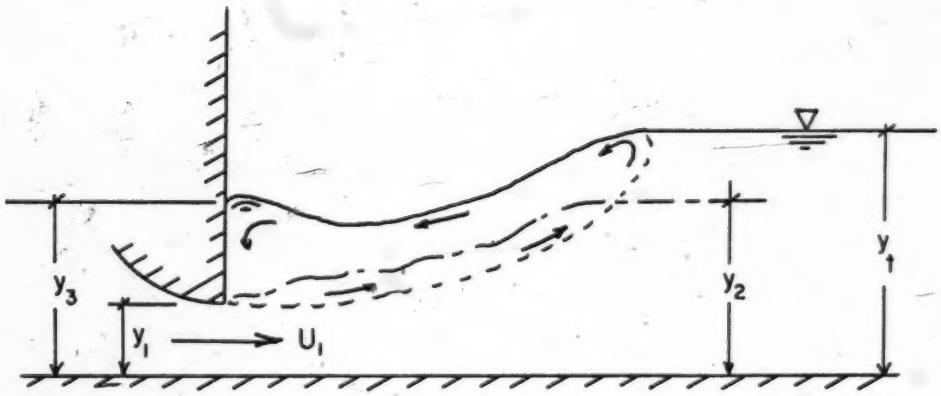

FIGURE 2 – THE SUBMERGED HYDRAULIC JUMP

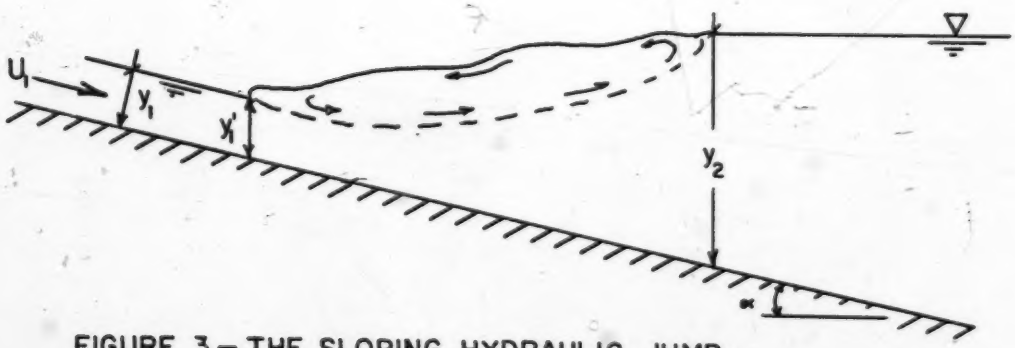

FIGURE 3 – THE SLOPING HYDRAULIC JUMP

reverses (the surface roller). The violent nature of the transition results in a substantial loss of energy.

Analysis of the classical hydraulic jump is carried out by assuming that the momentum is conserved, that velocity distributions are uniform and pressure distributions are hydrostatic upstream and downstream of the jump, and that turbulent fluctuations and boundary shear are negligible. The result is the well known Belanger momentum equation relating the sequent or conjugate depths in the following manner:

$$\frac{y_2}{y_1} = \frac{1}{2}\left(\sqrt{1 + 8\,F_1^2} - 1\right) \qquad (1)$$

where the supercritical Froude number F_1 is defined as:

$$F_1 = \frac{U_1}{\sqrt{g y_1}} \qquad (2)$$

As previously pointed out, the classical hydraulic jump has been studied extensively and a great deal is known not only of the global behavior but of the internal flow structure as well. Rajaratnam (1967) presents a summary and analysis of the various contributions to this field of study.

1.2.2 The Submerged Hydraulic Jump

If the depth of flow downstream of a supercritical stream is that predicted by the Belanger momentum equation,

the result will be a stationary hydraulic jump. A lower depth will result in movement of the jump downstream as a negative surge and a greater depth will result in a positive-type surge upstream. If the supercritical stream issues from an orifice as in Figure 2, a large downstream depth will result in a drowned or submerged jump.

Govinda Rao and Rajaratnam (1963) found that the parameters which define the submerged jump are the degree of submergence and the supercritical Froude number F_1. By applying the momentum equation to the efflux section and the end of the jump, the following relation was derived:

$$\phi = \left[\frac{(1+S)^2}{4}\phi^2 - 2F_1^2 + \frac{4F_1^2}{\phi(1+S)}\right]^{0.5} \tag{3}$$

where, using the notation of Figure 2:

$$\psi = \text{inlet depth factor} = y_3/y_1 \tag{4}$$

$$S = \text{submergence factor} = (y_t - y_2)/y_2 \tag{5}$$

$$y_2 = \text{sequent depth of supercritical stream} \tag{6}$$

$$\phi = (\sqrt{1 + 8F_1^2} - 1) \tag{7}$$

$$F_1 = \frac{U_1}{\sqrt{gy_1}} \tag{8}$$

Further studies by Rajaratnam (1965) examined the internal flow structure in submerged jumps and gave relations to predict the surface profile. A summary of the foregoing work and the work of others is given in Rajaratnam (1967).

1.2.3 The Sloping Hydraulic Jump

In the previous two situations the momentum equation could be applied without knowledge of the shape or extent of the transition region. In the case of the hydraulic jump on a sloping surface, however, analysis of horizontal momentum must include the horizontal component of pressure force that the body of the jump exerts on the floor. Since, at this time, it is impossible to predict this quantity initially, the problem of the sloping hydraulic jump must be dealt with in a semi-empirical manner.

Studies of the sloping hydraulic jump go back as far as those on the classical jump, but the first rational and successful approach to the problem was by Kindsvater (1944) who developed the following relation based on a momentum analysis:

$$\frac{y_2}{y_1} = \frac{1}{2\cos\alpha}\left[\sqrt{\frac{8\,U_1^2\cos^3\alpha}{g\,y_1(1 - 2\,\phi\,\tan\alpha)}} + 1 - 1\right] \qquad (9)$$

where the value of ϕ is a semi-empirical parameter used to account for the pressure of the jump body on the floor. Kindsvater initially assumed that the value of ϕ was dependent on what he termed the kinetic flow factor $\lambda = U_1^2/2g$, which in a nondimensional manner implies that ϕ is a function of the supercritical Froude number. However, further studies by Peterka (1963) indicate that this parameter is not strongly affected by Froude number but is more closely related to the slope of the floor, $\tan\alpha$. A

complete re-analysis of the problem was conducted by Rajaratnam (1966) who presented the following Belanger-type relation,...

$$\frac{y_2}{y_1} = \frac{1}{2}\left[\sqrt{1 + 8\,G_1^2} - 1\right] \qquad (10)$$

where,...

$$G_1^2 = \Gamma^2\, F_1^2 \qquad (11)$$

$$\log_{10}\Gamma \simeq 0.027\alpha \qquad (12)$$

$$y_1' = y_1/\cos\alpha \qquad (13)$$

Rajaratnam further discussed the variety of sloping jumps that can occur and their analysis. The present study, however, is confined to the D-type jump as in Figure 3. The internal flow structure of sloping jumps was investigated by Rajaratnam and Murahari (1974).

Studies of the free surface hydraulic jump also include jumps which occur at abrupt drops and expansions, jumps in non-rectangular channels and non-prismatic channels, jumps in conduits, forced jumps and jumps involving two-phase flow. For a concise discussion of these phenomena the reader is referred to Rajaratnam (1967).

1.3 INTERNAL HYDRAULIC JUMPS

The first attempt at analytically predicting the global parameters defining internal hydraulic jumps was the analysis of Yih and Guha (1955). By starting with the assumption of no entrainment between layers, no bed or interfacial shear, uniform velocity distributions in each layer upstream and downstream of the jump and a hydrostatic pressure distribution over the body of the jump in the lower layer, a momentum analysis of a two-layer flow (see Figure 4) was conducted. The combined momentum equations for the upper and lower layers resulted in a ninth-order polynomial.

Yih and Guha discussed the solution of this equation and pointed out that one root was trivial and four were non-real which implied that only three states can possibly exist conjugate to the given state. They further pointed out that if the motion of one layer is dynamically dominant, the downstream state is uniquely determined by the following Belanger-type relation:

$$\frac{y_2'}{y_2} = \frac{1}{2}\left[\sqrt{1 + 8\,F_{2*}^2} - 1\right] \qquad (14)$$

where F_{2*} is the densimetric Froude number of the flow in the dominant layer defined as:

$$F_{2*}^2 = q_2^2/g\,(\Delta\rho/\rho)\,y_2^3 \qquad (15)$$

where,...

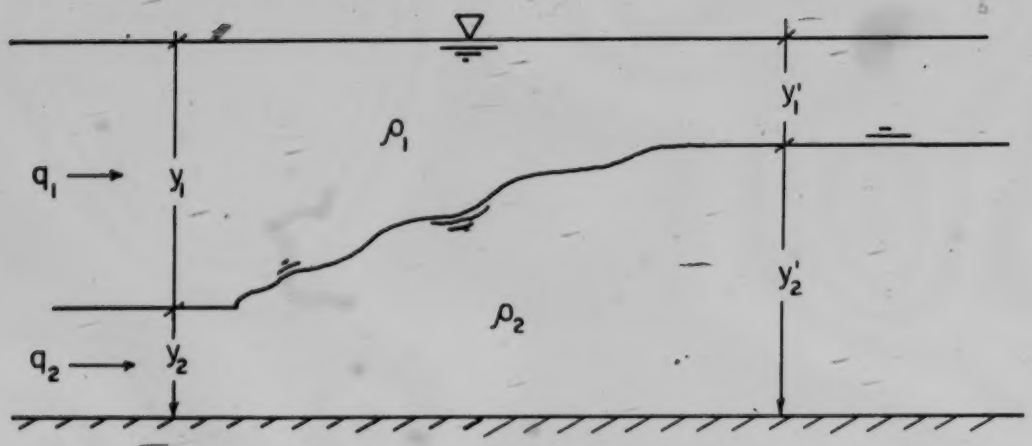

FIGURE 4 THE INTERNAL HYDRAULIC JUMP

(After Yih & Guha, 1955)

$\Delta\rho$ = the density difference between the two fluids

$= \rho_2 - \rho_1$

ρ = the characteristic density of the flow field

$\simeq \rho_2$

Experiments conducted by Yih and Guha on a hydraulic jump occurring in a flowing denser layer in a quiescent ambient showed that equation (14) consistently overestimated the downstream depth, the discrepancy increasing as the density difference between the two fluids increased. Yih and Guha attributed this anomaly to the effects of interfacial shear. However, the fluids used in the experiment were

immiscible (water and oil) and it is felt that the departure from theory was more likely due to energy losses arising due to the entrainment and subsequent detrainment of ambient fluid by the flowing denser layer.

Yih and Guha's initial discussion of the solution of the momentum equation was a purely mathematical one and did not consider some of the physical characteristics of the problem, likely since no observations of the phenomenon had previously been made. Other researchers dealt with the problem by modelling it initially as a two-layer flow in a duct (Mehrotra (1973) and Mehrotra and Kelly (1973)), and by imposing physical constraints such as energy loss across the jump (Hayakawa (1970) and Chu and Baddour (1977)). The result of these refinements was that for two flowing fluid layers of different density at an overall supercritical state (the sum of the densimetric Froude numbers of each layer greater than unity) there exist only two physically meaningful conjugate states, and further, that only the state closest to the original will be physically realized.

While the previous discussion may imply a complete solution to the problem it should be pointed out that these analyses were only of a global nature and that all assumed that no entrainment of one fluid by the other takes place. It is known that a density gradient tends to inhibit mixing since the buoyant forces tend to damp out turbulent fluctuations in the flow. However, it should not be assumed implicitly that no mixing takes place in a turbulent

stratified flow, including the situation of an internal hydraulic jump. A number of researchers have recognized this and attempted to account for entrainment in the analysis of internal hydraulic jumps.

One of the earliest attempts at analysing an entraining jump was by Wilkinson and Wood (1971). Their study dealt with a supercritical stream of denser fluid discharging into a lighter semi-infinite ambient field. The nomenclature employed by Wilkinson and Wood proposed that the term "density jump" describes a situation which includes a zone occupied by an entraining denser wall jet followed by a roller region where the actual jump phenomenon occurs (Figure 5). They observed that nearly all of the entrainment of the ambient fluid occurred in the "entraining region" and that entrainment by the roller region was negligible. They also discussed, in a qualitative manner, how a rise in tailwater (y_2) would force the jump upstream in a manner analagous to the open channel jump until the roller region occupies the entire jump and entrainment effectively ceases. They further observed that an additional increase in the downstream depth would result in a situation analagous to the submerged open channel jump and that this situation was similarly non-entraining.

The experiments conducted by Wilkinson and Wood used a weir to control the downstream depth of the flowing denser layer. It was assumed that the flow would be "critical" at this section (the densimetric Froude number of the flow in

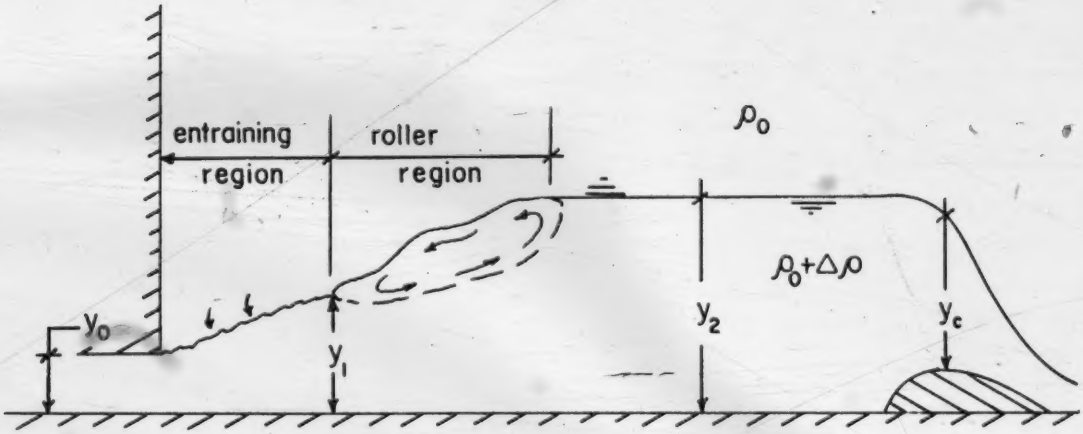

FIGURE 5 DENSITY JUMP

(After Wilkinson & Wood, 1971)

the denser layer equal to one). Therefore, for a given head on the downstream weir they were able to calculate, based on a momentum analysis, the depth downstream of the jump based on the upstream conditions, and indirectly, the rate of entrainment prior to jump formation.

Further investigations by Wood and Simpson (1984) dealt with a number of rapidly varied phenomena in two-layered systems and expanded on the work of Wilkinson and Wood. These investigations showed that if the stationary entraining jump is in a co-flowing ambient, the amount of entrainment increases over that of the jump in a quiescent ambient.

The effects of a limited depth of field on internal hydraulic jumps were first investigated by Stefan and Hayakawa (1972). Using a momentum analysis and numerically solving the resulting equation, they developed plots showing how entrainment varied with outlet densimetric Froude number and ambient depth. Their plots indicate that for a given ambient depth, entrainment by the flowing denser layer asymptotically approaches some terminal value as the outlet densimetric Froude number is increased indefinitely. Later analyses by Jirka and Harleman (1979) and Baddour and Abbink (1983) discussed the shortcomings of the Stefan and Hayakawa approach by pointing out that if all other physical characteristics of the system are held constant, an indefinite increase in the outlet densimetric Froude number of a denser flow into a limited ambient will result in a complete breakdown of the stratified environment as the flow begins to "interact" with the upper boundary of the ambient field. Both papers termed this condition an instability.

The paper by Baddour and Abbink is one of the most lucid and comprehensive on the subject. Once again, a momentum analysis is carried out and the resulting equation is solved by imposing a number of physical constraints such as a loss of energy across the jump, no reduction of discharge intensity across the jump, and sequent depth of the supercritical stream less than the total field depth. The subsequent discussion and presentation of experimental results brings forth some useful and interesting points. The

authors' analysis predicts that for a given set of conditions, entrainment increases with outlet densimetric Froude number until a maximum is reached at a densimetric Froude number of $F_{o_*} \simeq H^{2/3}$, where H is the ratio of the total field depth to the depth of the supercritical stream at the outlet. Until this point is reached, the flow behaves as essentially unconfined. An increase in densimetric Froude number beyond this point results in a decrease in entrainment until the flow becomes "unstable" at a Froude number of $F_{o_*} \simeq H/\sqrt{2}$. Baddour and Abbink also discuss the phenomenon of the submerged internal jump and give an equation for the downstream control which will result in a jump on the drowned/free borderline for a given densimetric Froude number at the outlet. They point out, however, that this borderline is poorly defined in reality, with the jump alternating between a drowned and free state.

All of the foregoing papers dealing with entraining internal jumps have either assumed that the mechanism by which the jump entrains ambient fluid is turbulent entrainment or made no reference to the mode of entrainment at all. Regardless of the assumed entrainment mechanism, all of the foregoing analyses were of a global nature and considered only the effects of entrainment on the global flow parameters at a given section.

One of the first studies of turbulent entrainment in stratified flows was that of Ellison and Turner (1959). They assumed that the phenomenon could be analysed in a manner

similar to that employed in the study of buoyant plumes; that is, that the entrainment velocity induced in the ambient field by the turbulent flow is directly proportional to the mean flow velocity. Their results indicated that the constant of proportionality in this relation was strongly dependent on the densimetric Richardson number of the stratified flow which they defined as $R_{i*}=1/F_o{}^2{}_*$. Their results showed that the entrainment constant was the same as that for a neutral jet at $R_{i*}\simeq 0$ but that it rapidly decreased for flows of increasing Richardson number. Similar results were obtained in a study by Chu and Vanvari (1976). The paper by Chu and Vanvari goes further by examining the internal flow structure in turbulent stratified flows and also mentions other entrainment mechanisms. They discuss the internal hydraulic jump, and along with previous researchers point out that the roller region accounts for very little entrainment. They also point out, however, that some small amount of entrainment does occur in this region, but rather than being turbulent entrainment, it is typically the result of ambient fluid being entrapped by breaking interfacial waves. A study by Christodolou (1986) consolidates data from a number of studies and analyses it in the same manner as Ellison and Turner. Cristodolou plotted the nondimensional entrainment velocity versus the Richardson number and defined four regions describing the relationship between entrainment, Richardson number and the associated entrainment mechanism.

Further discussion of entrainment can be found in a paper by Macagno and Macagno (1975). Based on studies of open channel jumps they proposed that most of the entrainment in internal jumps occurs at the toe of the jump, a region of high turbulence production and low dissipation.

1.4 SUMMARY

Despite the enormous advances that the previously discussed works represent, a comprehensive understanding of stratified flow in general and internal hydraulic jumps in particular is far from being realized. A review of the literature in this area reveals the great complexity of turbulent stratified flows and shows how simplistic the usual global analyses are given the complexity of the problem. The analyses to be presented in this thesis are similarly simplistic in that they attempt to extend relations developed for open channel jumps to internal jumps. It is hoped that this information will be of some use in future studies of internal hydraulic jumps.

2. PART TWO: THEORETICAL DEVELOPMENT

2.1 GENERAL STRATIFIED FLOW

Let us initially consider the general case where a heavier fluid of density ρ is flowing beneath a deep, quiescent layer of less dense fluid of density ρ_a. In this situation, the Navier-Stokes equations for planar motion in a cartesian coordinate system, as in Figure 6, will be,...

$$\frac{\partial u}{\partial t} + u\frac{\partial u}{\partial x} + v\frac{\partial u}{\partial y} = -\frac{1}{\rho}\frac{\partial p}{\partial x} + \nu\nabla^2 u + g\frac{\partial h}{\partial x} \qquad (16)$$

$$\frac{\partial v}{\partial t} + u\frac{\partial v}{\partial x} + v\frac{\partial v}{\partial y} = -\frac{1}{\rho}\frac{\partial p}{\partial y} + \nu\nabla^2 v - g\frac{\partial h}{\partial y} \qquad (17)$$

$$\frac{\partial u}{\partial x} + \frac{\partial v}{\partial y} = 0 \qquad (18)$$

Equations (16) and (17) are the momentum conservation equations in the x and y directions, respectively, and equation (18) is the equation of continuity. Equations (16) and (17) could also be written as,...

$$\frac{\partial u}{\partial t} + \frac{\partial u^2}{\partial x} + \frac{\partial uv}{\partial y} = -\frac{1}{\rho}\frac{\partial p}{\partial x} + \nu\nabla^2 u + g\frac{\partial h}{\partial x} + u\left(\frac{\partial u}{\partial x} + \frac{\partial v}{\partial y}\right) \qquad (16a)$$

$$\frac{\partial v}{\partial t} + \frac{\partial uv}{\partial x} + \frac{\partial v^2}{\partial y} = -\frac{1}{\rho}\frac{\partial p}{\partial y} + \nu\nabla^2 v - g\frac{\partial h}{\partial y} + v\left(\frac{\partial u}{\partial x} + \frac{\partial v}{\partial y}\right) \qquad (17a)$$

By continuity, the last terms in each of the above equations reduce to zero, and we get,...

$$\frac{\partial u}{\partial t} + \frac{\partial u^2}{\partial x} + \frac{\partial uv}{\partial y} = -\frac{1}{\rho}\frac{\partial p}{\partial x} + \nu\nabla^2 u + g\frac{\partial h}{\partial x} \qquad (16b)$$

$$\frac{\partial v}{\partial t} + \frac{\partial uv}{\partial x} + \frac{\partial v^2}{\partial y} = -\frac{1}{\rho}\frac{\partial p}{\partial y} + \nu\nabla^2 v - g\frac{\partial h}{\partial y} \qquad (17b)$$

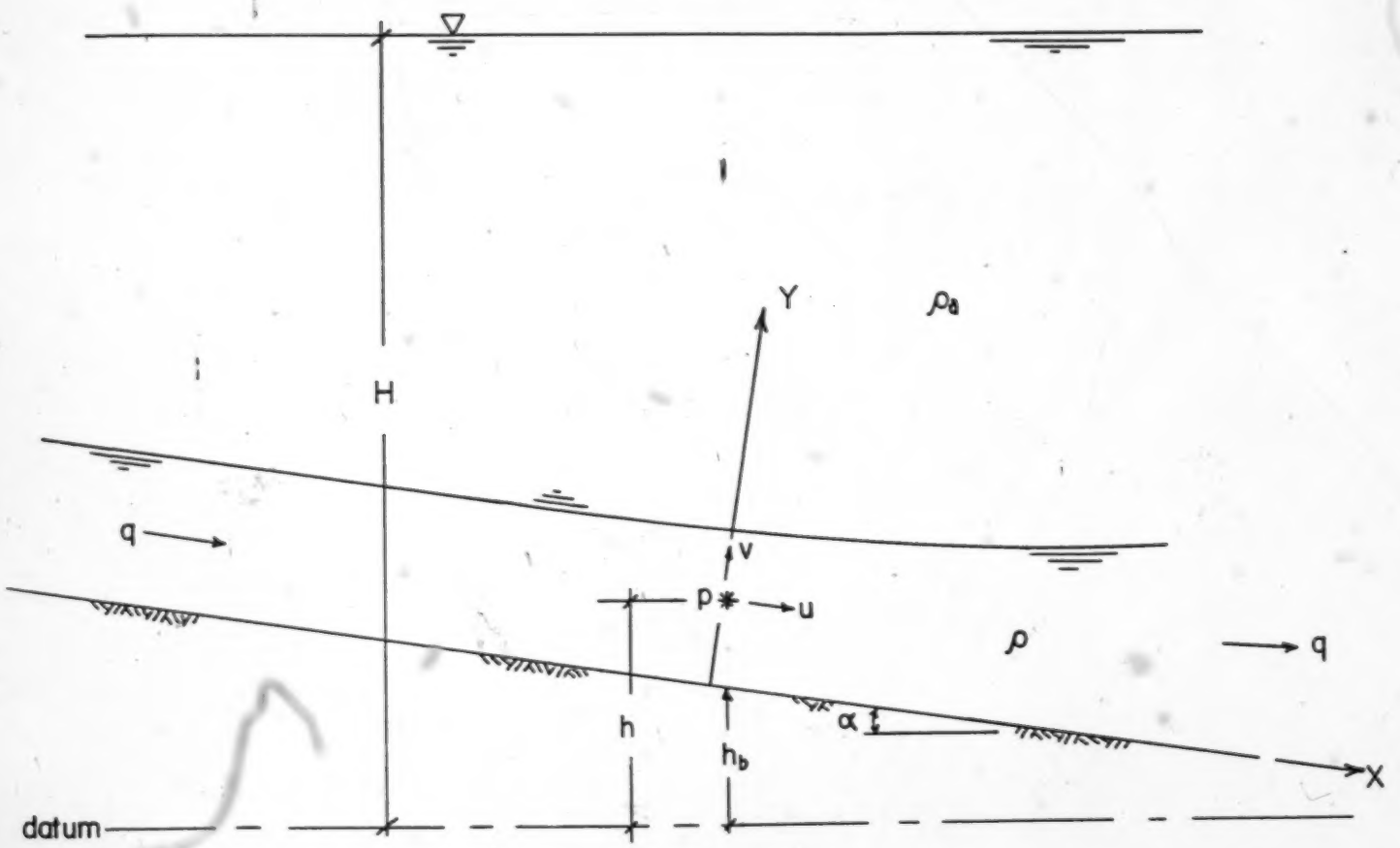

FIGURE 6-STRATIFIED FLOW

Let us now confine our attention to turbulent flows where, according to the rules of Reynolds decomposition, the dynamic variables in the above equations can be assumed to be made up of the sum of a time averaged or mean quantity and a fluctuating quantity. For example,...

$$u=\bar{u}+u'$$

$$v=\bar{v}+v'$$

$$p=\bar{p}+p'$$

$$\rho=\bar{\rho}+\rho'$$

If we expand equations (16b) and (17b) and assume that the fluid is incompressible we will end up with the familiar Reynolds equations for two dimensional flow.

$$\frac{\partial \bar{u}}{\partial t}+\bar{u}\frac{\partial \bar{u}}{\partial x}+\bar{v}\frac{\partial \bar{u}}{\partial y}=-\frac{1}{\rho}\frac{\partial \bar{p}}{\partial x}+\nu\nabla^2\bar{u}-\left(\frac{\partial \overline{u'^2}}{\partial x}+\frac{\partial \overline{u'v'}}{\partial y}\right)+g\frac{\partial h}{\partial x} \qquad (18)$$

$$\frac{\partial \bar{v}}{\partial t}+\bar{u}\frac{\partial \bar{v}}{\partial x}+\bar{v}\frac{\partial \bar{v}}{\partial y}=-\frac{1}{\rho}\frac{\partial \bar{p}}{\partial y}+\nu\nabla^2\bar{v}-\left(\frac{\partial \overline{u'v'}}{\partial x}+\frac{\partial \overline{v'^2}}{\partial y}\right)-g\frac{\partial h}{\partial y} \qquad (19)$$

$$\frac{\partial \bar{u}}{\partial x}+\frac{\partial \bar{v}}{\partial y}=0 \qquad (20)$$

wherein:

-$\bar{u}$ and $\bar{v}$ are the time averaged values of horizontal and vertical velocities, respectively;

-u' and v' are the instantaneous values of the fluctuating components of the turbulent velocity field;

-$\bar{p}$ is the mean pressure at a point;

-ρ is the mass density of the heavier fluid;

-h is the height of the fluid particle above some datum;

-ν is the kinematic viscosity of the fluid in motion;

-g is the acceleration due to gravity;

and the overscores indicate that the values have been averaged over some physically meaningful time scale. Hereafter, the overscores will be neglected for convenience of notation.

If we now write the pressure and density terms as,...

$$p = \rho_a g (H - h) + \Delta p \tag{21}$$

$$\rho = \rho_a + \Delta\rho \tag{22}$$

we can say,...

$$\frac{\partial p}{\partial x} = - g\rho_a \frac{\partial h}{\partial x} + \frac{\partial \Delta p}{\partial x}$$

$$- \frac{\partial p}{\partial x} - \rho g \frac{\partial h}{\partial x} = g\rho_a \frac{\partial h}{\partial x} - \frac{\partial \Delta p}{\partial x} - g (\rho_a + \Delta\rho) \frac{\partial h}{\partial x}$$

$$- \frac{\partial p}{\partial x} - \rho g \frac{\partial h}{\partial x} = \frac{\partial \Delta p}{\partial x} - \Delta\rho g \frac{\partial h}{\partial x}$$

Let us now define

$$g' = g\Delta\rho/\rho \tag{23}$$

$$\Delta p_* = \Delta p + gh\,\Delta\rho \tag{24}$$

If we use the above definition and further assume that vertical accelerations are relatively small, that the viscous and turbulent stress terms in equations (18) and (19) can be expressed as the total stress τ and that the motion is steady, we can write,...

$$u \frac{\partial u}{\partial x} + v \frac{\partial u}{\partial y} = - \frac{1}{\rho} \frac{\partial \Delta p_*}{\partial x} + \frac{1}{\rho} \frac{\partial \tau}{\partial y} \qquad (25)$$

Now, let us integrate equation (25) from the channel bed (y=0) to the light-dense interface ($y=\bar{y}$). The first term on the left side of the equation will become,...

$$\int_0^{\bar{y}} u \frac{\partial u}{\partial x} dy = \frac{1}{2} \int_0^{\bar{y}} \frac{\partial u^2}{\partial x} dy = \frac{1}{2} \left\{ \frac{d}{dx} \int_0^{\bar{y}} u^2 dy - u_{\bar{y}}^2 \frac{d\bar{y}}{dx} \right\}$$

by using the Liebnitz Theorem. The second term on the left side of equation (25) can be integrated by parts as follows:

$$\int_0^{\bar{y}} v \frac{\partial u}{\partial y} dy = uv \Big|_0^{\bar{y}} - \int_0^{\bar{y}} u \frac{\partial v}{\partial y} dy$$

Recalling that the equation of continuity says $\frac{\partial v}{\partial y} = - \frac{\partial u}{\partial x}$, we can write,...

$$\int_0^{\bar{y}} v \frac{\partial u}{\partial y} dy = u_{\bar{y}} v_{\bar{y}} + \int_0^{\bar{y}} u \frac{\partial u}{\partial x} dy$$

It can be said that,...

$$\underline{u}_{\bar{y}}\,\underline{v}_{\bar{y}} = \underline{u}_{\bar{y}} \int_0^{\bar{y}} \frac{\partial v}{\partial y}\, dy$$

which, by continuity is equivalent to saying,...

$$\underline{u}_{\bar{y}}\,\underline{v}_{\bar{y}} = -\underline{u}_{\bar{y}} \int_0^{\bar{y}} \frac{\partial u}{\partial x}\, dy$$

Now we have,...

$$\int_0^{\bar{y}} v\,\frac{\partial u}{\partial y}\, dy = -\underline{u}_{\bar{y}} \int_0^{\bar{y}} \frac{\partial u}{\partial x}\, dy + \int_0^{\bar{y}} u\,\frac{\partial u}{\partial x}\, dy$$

If we once again apply the Liebnitz Theorem we will get,...

$$\int_0^{\bar{y}} v\,\frac{\partial u}{\partial y}\, dy = -\underline{u}_{\bar{y}} \left\{\frac{d}{dx} \int_0^{\bar{y}} u\, dy - \underline{u}_{\bar{y}} \frac{\partial \bar{y}}{dx}\right\} + \int_0^{\bar{y}} u\,\frac{\partial u}{\partial x}\, dy$$

and the left hand side of equation (25) can be expressed as,...

$$\frac{d}{dx} \int_0^{\bar{y}} u^2\, dy - \underline{u}_{\bar{y}}\, \frac{d}{dx} \int_0^{\bar{y}} u\, dy$$

Now let us assume that the slope $S_o = -\left(\frac{\partial}{\partial x}(h_b)\right)$ is small. If this is the case, then the first term on the right hand side of equation (25) will be,...

$$\frac{\partial \Delta p_*}{\partial x} \simeq \frac{d\Delta p}{dx} + g\frac{d}{dx}(\Delta\rho\,(h_b + y)) \simeq \frac{d\Delta p}{dx} + g\Delta\rho\frac{dh_b}{dx}$$

and integration with respect to y will give us,...

$$\int_0^{\bar{y}} \frac{\partial \Delta p_*}{\partial x}\,dy = \int_0^{\bar{y}} \frac{d\Delta p}{dx}\,dy - \int_0^{\bar{y}} gS_0\frac{d\Delta\rho}{dx}\,dy$$

The stress term in equation (25) can be integrated if we let the stress at the bed be τ_o and the interfacial stress be τ_i, as follows,...

$$\int_0^{\bar{y}} \frac{\partial \tau}{\partial y}\,dy = \tau\Big|_0^{\bar{y}} = -(\tau_0 - \tau_i)$$

since τ_o and τ_i are opposite in sign by definition.

Now let us qualify the argument by saying that the entrainment between layers is negligible. Under such conditions it can be said that,...

$$\underline{u}_{\bar{y}}\frac{d}{dx}\int_0^{\bar{y}} u\,dy = 0$$

and,...

$$g \frac{d}{dx} (\Delta\rho h_b) = g\Delta\rho \frac{dh_b}{dx}$$

Under these conditions, all of the foregoing work reduces to,...

$$\frac{d}{dx} \int_0^{\bar{y}} (\Delta p + \rho u^2)\, dy = -(\bar{\tau_0} + \tau_i) - S_0\, g\Delta\rho\bar{y} \qquad (26)$$

Equation (26) states that the rate of change of the total pressure and momentum from one section to another in the flowing denser layer is the result of a destructive shearing force and a gravitational driving force due to the density difference between the two layers.

Let us now assume that our region of interest is a relatively short reach where the energy losses due to viscous and turbulent dissipation are negligibly small, and further, that the fluid motion is irrotational and steady. Such assumptions, when applied to equations (15) and (16) will result in the following expressions,...

$$u \frac{\partial u}{\partial x} + v \frac{\partial u}{\partial y} \simeq - \frac{1}{\rho} \frac{\partial \Delta p_*}{\partial x} \qquad (27)$$

$$u \frac{\partial v}{\partial x} + v \frac{\partial v}{\partial y} \simeq - \frac{1}{\rho} \frac{\partial \Delta p_*}{\partial y} \qquad (28)$$

The assumption of irrotationality implies that the component of vorticity in the z direction is zero. By definition, this

means,...

$$\frac{\partial v}{\partial x} = \frac{\partial u}{\partial y}$$

Therefore we can write equation (27) as,...

$$\rho \frac{\partial}{\partial x} \left(\left(\frac{u^2}{2} + \frac{v^2}{2} \right) + \Delta p_* \right) = 0$$

Which, if integrated with respect to y becomes,...

$$\rho/2 \ (u^2 + v^2) + \Delta p_* = f(y) \qquad (29)$$

Equation (28) can similarly be written as,...

$$\frac{\partial}{\partial y} \left(\rho/2 \ (u^2 + v^2) + \Delta p_* \right) = 0 \qquad (30)$$

If equation (29) is differentiated with respect to y and compared to equation (30) it can be seen that $\frac{\partial}{\partial y}(f(y)) = 0$ or $f(y)$=constant. Therefore, if we define the total velocity vector as $V^2 = u^2 + v^2$, then we will get,...

$$\Delta p_* + \frac{\rho V^2}{2} = \text{constant} \qquad (31)$$

Equation (31) above is a Bernoulli-type expression which implies that the specific energy at any section in the

flow is a constant. However, the assumptions used in the derivation are such that this will only be true over very short reaches where the flow is reasonably tranquil. Nevertheless, the concept of specific energy is a useful tool and will be employed later.

2.2 THE FREE INTERNAL JUMP

All of the studies of the past which dealt with hydraulic jumps in stratified flows have used a control volume or macro approach in the analysis. The present analysis, while reducing to the control volume approach in the evaluation of integral terms, goes back one step to the integral form of the Reynolds equations as previously developed. The following analysis is confined to the case where one layer of a two-layer system is in motion. It can also be applied to the case of both layers in motion but it becomes much more cumbersome algebraically.

The definition sketch to be considered will be as in Figure 7. If we assume that the bed is horizontal and that the shear forces along the bed and interface can be neglected, then equation (26) becomes,...

$$\frac{d}{dx} \int_0^{\bar{y}} (\Delta p + \rho u^2)\, dy = 0 \qquad (26a)$$

or

$$\int_0^{\bar{y}} (\Delta p + \rho u^2)\, dy = \text{constant, say A} \qquad (26b)$$

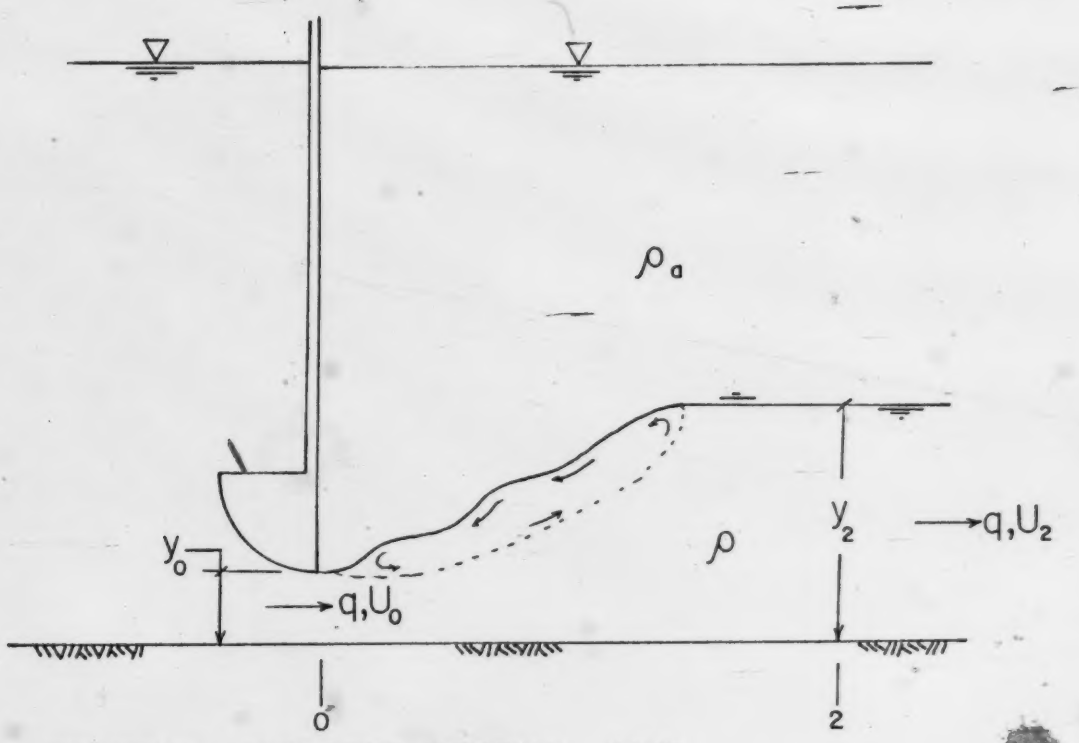

FIGURE 7 – THE FREE INTERNAL JUMP

If we apply equation (26b) at sections 0 and 2 we will get

$$\int_0^{y_0} (\Delta p + \rho u^2)\, dy = \rho U_0^2\, y_0 + \frac{1}{2}\, g\Delta\rho y_0^2 = A \qquad (32)$$

$$\int_0^{y_2} (\Delta p + \rho u^2)\, dy = \rho U_2^2\, y_2 + \frac{1}{2}\, g\Delta\rho y_2^2 = A \qquad (33)$$

In our idealized situation we are assuming that momentum is conserved and the two expressions above can be equated, resulting in,...

$$\frac{1}{2}\, g\Delta\rho\, (y_2^2 - y_0^2) = \rho\, (U_0^2\, y_0 - U_2^2\, y_2) \qquad (34)$$

Recalling that we have invoked the condition of no

entrainment in the derivation of equation (26), we can say that the discharge intensity remains constant, or,...

$$U_o y_o = U_2 y_2 = q$$

and we can rearrange equation (34) to get,...

$$g\Delta\rho\ (y_2 - y_0)\ (y_2 + y_0) = 2\rho\ U_0^2\ y_0\ (y_2 - y_0)/y_2 \qquad (35)$$

If we now define a densimetric or modified Froude number as,...

$$F_\star = \frac{U}{\sqrt{gy\Delta\rho/\rho}}$$

then expression (35) becomes the quadratic,...

$$(y_2/y_0)^2 + (y_2/y_0) - 2\ F_{0\star}^2 = 0 \qquad (36)$$

the real solution of which is,...

$$\frac{y_2}{y_0} = \frac{1}{2}\left[\sqrt{1 + 8\ F_{0\star}^2} - 1\right] \qquad (37)$$

Equation (37) is analagous to the classic Belanger equation for hydraulic jumps in rectangular open channels, the difference being in the definition of the Froude number.

The energy loss in a free internal jump can be expressed as the difference between the specific energy upstream and downstream of the jump as calculated from conditions described by equation (37). Using the notation of Figure 7, the energy of a fluid particle at the light-dense interface at section 0 can be written as,...

$$E_0 = g\Delta\rho\, y_0 + \frac{\rho U_0^2}{2}$$

by using equation (31). Similarly, the energy at section 2 will be,...

$$E_2 = g\Delta\rho\, y_2 + \frac{\rho U_2^2}{2}$$

The resulting energy loss incurred by the flow transition can now be expressed nondimensionally as,...

$$\frac{E_0 - E_2}{E_0} = \frac{g\Delta\rho y_0 + \rho U_0^2/2 - g\Delta\rho y_2 - \rho U_2^2/2}{g\Delta\rho\, y_0 + \rho U_0^2/2} \qquad (38)$$

Dividing both the numerator and denominator of equation (38) by $g\Delta\rho y_0$ and using the continuity relation, the nondimensional energy loss across the jump can be written as,...

$$\frac{\Delta E}{E_0} = \frac{1 - \phi + \frac{F_{0*}^2}{2}(1 - 1/\phi^2)}{1 + F_{0*}^2/2} \qquad (39)$$

where,...

$$F_{0*}^2 = \frac{U_0^2}{y_0 g'}$$

$$g' = g \frac{\Delta\rho}{\rho}$$

$$\phi = \frac{y_2}{y_0} = \frac{1}{2}\left[\sqrt{1 + 8 F_{0*}^2} - 1\right]$$

as defined previously.

2.3 THE SUBMERGED INTERNAL JUMP

There have been a number of papers written in the past on the subject of hydraulic jumps in stratified flows which have remarked on the existence of drowned or submerged jumps, among them studies by Wilkinson and Wood (1971), Stefan and Hayakawa (1972), and Baddour and Abbink (1983). However, the remarks dealt mainly with the conditions which would cause submergence and were generally inserted as an aside to the discussion of the problems being addressed in the study. The following analysis is meant to more completely define the submerged internal jump and to present a method of calculating some of the salient parameters associated with this phenomenon. The present analysis draws heavily on material presented by Rajaratnam (1963,1965) in papers which outlined the results of investigations of submerged open channel jumps. We shall begin by referring to Figure 8 as our definition sketch and we will employ the arguments developed in the preceding sections.

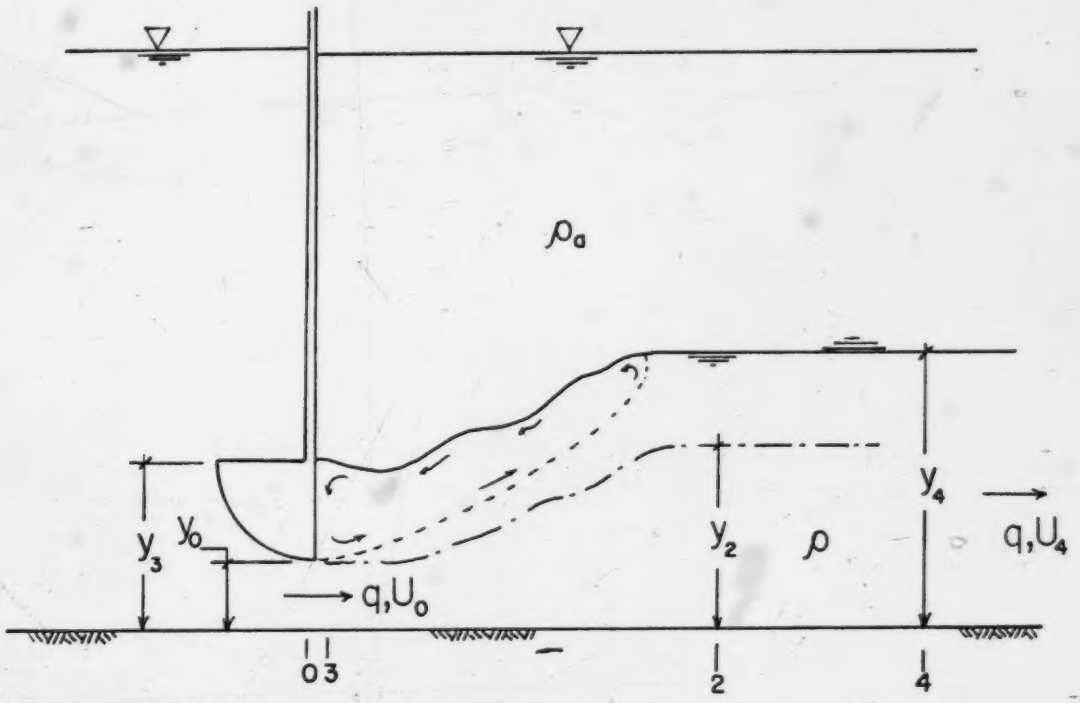

FIGURE 8 – THE SUBMERGED INTERNAL JUMP

If the depth of the denser layer downstream of the jump is such that a jump forms at section 3 and is stable, then the upstream and downstream depths are related by the following expression,...

$$\phi = \frac{y_2}{y_0} = \frac{1}{2}\left[\sqrt{1 + 8\,F_{0*}^2} - 1\right] \qquad (40)$$

as developed in the previous section (for a deep, quiescent ambient).

Now, if the downstream depth at section 4 is greater than y_2 such that the jump moves upstream, the efflux section will become submerged. If we apply our integral

momentum equation (eq'n (26b)) at sections 3 and 4, we will get,...

$$\int_0^{y_3} (\Delta p + \rho u^2)\, dy = \rho U_3^2 y_3 + \frac{1}{2} g\Delta\rho\, y_3^2 = A \qquad (41)$$

$$\int_0^{y_4} (\Delta p + \rho u^2)\, dy = \rho U_4^2 y_4 + \frac{1}{2} g\Delta\rho\, y_4^2 = A \qquad (42)$$

We will once again neglect any entrainment such that,...

$$q=U_0y_0=U_2y_2=U_3y_3=U_4y_4$$

and following Rajaratnam we will define the following terms:

Submergence factor $S=(y_4-y_2)/y_2$ (43)

Inlet depth factor $\psi=(y_3/y_0)$ (44)

Using these identities, equations (41) and (42) can be reduced and written as,...

$$\phi^2 y_0^2 - \phi^2 y_0^2 (S+1)^2 = \frac{2q^2}{g'} \left(\frac{1}{\phi y_0 (S+1)} - \frac{1}{y_0}\right) \qquad (45)$$

Further manipulation will result in an equation for the inlet depth factor as a function of flow conditions at the nozzle and the depth of the subcritical stream as follows,...

$$\psi = \left[\phi^2 (S+1)^2 - 2F_{0*}^2 + \frac{2F_{0*}^2}{\phi (S+1)}\right]^{0.5} \qquad (46)$$

As with the similarity between equation (37) and the classic Belanger equation, equation (46) is identical to that developed by Rajaratnam for submerged open channel jumps, with the densimetric Froude number replacing the traditional Froude ratio.

The energy loss in a submerged internal jump can be calculated in a manner similar to that employed in the calculation of the energy loss in a free internal jump. Referring once again to Figure 8, the specific energy at section 3 can be expressed as,...

$$E_3 = g\Delta\rho\, y_3 + \frac{1}{2}\rho U_0^2 \qquad (47)$$

Or recalling that $\psi=(y_3/y_0)$, equation (47) can be written as,...

$$E_3' = \psi + \frac{1}{2} F_{0*}^2 \qquad (48)$$

The specific energy of a fluid particle at the density interface of section 4 will be,...

$$E_4 = g\Delta\rho\, y_4 + \frac{1}{2}\rho U_4^2 \qquad (49)$$

As with the free jump, we can express the energy loss in a submerged jump relative to the inlet energy with the following expression,...

$$\frac{\Delta E}{E_3'} = \frac{E_3 - E_4}{E_3'} = \frac{[\phi - \phi\,(S + 1] + \frac{1}{2} F_{0*}^2 [1 - 1/\phi^2\,(S + 1)^2]}{\phi + \frac{1}{2} F_{0*}^2} \qquad (50)$$

2.4 THE SLOPING INTERNAL JUMP

It appears that the problem of predicting the sequent depth of a free internal jump forming on a sloping bed has not been previously investigated. As with the sloping open channel jump, a momentum analysis of a sloping internal jump is complicated by the additional horizontal component of force exerted by the sloping floor on the control volume used in the global analysis. Solution of this problem would require an analytic expression relating the length and shape of the jump to the upstream conditions. Unfortunately, such an expression has not yet been developed. However, it was felt that sloping internal jumps could be analysed in the same semi-empirical manner as sloping open channel jumps, and further, that the empirical coefficients derived from open channel experiments could be employed in the analysis of sloping internal jumps. As before, the integral form of the momentum equation will be developed before going to the control volume analysis. Our definition sketch will be as in Figure 9.

Our Reynolds equations will be,...

$$u \frac{\partial u}{\partial x} + v \frac{\partial u}{\partial y} = - \frac{1}{\rho} \frac{\partial p}{\partial x} + g \sin\alpha + \nu \nabla^2 u - \left(\frac{\partial \overline{u'^2}}{\partial x} + \frac{\partial \overline{u'v'}}{\partial y}\right) \qquad (51)$$

$$u \frac{\partial v}{\partial x} + v \frac{\partial v}{\partial y} = - \frac{1}{\rho} \frac{\partial p}{\partial y} - g \cos\alpha + \nu \nabla^2 v - \left(\frac{\partial \overline{u'v'}}{\partial x} + \frac{\partial \overline{v'^2}}{\partial y}\right) \qquad (52)$$

$$\frac{\partial u}{\partial x} + \frac{\partial v}{\partial y} = 0 \qquad (20)$$

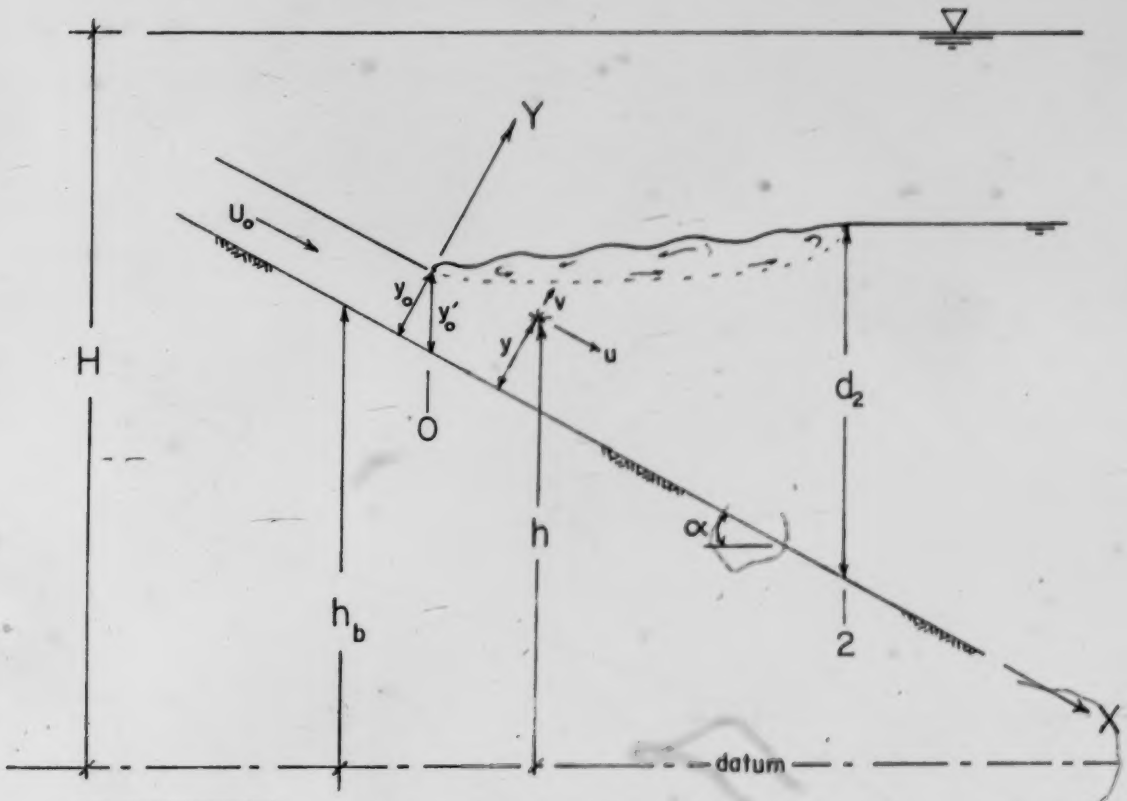

FIGURE 9 — THE SLOPING INTERNAL JUMP

By using an order of magnitude analysis and the integrated form of equation (52) we can write,...

$$u \frac{\partial u}{\partial x} + v \frac{\partial u}{\partial y} = - \frac{1}{\rho} \frac{\partial p}{\partial x} + g \sin\alpha + \frac{1}{\rho} \frac{\partial \tau}{\partial y}$$

where τ is the total shear stress, as before. If we now define the following terms,...

$$h - h_b = \frac{y}{\cos\alpha}$$

$$\frac{\partial h_b}{\partial x} = - \sin\alpha$$

$$\rho = \rho_a + \Delta\rho$$

$$p = g\rho_a (H - h) + \Delta p$$

then, in a manner similar to that used in the discussion of general stratified flow we can develop the expression,...

$$u \frac{\partial u}{\partial x} + v \frac{\partial u}{\partial y} = - \frac{1}{\rho} \frac{\partial \Delta p_*}{\partial x} + \frac{1}{\rho} \frac{\partial \tau}{\partial y}$$

Now, if we integrate this expression from the channel bed (y=0) to the light-dense interface ($y=\bar{y}$) and assume that no ambient fluid is entrained we will get,...

$$\frac{d}{dx} \int_0^{\bar{y}} (\Delta p + \rho u^2) \, dy = g \Delta \rho \, \bar{y} \sin\alpha - (\tau_0 - \tau_i) \qquad (53)$$

Even if the shear stresses on the bed and interface are ignored, equation (53) is essentially insoluble since $\bar{y}$ is an unknown function of x and the parameter defining the limits of integration in equation (53), the jump length, is not initially known. Therefore, we will conduct an analysis of the horizontal momentum in the same manner as Kindsvater (1944) and Rajaratnam (1966,1967). The pressure and momentum influx at section 0 in Figure 9 will be,...

$$\Delta P_0 + M_0 = \frac{\Delta \rho g \, y_0^2}{2 \cos^2\alpha} + \rho U_0^2 \cos\alpha \qquad (54)$$

and the pressure and momentum efflux at section 2 will be,...

$$\Delta P_2 + M_2 = \frac{1}{2} \Delta \rho g \, d_2^2 + \frac{\rho U_0^2 \, y_0^2}{d_2} \qquad (55)$$

The deviatoric pressure component of the floor on the body of the jump can be expressed empirically as,...

$$\Delta P = 2K \left(\Delta\rho g \, d_2^2/2 - \Delta\rho g \, y_0^2/2 \cos^2\alpha\right) \tan\alpha \qquad (56)$$

where K is an empirical parameter and the form of the above expression has been chosen to facilitate algebraic operations. If we say that the change in momentum from section 0 to section 2 is equal to the sum of the horizontal pressure forces acting on the control volume, then equations (54) to (56) will combine to yield,...

$$\frac{d_2}{y_0/\cos\alpha} = \frac{1}{2}\left[\sqrt{1 + 8\, G_{0*}^2} - 1\right] \qquad (57)$$

where, following Rajaratnam (1966), the following terms are defined:

$$G_{0*}^2 = \Gamma_0^2 \, F_{0*}^2 \qquad (58)$$

$$\Gamma_0^2 = \frac{\cos^3\alpha}{1 - 2K\tan\alpha} \qquad (59)$$

$$\log_{10}\Gamma_0 = 0.027\alpha \qquad (13)$$

and the densimetric Froude number F_{o_*} of the supercritical flow is as previously defined. The conjecture in this analysis is that the parameter Γ_o is a function only of bed slope α, and that this function is of the same form as that derived for dynamically similar open channel jumps (equation (13)).

The energy loss expression for sloping internal jumps can be derived in a manner similar to that employed in the derivation of energy loss expressions for the ordinary and submerged internal jumps. The specific energy at section 0 in Figure 9 (relative to the bed level at section 2) will be,...

$$E_0 = (L_{SLJ} \tan\alpha + y_0/\cos\alpha)\ g\Delta\rho + \frac{1}{2}\rho U_0^2$$

which, for simplicity can be approximated as,...

$$E_0 \simeq (L_{SLJ} \tan\alpha + y_0)\ g\Delta\rho + \frac{1}{2}\rho U_0^2$$

The energy at section 2 can be written as,...

$$E_2 = g\Delta\rho\ d_2 + \rho U_0^2\ y_0^2/2\ d_2^2$$

The energy loss relative to the inlet energy can subsequently be written as,...

$$\frac{E_0 - E_2}{E_0} = \frac{\Delta E}{E_0} = \frac{\left[(1 - d_2/y_0) + \frac{1}{2} F_{0*}^2\ (1 - (d_2/y_0)^2) + L_{SLJ} \tan\alpha/y_0\right]}{\left[1 + \frac{1}{2} F_{0*}^2 + L_{SLJ} \tan\alpha/y_0\right]} \quad (60)$$

3. PART THREE: EXPERIMENTS

3.1 INTRODUCTION

All experiments for this study were performed in the T. Blench Graduate Hydraulics Laboratory at the University of Alberta. The density difference between the two fluid layers was created by using hot and cold water as the lighter and denser fluids, respectively. The following is a general discussion of the apparatus and procedures used in the investigation. A schematic representation of the experimental setup appears in Figure 10.

3.2 APPARATUS

3.2.1 Flume

All experiments were performed in a glass-walled flume 5.50 m long, 0.310 m wide and 0.50 m deep. The slope of the flume was adjustable but was kept level throughout the investigation.

A metal undershot gate with a streamlined efflux nozzle separated the cold water reservoir from the hot water field downstream. The gate was insulated with closed-cell plastic foam to inhibit the transfer of heat across it. The gate opening could be manually adjusted but with poor precision. In order to accurately fix the gate opening, metal plates of known thickness would be inserted below the gate and the gate adjusted until the bottom fitted snugly against the

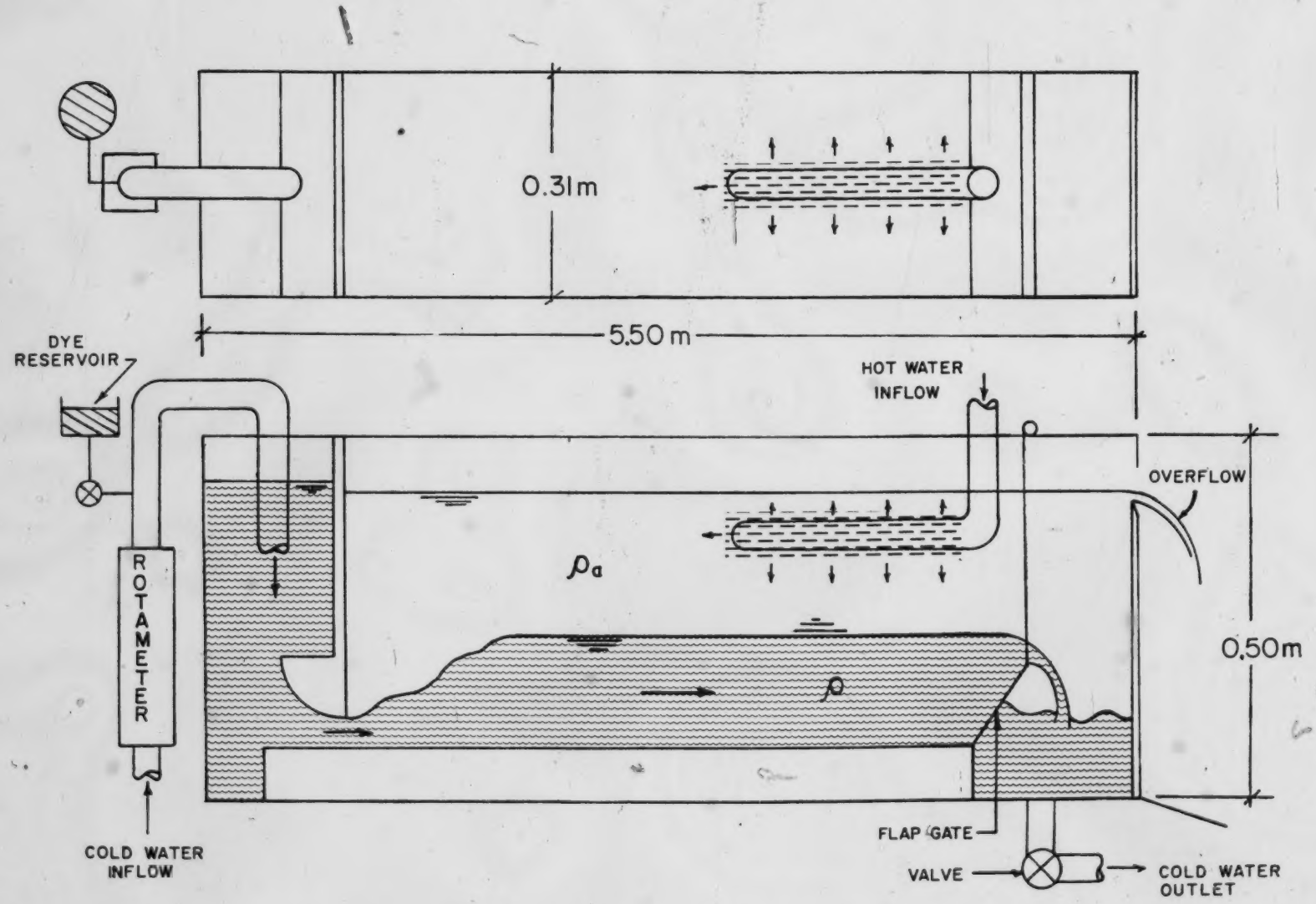

FIGURE 10 – SCHEMATIC DIAGRAM OF TEST APPARATUS

plates. These metal spacer plates would then be carefully removed and the gate would be sealed.

To facilitate the outflow of the cold water at the downstream end of the flume, an adjustable valve was installed in the bed of the flume. Total water levels in the flume were regulated by an overflow section at the downstream end. The depth of the flowing cold water layer was regulated by an adjustable metal flap gate located just upstream of the outlet valve.

3.2.2 Cold Water Supply

Cold water was conveyed under city water pressure to a constant head overflow tank located about 3 m above the flume. From the constant head tank, the water flowed through a flexible rubber hose to a rotameter which measured the discharge. From the rotameter, water travelled through another hose to the cold water reservoir of the flume.

Since the accuracy of the rotameter readings can be affected by the temperature of the water due to the associated fluid viscosity variation, the rotameter was calibrated using cold water at what was felt to be a temperature representative of conditions for the entire range of experiments. The resulting calibration chart appears in Figure 11.

FIGURE 11
ROTAMETER CALIBRATION CHART
T=7.0°C

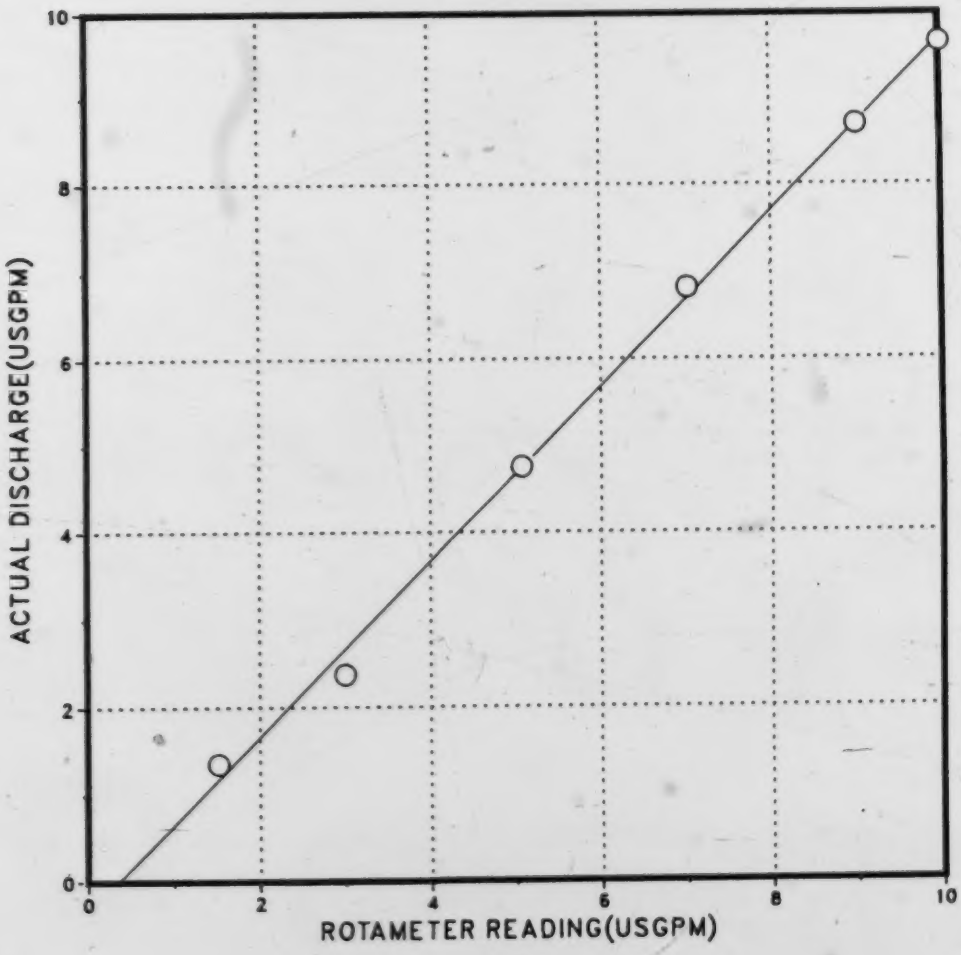

3.2.3 Hot Water Supply

The temperature of the hot water ambient field was held constant by continually recharging it with heated water. The source of the hot water was city water passed through a Delta Hot Water Blast Cleaning System rated at 900,000 Btu.

From the heater, the hot water was conveyed to the flume by a rubber hose and was discharged through a diffuser suspended at the downstream end of the flume. The discharge rate was small such that any circulation induced in the ambient field by this recharge was negligible. It is known that the temperature of the hot water supply varied, the amount of variation increasing with temperature. That the temperature variations caused by the hot water supply were damped by the large volume of the ambient field was evident in the consistency of the ambient temperature readings for each run.

3.2.4 Thermometer

The thermometer used in this study was a Fluke 2180 RTD digital thermometer. Accuracy of the readings was checked against a mercury thermometer and the instrument was found to be accurate to within a tenth of a degree celsuis.

3.2.5 Photographic Equipment

Photographs of the steady flow situation were taken with a Pentax 35 mm camera using Kodak ASA 100 film. The setup was illuminated for the photographs by two ColorTran

arc lamps rated at 650 Watts each.

3.2.6 Modifications

The foregoing was a general description of the apparatus employed in the study. Minor alterations were made to the general setup to facilitate the various jump configurations studied. The following is a brief description of these modifications.

3.2.6.1 Free Internal Jump

It was found that channel friction and the imprecise outflow control did not allow for the formation of free jumps except at relatively high densimetric Froude numbers. To correct this, a false plywood floor approximately 4.5 m long was installed in the bed of the flume (see Figure 10). With the addition of this false floor, a much wider range of tailwater depths could be achieved.

3.2.6.2 Sloping Internal Jump

A sloping bed was constructed by placing sheets of plywood at predetermined slopes below the gate separating the cold water reservoir and the hot water field.

3.3 EXPERIMENTAL PROCEDURE

The general procedure was basically the same for all experiments. The flume was initially filled with hot water of a given temperature. The cold water discharge which would result in a specific densimetric Froude number at the outlet was calculated using an assumed cold water temperature. Cold water was introduced to the cold water reservoir at the specified rate and the outlet valve was adjusted until the water levels in the flume and reservoir remained constant. The setup was then allowed to run until a distinct cold water layer was flowing at the bottom of the flume with the efflux section submerged by the flow downstream such that entrainment of the hot water did not occur. The cold water inflow and outflow were then adjusted to the desired rate and the depth of the flowing cold water layer downstream of the gate was manipulated by adjusting the flap gate until the desired flow configuration was achieved.

For the free and sloping jumps, the "tailwater level" of the cold water flow was adjusted until the jump formed as close to the gate as possible without submergence (usually within one centimetre). Under such conditions, it was assumed that entrainment of ambient fluid prior to jump formation would be negligible.

For the submerged jumps, the depth of the flowing cold water layer was adjusted to create a number of levels of submergence for each densimetric Froude number.

Once the desired state had been achieved, the average temperature of the ambient fluid was determined by averaging temperature readings from four locations immediately downstream of the gate separating the cold and hot water reservoirs. The temperature of the cold water was taken as the average of two readings taken in the cold water reservoir upstream of the gate. For the free and sloping jumps, four readings were taken in the flowing cold water layer downstream of the jump, as well.

Injection of small slugs of dye into the ambient field indicated that the underflow induced little or no motion in the ambient, and therefore, that the experiments simulated denser underflow in a semi-infinite ambient field. Careful injection of dye into the surface roller of each jump helped to visually determine the location of the end of the roller. This location was marked on the glass wall of the flume with tape. Dye injection was also used to verify, to some extent, the assumption that little or no entrainment was occurring in the jump.

Once the salient parameters had been recorded, a neutral dye was introduced to the cold water flow from a small reservoir which tapped into the cold water supply line (see Figure 10). After the dye had colored the flowing cold water layer, a number of photographs were taken of the jump. Care was taken to position the camera at the same level as the hot/cold interface downstream of the jump so that the depth of the denser layer would not be distorted by

parralax. A set of orthogonal scales were affixed to the glass walls of the flume so that each photograph would have its own reference scale. The depth of the downstream flow, length of the jump and jump profile were recorded as the average of measurements taken from each print.

Plates 1 to 6 are typical dye photographs for each of the jump types studied and plate 7 shows the flap gate used to adjust the depth of the flowing cold water layer.

It is worth noting that the setup and procedure described in the preceding text produced a remarkably stable stratified flow which could be run for a number of hours without degenerating into a gradually or multiply stratified system.

PLATE 1:Free Internal Jump $F_* \simeq 4.0$

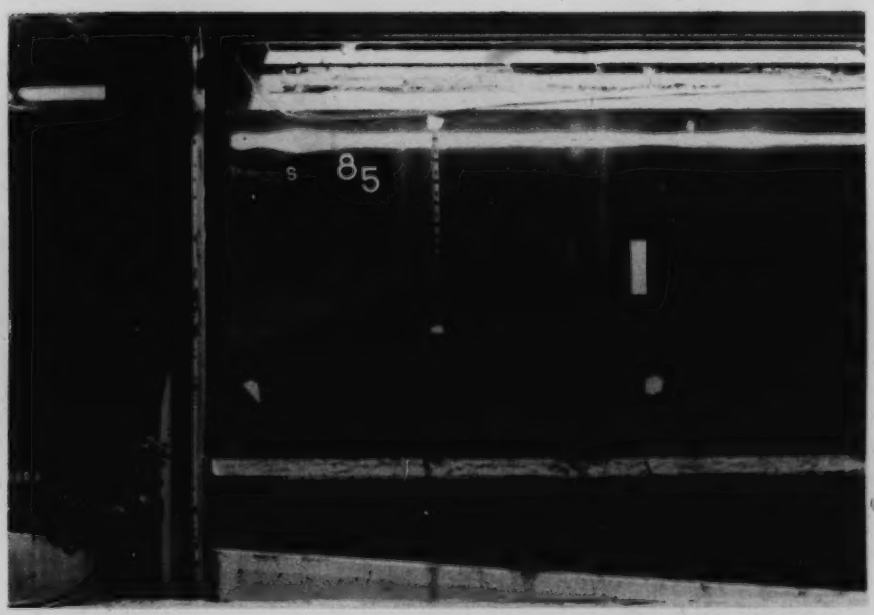

PLATE 2:Free Internal Jump $F_* \simeq 7.9$

PLATE 3:Submerged Internal Jump $F_* \simeq 3.8$, $S \simeq 0.80$

PLATE 4:Submerged Internal Jump $F_* \simeq 11.4$, $S \simeq 0.92$

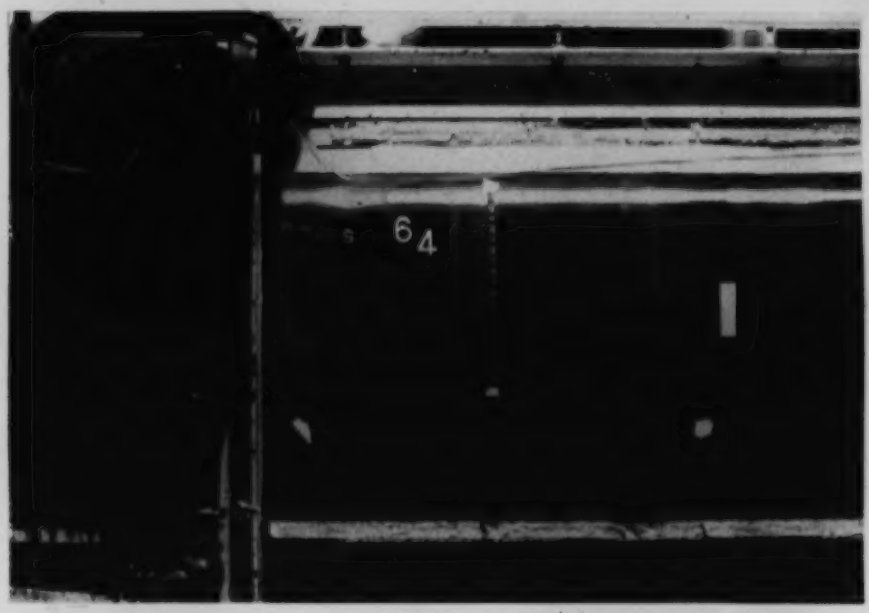

PLATE 5:Sloping Internal Jump $F_* \simeq 6.1$, $\alpha = 3.10$ deg.

PLATE 6:Sloping Internal Jump $F_* \simeq 4.4$, $\alpha = 5.71$ deg.

PLATE 7:Downstream depth control.

4. PART FOUR:ANALYSIS AND DISCUSSION OF RESULTS

4.1 THE FREE INTERNAL JUMP

Figures 12 through 14 are dimensionless plots of the profiles of the free denser internal jumps studied in the laboratory, and Table A1 of Appendix A lists the pertinent data associated with each test run.

The applicability of the Belanger-type relation (equation (37)) previously developed was investigated by plotting the measured sequent depth ratio (y_2/y_1) against the prediction from equation (37) as shown in Figure 15. The same data plotted against the densimetric Froude number at the efflux nozzle results in the plot of Figure 16. These two plots suggest that equation (37) tends to consistently underestimate the downstream depth required to form a stable jump at the nozzle, the amount of discrepancy increasing with the modified Froude number. This departure from theory can be explained, to some extent, by discussing some observations made during the course of the study.

As previously discussed in the section outlining experimental procedures, the free internal jump was formed by adjusting the downstream depth of the flowing cold water layer until it could be visually determined that the jump was forming just at the gate. Visual location of the jump was achieved by injecting dye into the flowing cold water layer and viewing the resulting situation both from the side and from above. By viewing the flow from above, it was

FIGURE 12
NONDIMENSIONAL PROFILES OF FREE INTERNAL JUMP
y_0=0.007 m

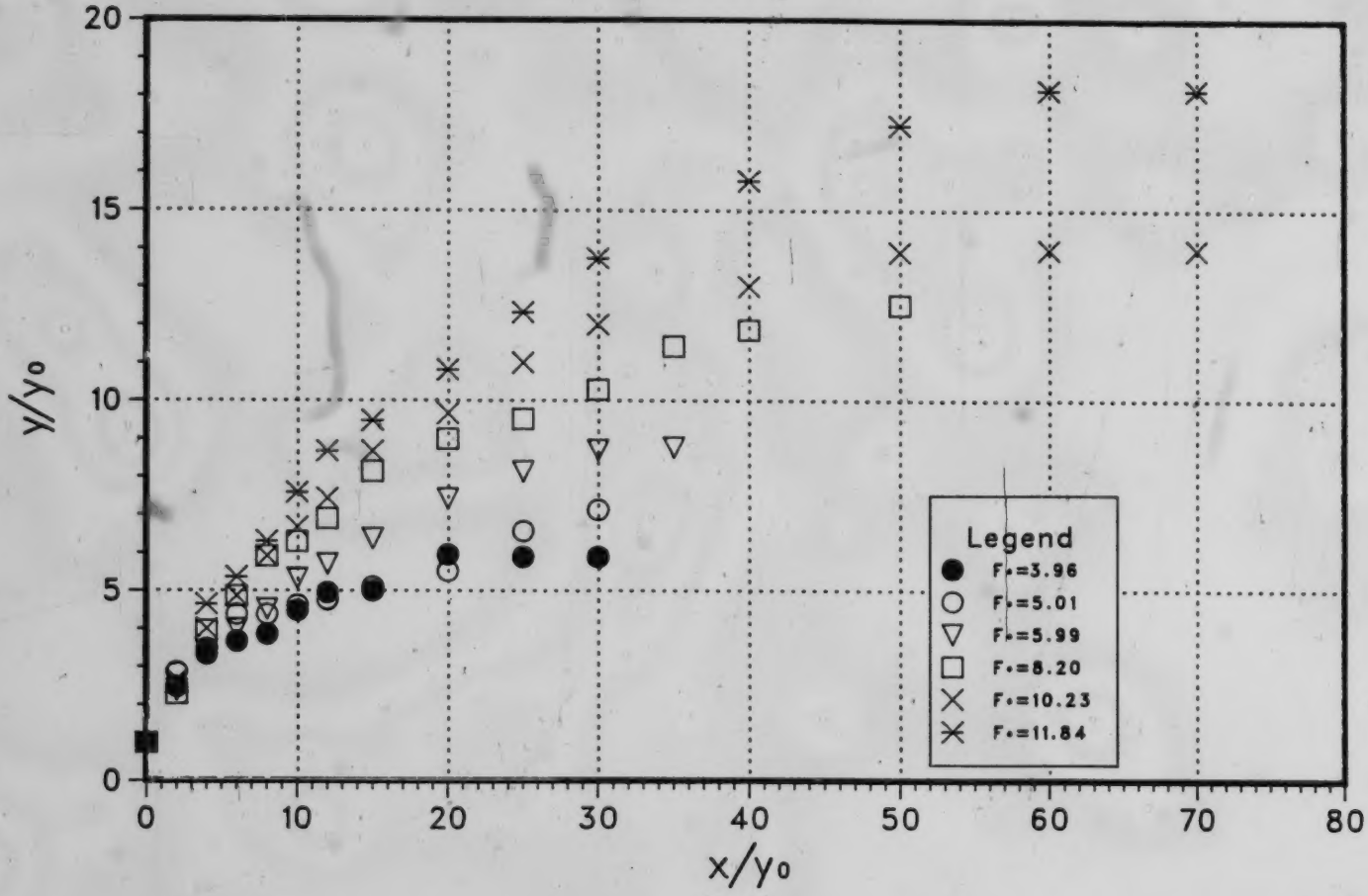

FIGURE 13
NONDIMENSIONAL PROFILES OF FREE INTERNAL JUMP
y_0=0.012 m

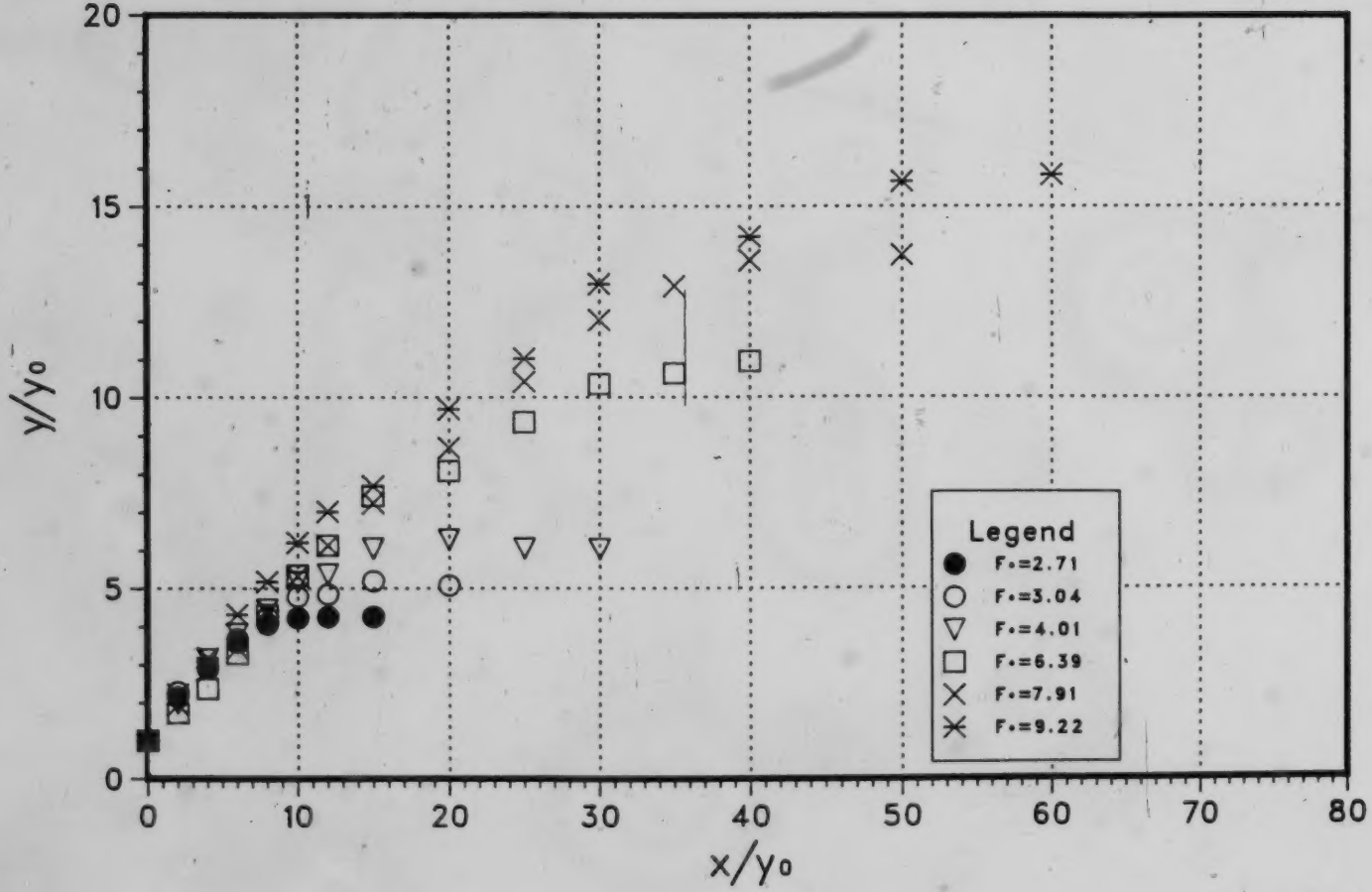

FIGURE 14
NONDIMENSIONAL PROFILES OF FREE INTERNAL JUMP
y_0=0.0195 m

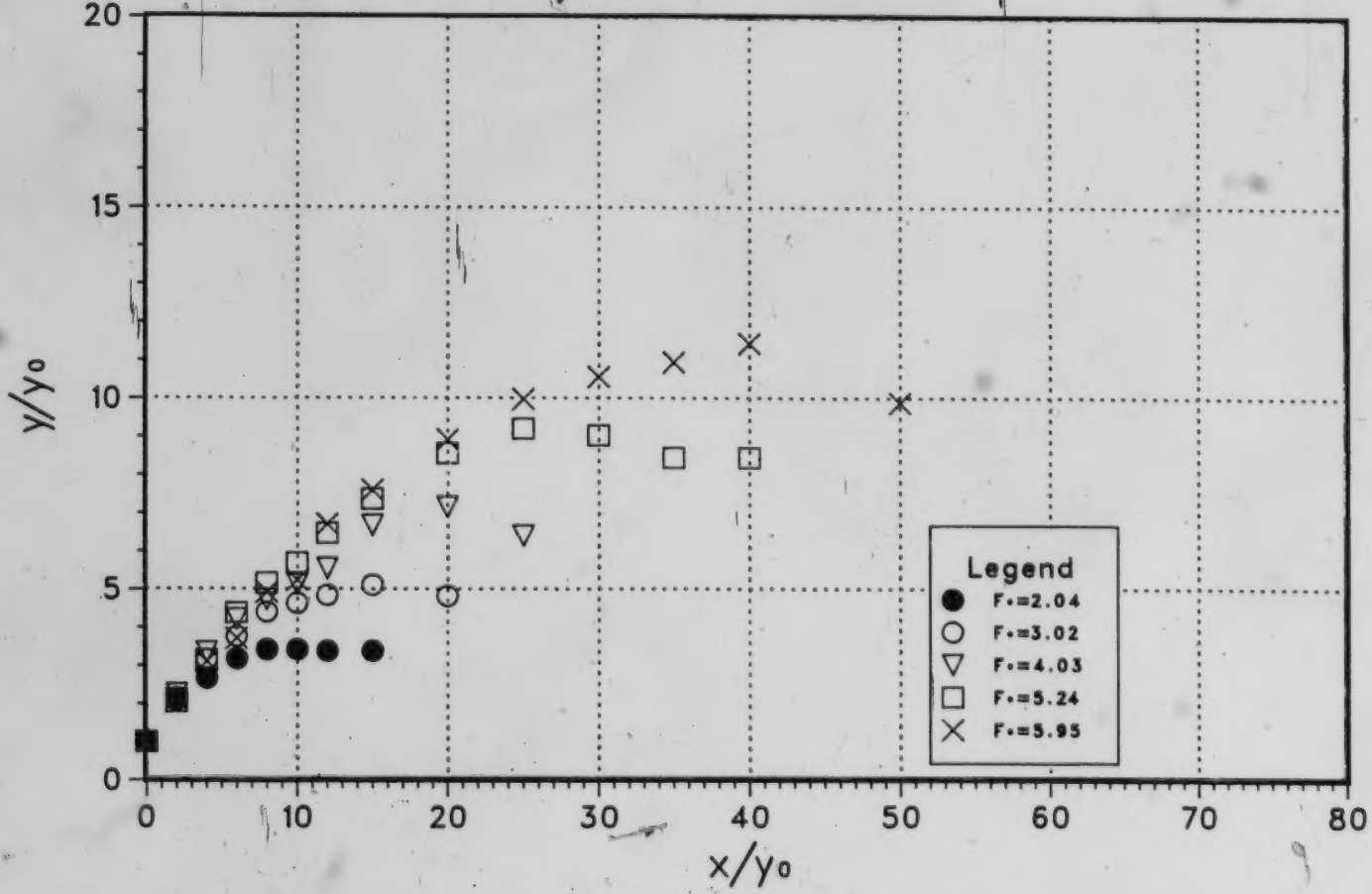

FIGURE 15
ORDINARY FREE INTERNAL JUMP
THEORETICAL VS. EXPERIMENTAL SEQUENT DEPTH RATIO

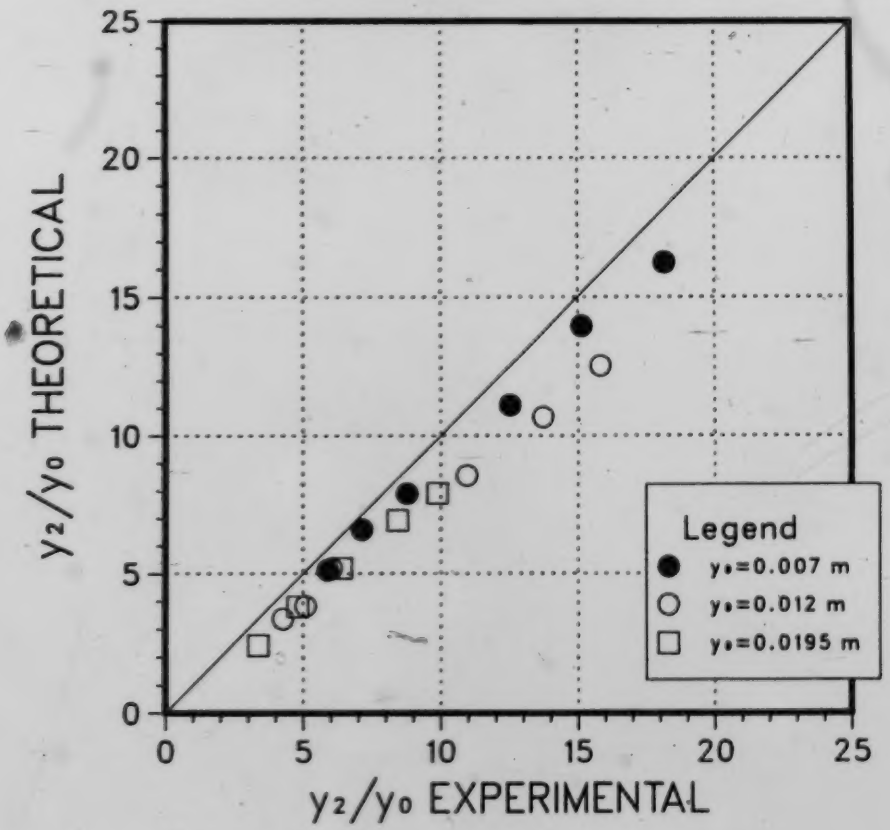

FIGURE 16
ORDINARY FREE INTERNAL JUMP
SEQUENT DEPTH RATIO VS. DENSIMETRIC FROUDE NUMBER

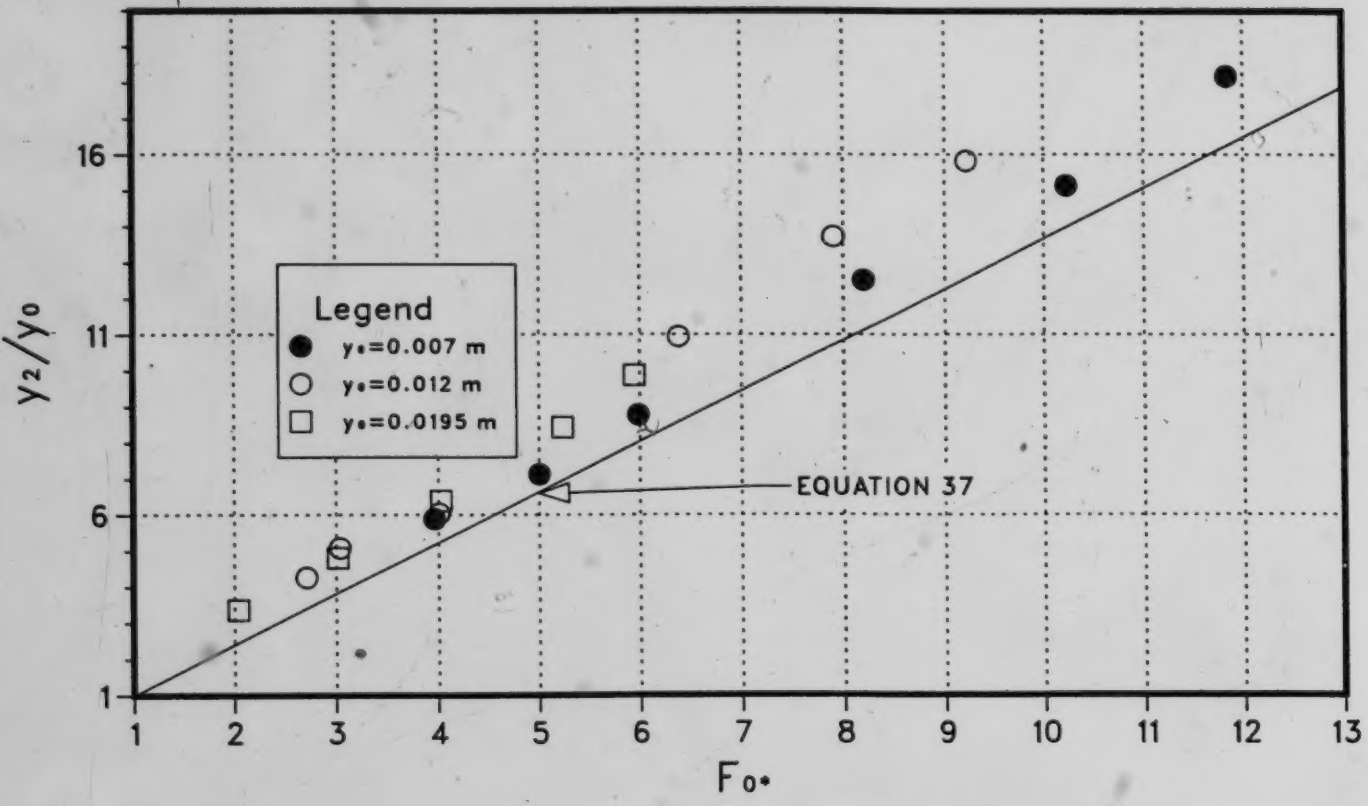

observed that the velocity distribution in the supercritical stream was not uniform across the channel but had a shape as shown in the following sketch:

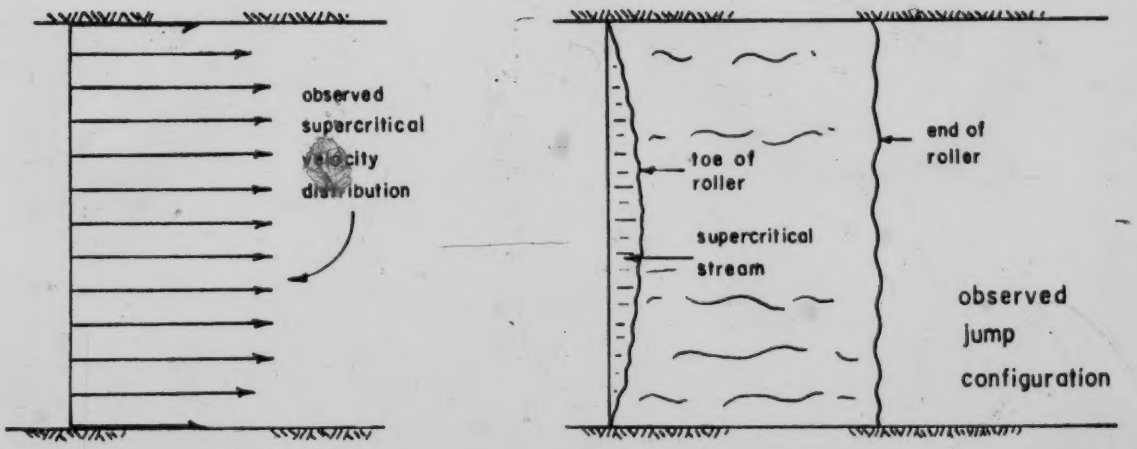

FIGURE 17 - PLAN VIEW OF FREE INTERNAL JUMP

It was also noted that the degree of non-uniformity increased with the outlet densimetric Froude number. Because the velocity was unevenly distributed across the channel, the toe of the roller was similarly pushed further downstream in mid-channel than at the edges. When locating the jump, an attempt was made to position the toe of the roller as near to the gate as possible across the entire channel width so as to reduce entrainment by the free jet. It can be seen that if the toe of the roller was forced to

form just at the gate in mid-channel, the jump would would be slightly submerged at the edges, and the associated downstream depth would be slightly greater than that required to form the jump at the gate if the supercritical velocity distribution was uniform across the channel.

Another possible reason for the observed departure from theory is that the assumption of no entrainment may not have been satisfied. It can be quite safely assumed that the amount of ambient fluid entrained by the roller region of the jump is negligible; any entrainment in this region seems to arise due to the breaking of waves at the density interface rather than from turbulent entrainment across the interface (Chu and Vanvari (1975)). However, observations by Baddour and Abbink (1983) and by the author suggest that the borderline between drowned and free jumps is not sharply defined, with the jump alternating between the two states if observed over time. As such the jet region, or supercritical stream, would be periodically "exposed" and allowed to entrain some ambient fluid. It was observed that this "unsteadiness" (at least in terms of small time scales) occurred as pulsations or bursts and that it increased with densimetric Froude number. This would seem consistent with results obtained by Chu and Vanvari which showed the turbulence intensity increasing in the same manner. It should also be noted that at least a small portion of the supercritical stream was always "exposed" in mid-channel, with the degree of exposure increasing with Froude number,

as previously mentioned.

An interesting feature related to the idea that entrainment of ambient fluid may have caused measured values to depart from theory can be discussed using Figure 16. While measured values of the sequent depth ratio are always greater then their theoretical counterparts, the amount of discrepancy between theory and experiment begins to increase at Froude numbers between about 3 and 5. Studies by Ellison and Turner (1959) and Chu and Vanvari (1975) suggest that the turbulent entrainment coefficient for a free denser jet goes from a maximum at a Richardson number of 0 ($F_{o_*}=\infty$) to almost zero at Richardson numbers between about 0.2 and 0.8 ($1.11 \leq F_{o_*} \leq 2.23$). Therefore, at lower Froude numbers between, say 1 and 3, it would be expected that the amount of entrainment of ambient fluid would be minimal even if the jet was somewhat exposed. If the data from the present study is taken to be "correct", however, it would seem that even for flows of low Froude number some entrainment is occurring prior to the formation of the jump. A study by Macagno and Macagno (1975) suggests that, at least for hydraulic jumps in stratified flows, another mechanism for entrainment may exist in addition to turbulent entrainment and interfacial entrapment by breaking waves. A certain amount of viscous drag occurs between the flowing denser layer and the "stagnant" ambient resulting in a thin layer of the ambient fluid being dragged along by the flowing layer. It is thought that at the toe of the jump where the reverse flow

in the roller is "turned under" by the impinging supercritical jet, a certain amount of the ambient fluid is also "dragged" into the jump as in the following sketch:

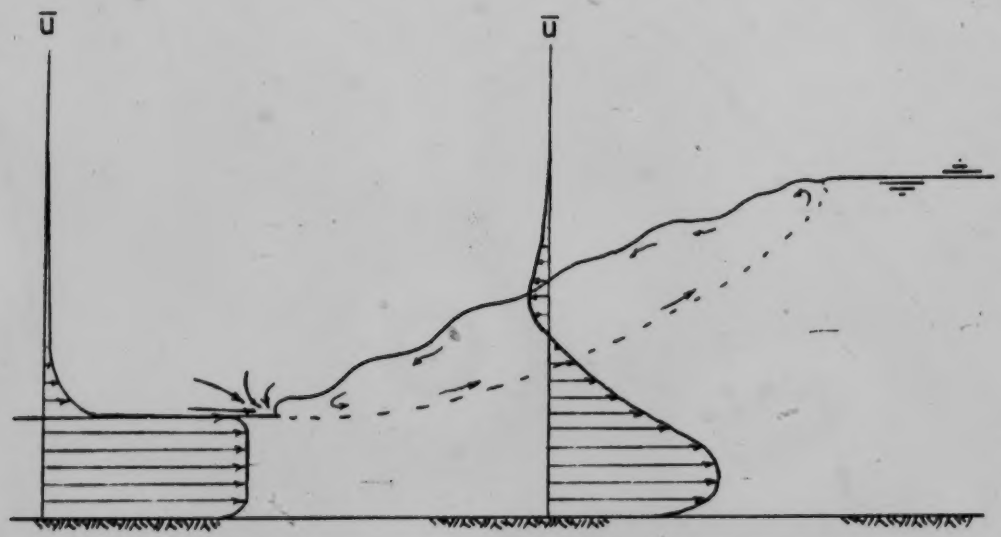

FIGURE 18 - ENTRAINMENT AT TOE OF JUMP

The methods employed in the present study as well as the present state of knowledge regarding the entrainment phenomena unfortunately preclude any definitive conclusions about entrainment to be made from the analysis of the present data.

As with open channel jumps, internal jumps increase in length as the densimetric Froude number increases. Defining the length of the of the jump is a controversial issue, but most investigators tend to define the end of the jump as the

section where the water surface (or density interface) first becomes level or where the mean surface (interface) elevation is a maximum. In the present study, it was felt that picking such a subjective point off of a photograph of relatively small scale would be so imprecise as to negate any value. In fact, an attempt was made to include jump length as part of the study but the data were widely scattered.

However, it was found that another length scale characteristic of the jump could be fixed with much greater accuracy. As previously described in the section describing experimental procedure, the end of the surface roller was visually located by carefully injecting dye into the flow and marking on the glass wall of the flume the mean location where the flow reached the density interface and reversed. The distance from the efflux nozzle to this point was termed the roller length L_{RJ} and a non-dimensional form of this quantity as measured is plotted against the outlet densimetric Froude number F_{o_*} for each experiment in Figure 19. Also appearing in Figure 19 is a curve describing the same relationship for open channel jumps from Rajaratnam (1967). The arrangement of the present data more closely resembles a curve presented by Rajaratnam in the same paper citing Rouse (1959) as the source.

It was found that the roller length could also be used to normalize the jump profiles. It was thought that if the jump length was a characteristic lateral dimension, the

FIGURE 19
ORDINARY FREE INTERNAL JUMP
ROLLER LENGTH VS. DENSIMETRIC FROUDE NUMBER

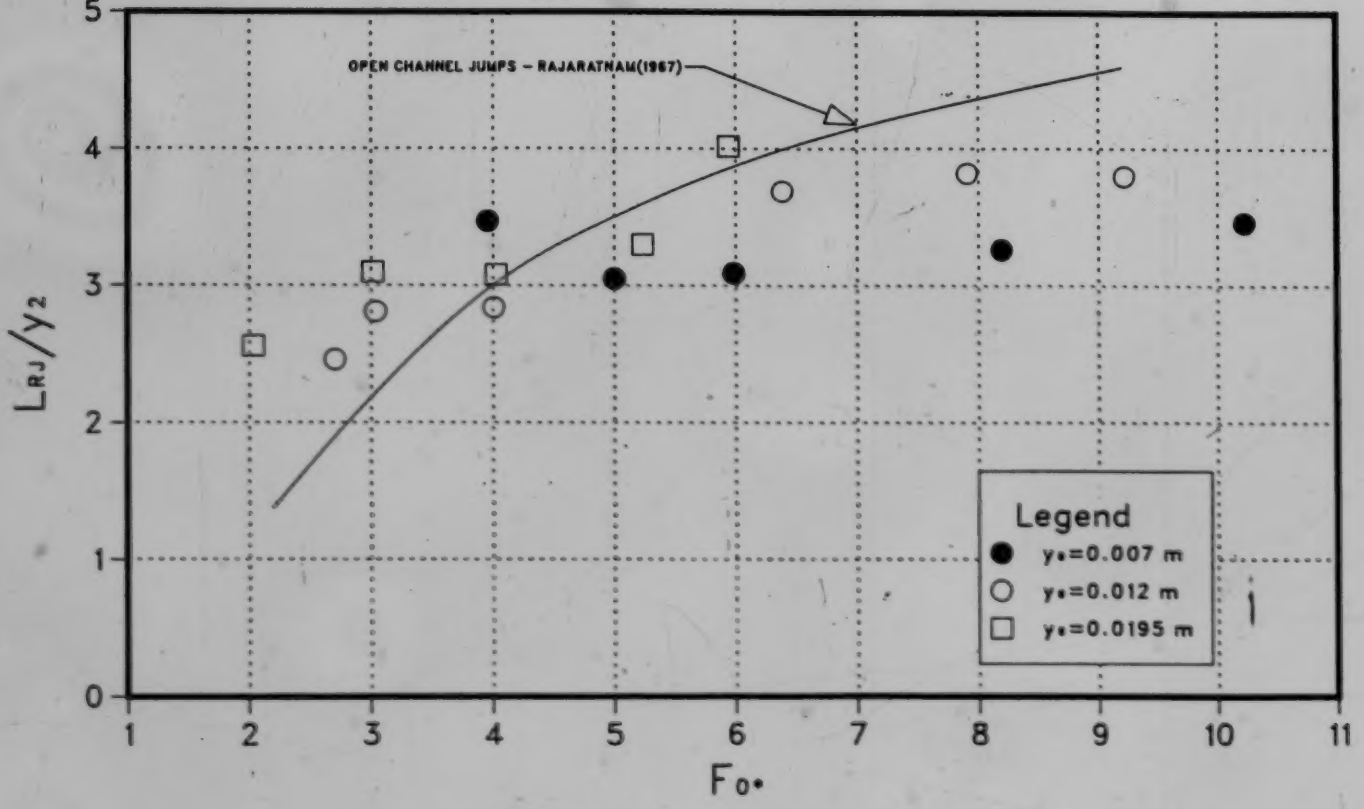

height of the jump at the crest of the roller (y_{LJ}) would be a corresponding characteristic vertical dimension. Figure 20 is a plot of the non-dimensional height of the density interface above the nozzle ($(y-y_o)/(y_{LRJ}-y_o)$) versus the non-dimensional distance from the nozzle (x/L_{RJ}) for all runs. The form is similar to the profile for open channel jumps (Rajaratnam and Subramanya (1968)).

The validity of the energy loss expression for the free internal jump (equation (39)) was checked by plotting the non-dimensional energy loss calculated using measured values of ϕ in equation (39) versus the same quantity determined using calculated values of ϕ. The result was the plot of Figure 21 which shows that the actual energy loss incurred in the jump is slightly less than that predicted by equation (39) using theoretical values of ϕ. This is consistent with the observed behavior of ϕ illustrated by Figures 15 and 16.

4.2 THE SUBMERGED INTERNAL JUMP

Dimensionless plots of the submerged denser internal jumps studied were plotted and appear in Figures 22 through 30. Table A2 in Appendix A lists the pertinent data associated with each test run.

The validity of equation (46) developed previously was checked by plotting the inlet depth factor as measured against the same quantity calculated using measured values of the depth of the denser layer downstream of the jump and densimetric Froude number (Figure 31). It was found that

FIGURE 20
ORDINARY FREE INTERNAL JUMP
NORMALIZED JUMP PROFILES

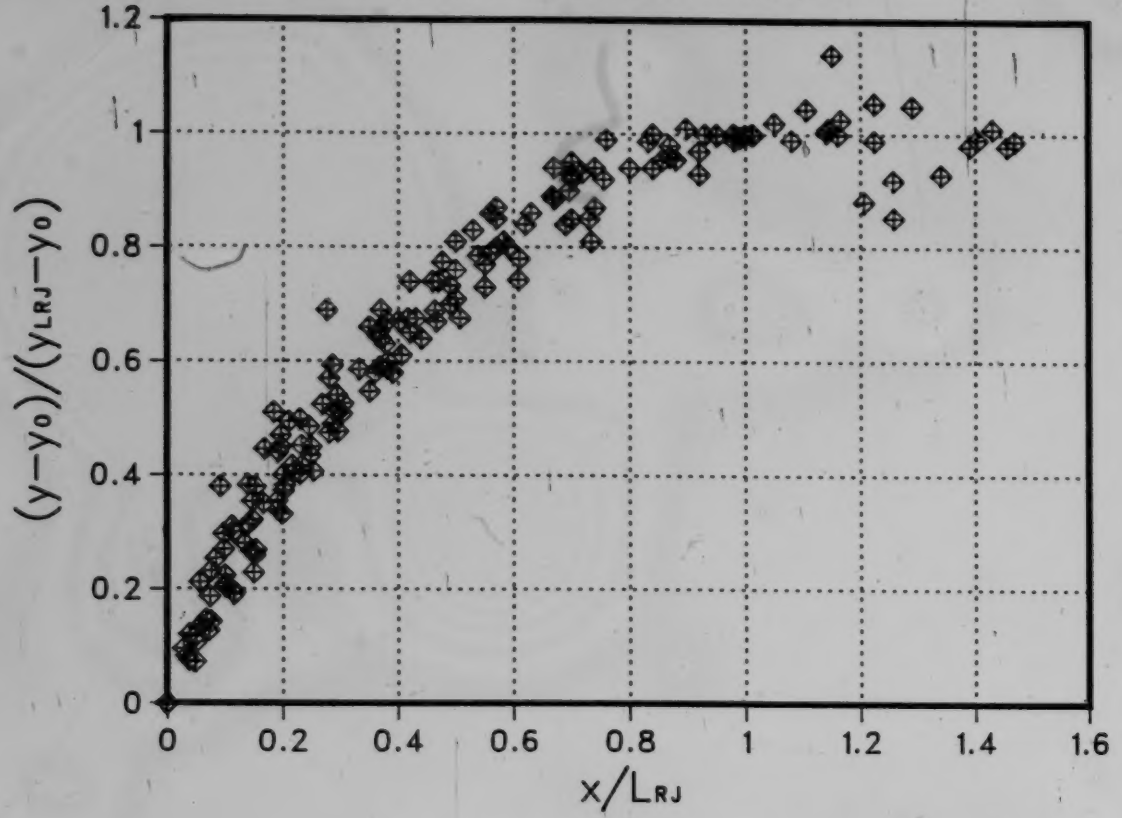

FIGURE 21
ORDINARY FREE INTERNAL JUMP
NONDIMENSIONAL ENERGY LOSS IN JUMP
THEORETICAL VS. EXPERIMENTAL

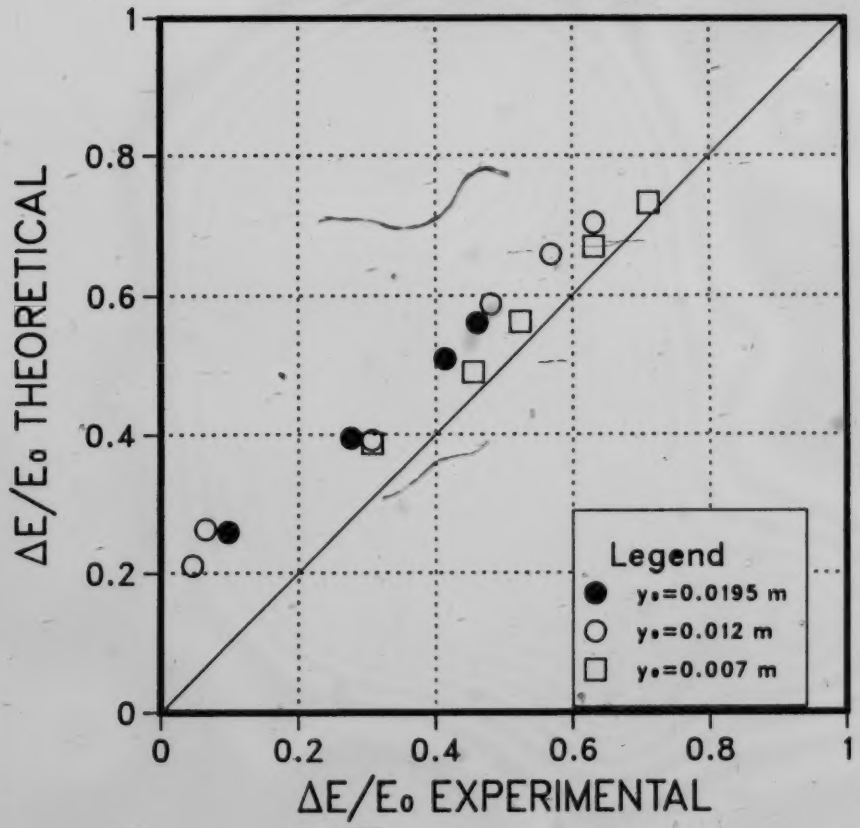

FIGURE 22
NONDIMENSIONAL PROFILES OF
SUBMERGED INTERNAL JUMPS
y_o=0.007 m

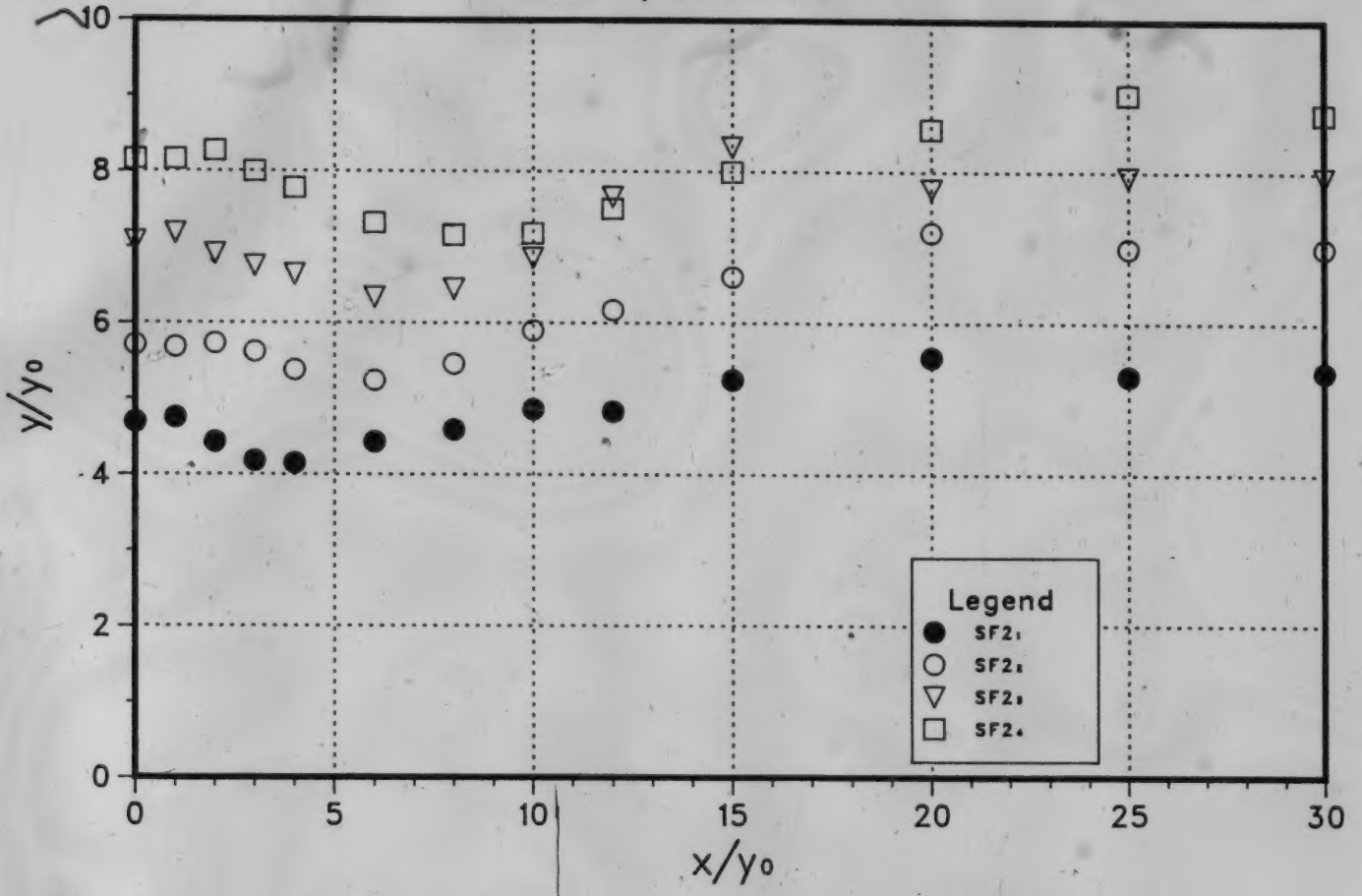

FIGURE 23
NONDIMENSIONAL PROFILES OF
SUBMERGED INTERNAL JUMPS
y_0=0.007 m

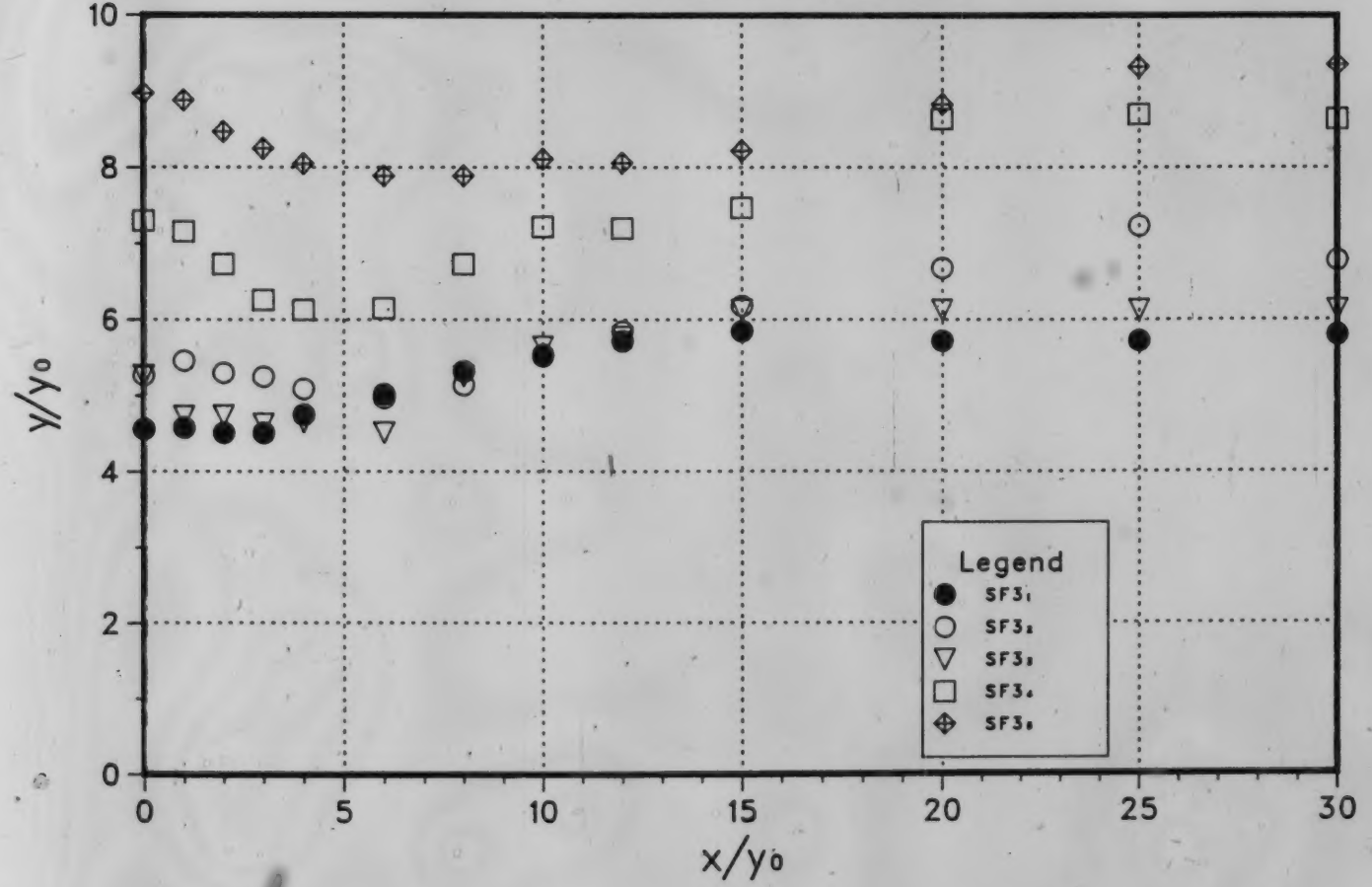

FIGURE 24
NONDIMENSIONAL PROFILES OF
SUBMERGED INTERNAL JUMPS
y_0=0.007 m

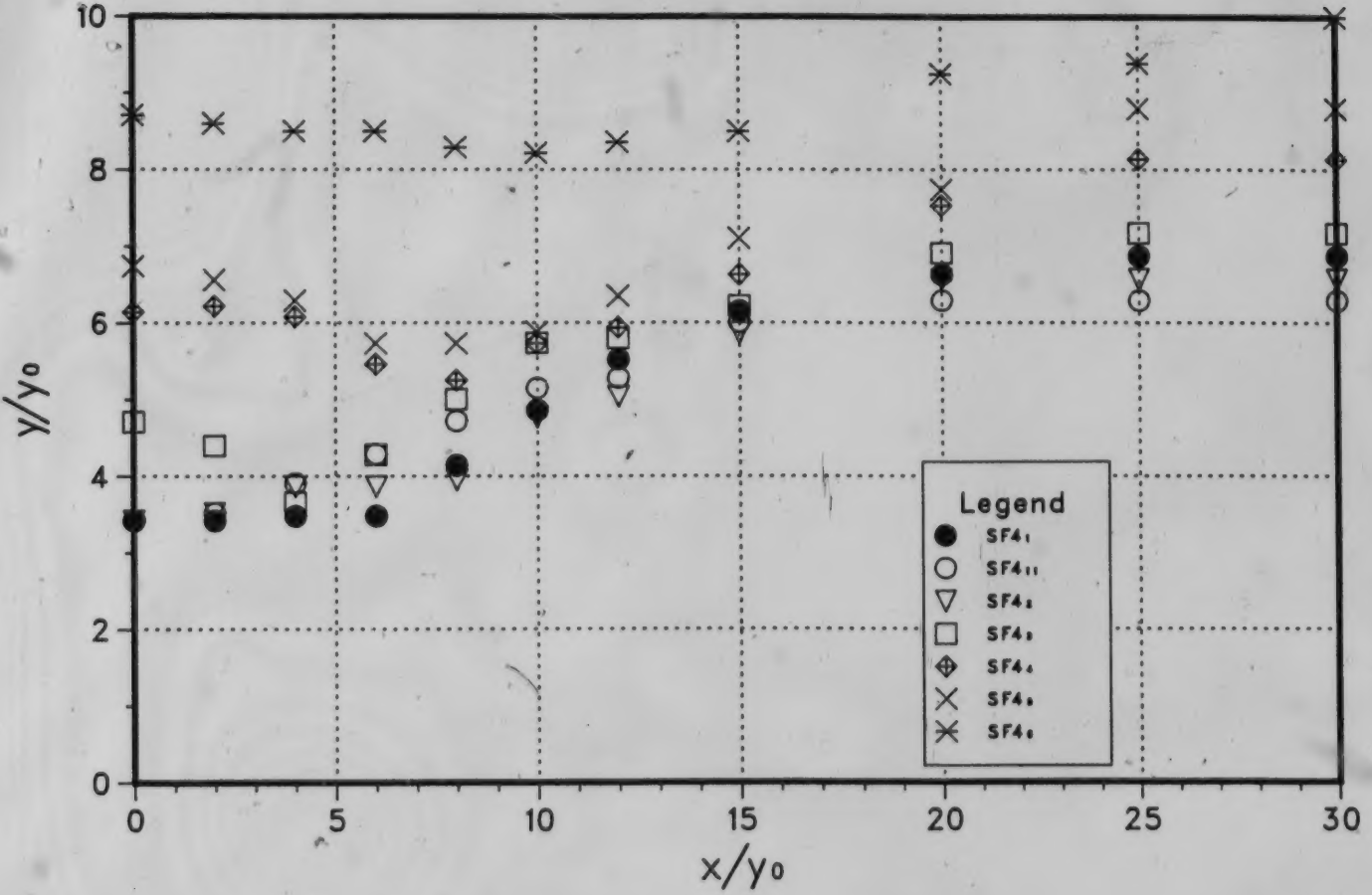

FIGURE 25
NONDIMENSIONAL PROFILES OF
SUBMERGED INTERNAL JUMPS
y_o=0.007 m

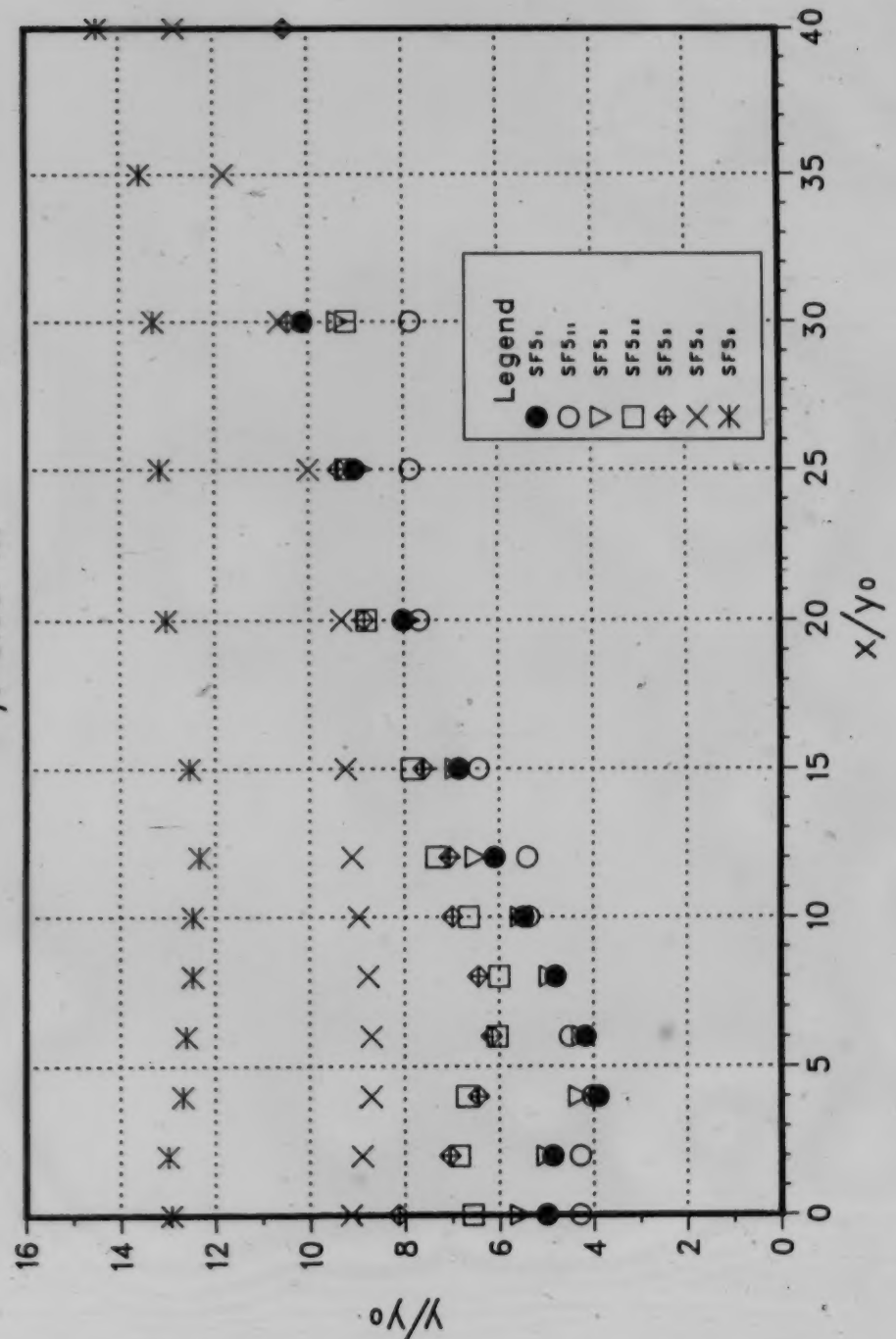

FIGURE 26
NONDIMENSIONAL PROFILES OF
SUBMERGED INTERNAL JUMPS
y_o=0.007 m

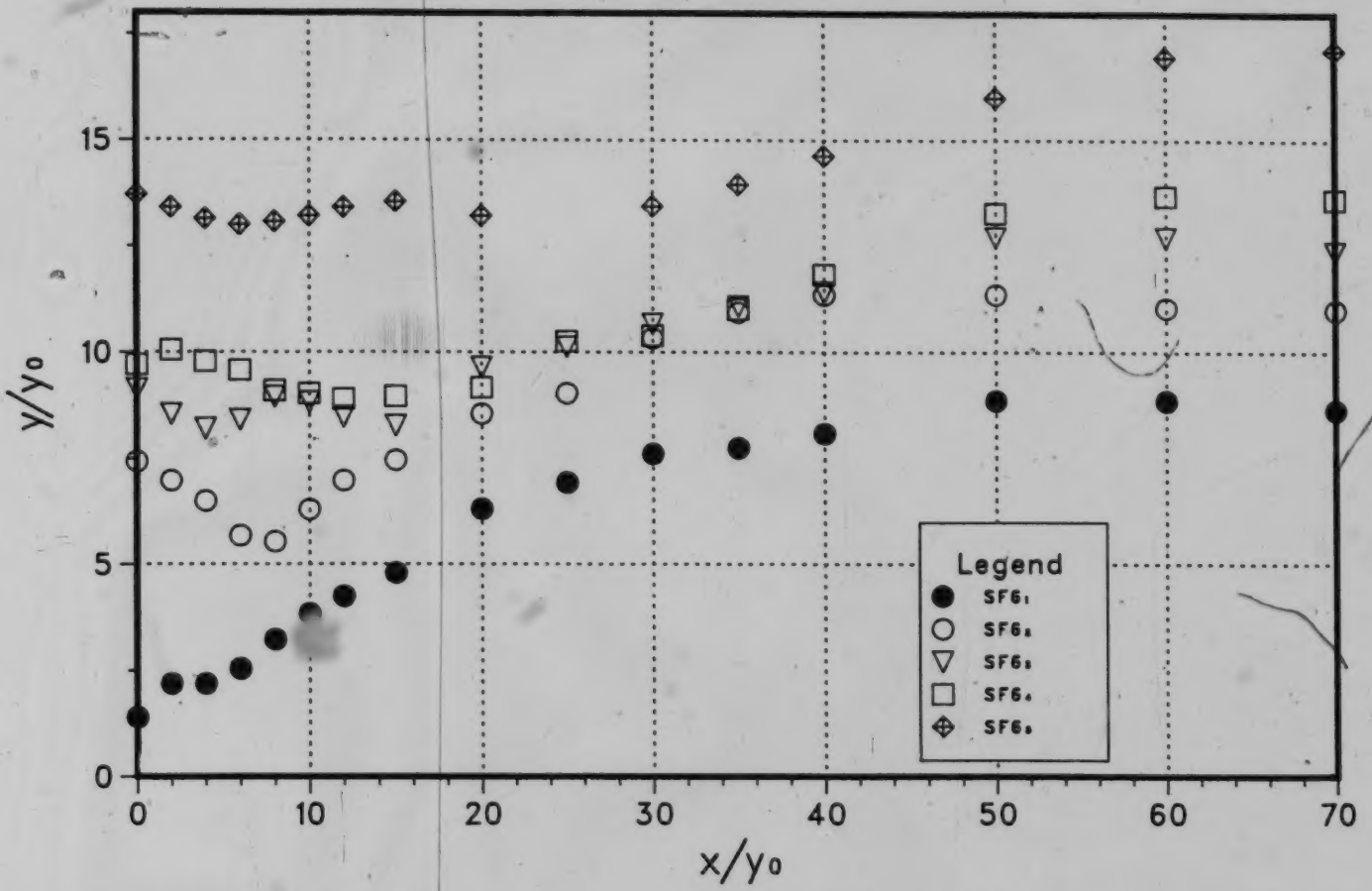

FIGURE 27
NONDIMENSIONAL PROFILES OF
SUBMERGED INTERNAL JUMPS
y_o=0.007 m

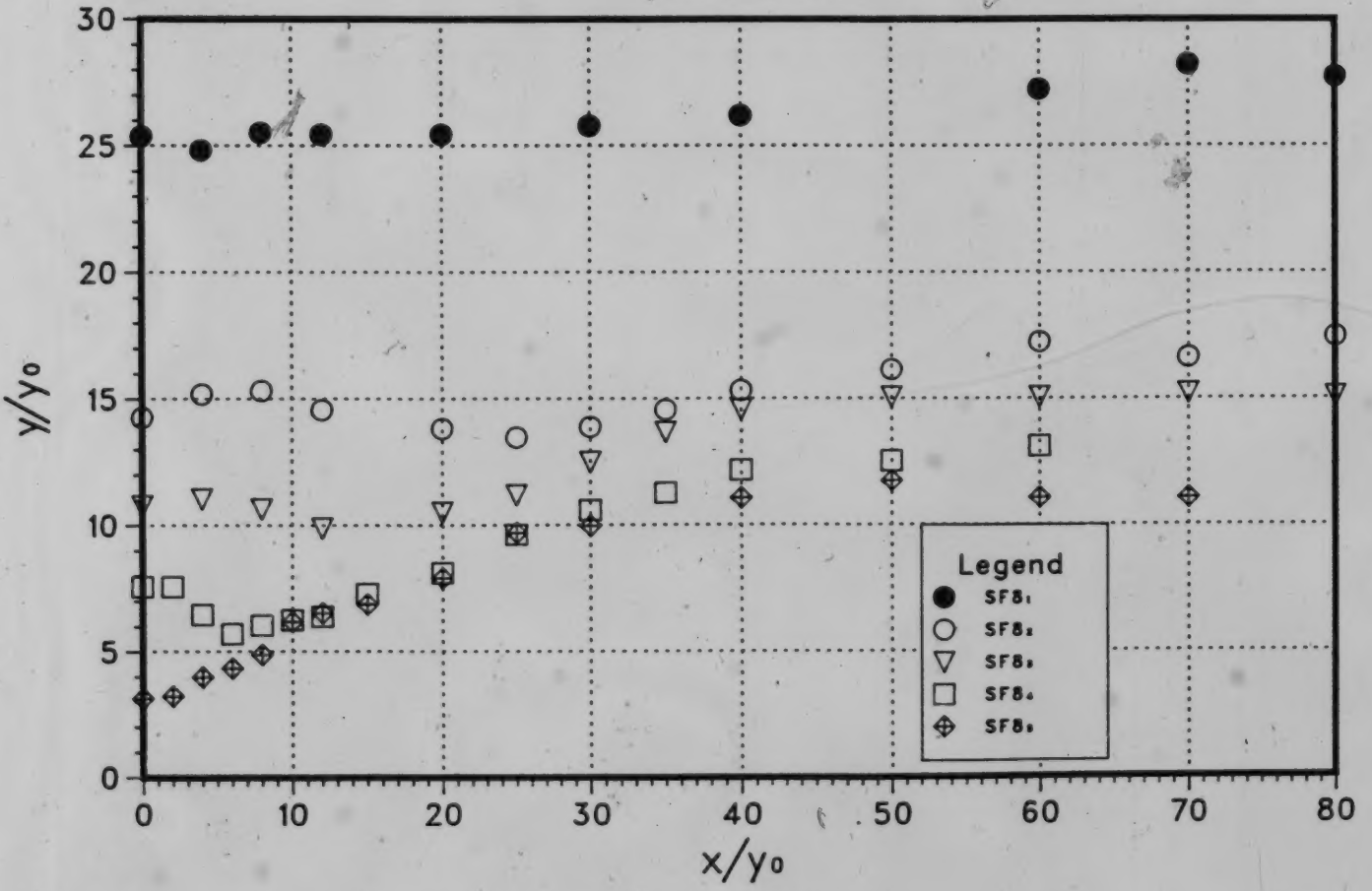

FIGURE 28
NONDIMENSIONAL PROFILES OF
SUBMERGED INTERNAL JUMPS
y_o=0.007 m

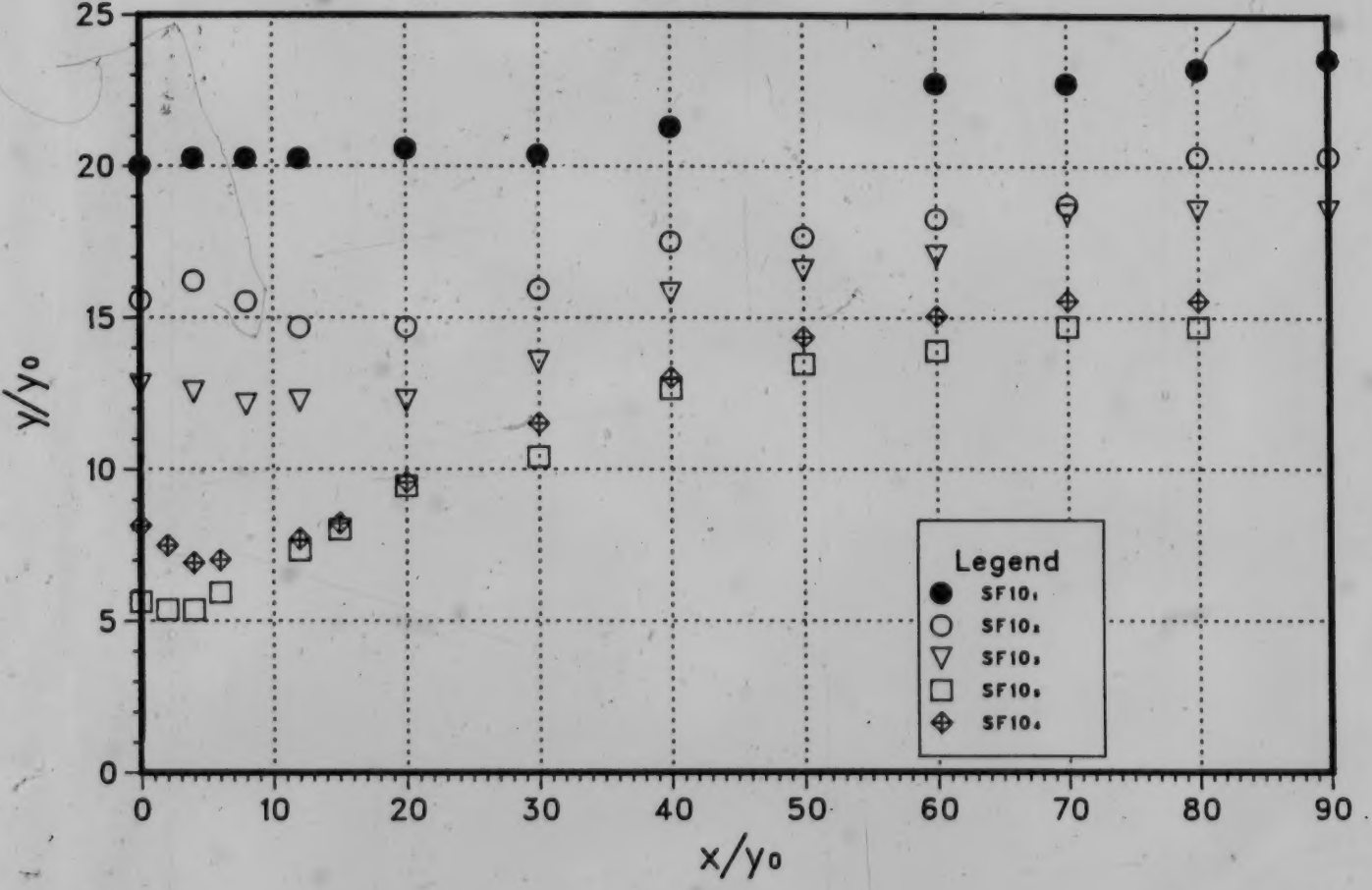

FIGURE 29
NONDIMENSIONAL PROFILES OF
SUBMERGED INTERNAL JUMPS
y_o=0.007 m

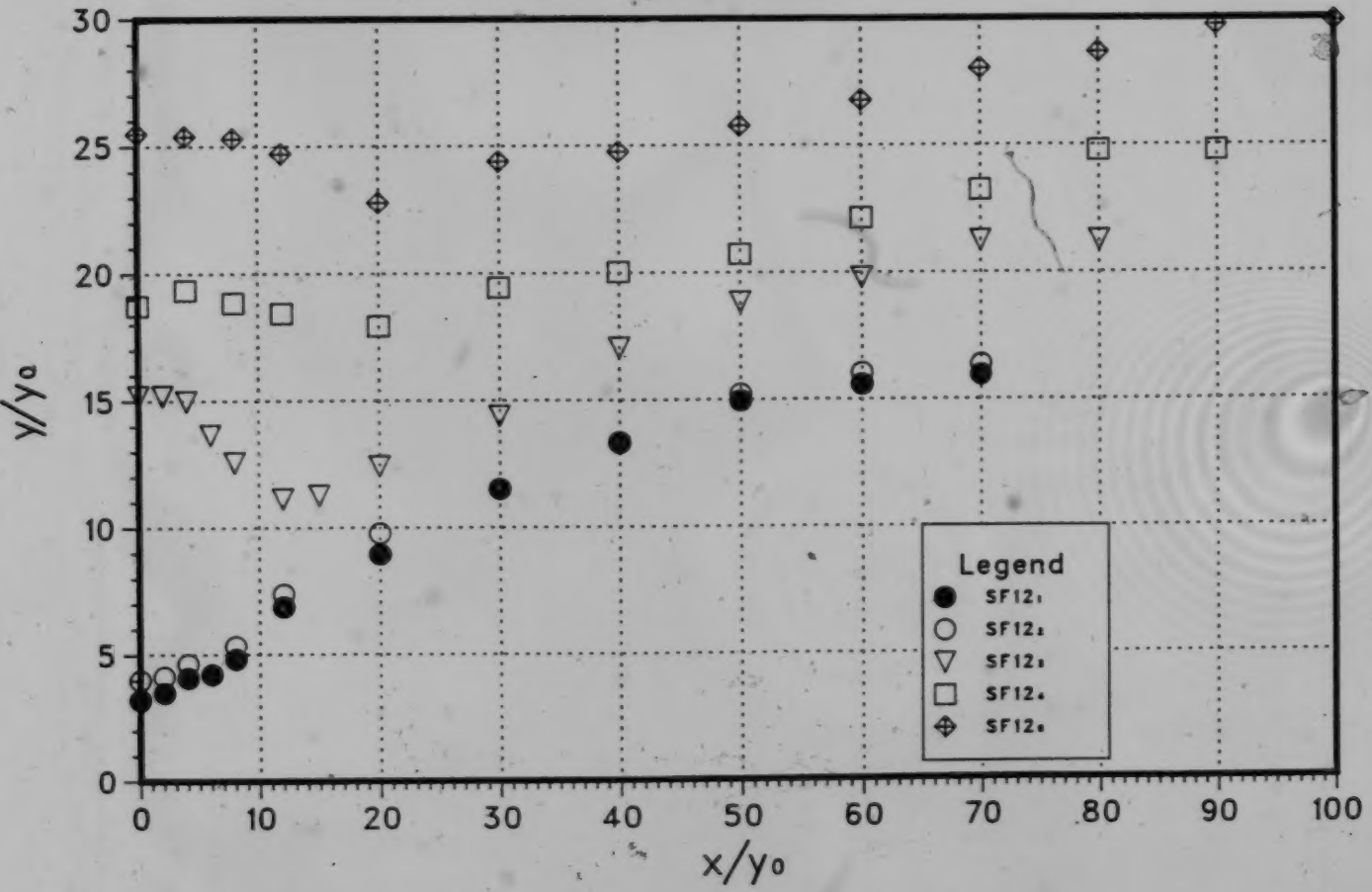

FIGURE 30
NONDIMENSIONAL PROFILES OF
SUBMERGED INTERNAL JUMPS
y_o=0.007 m

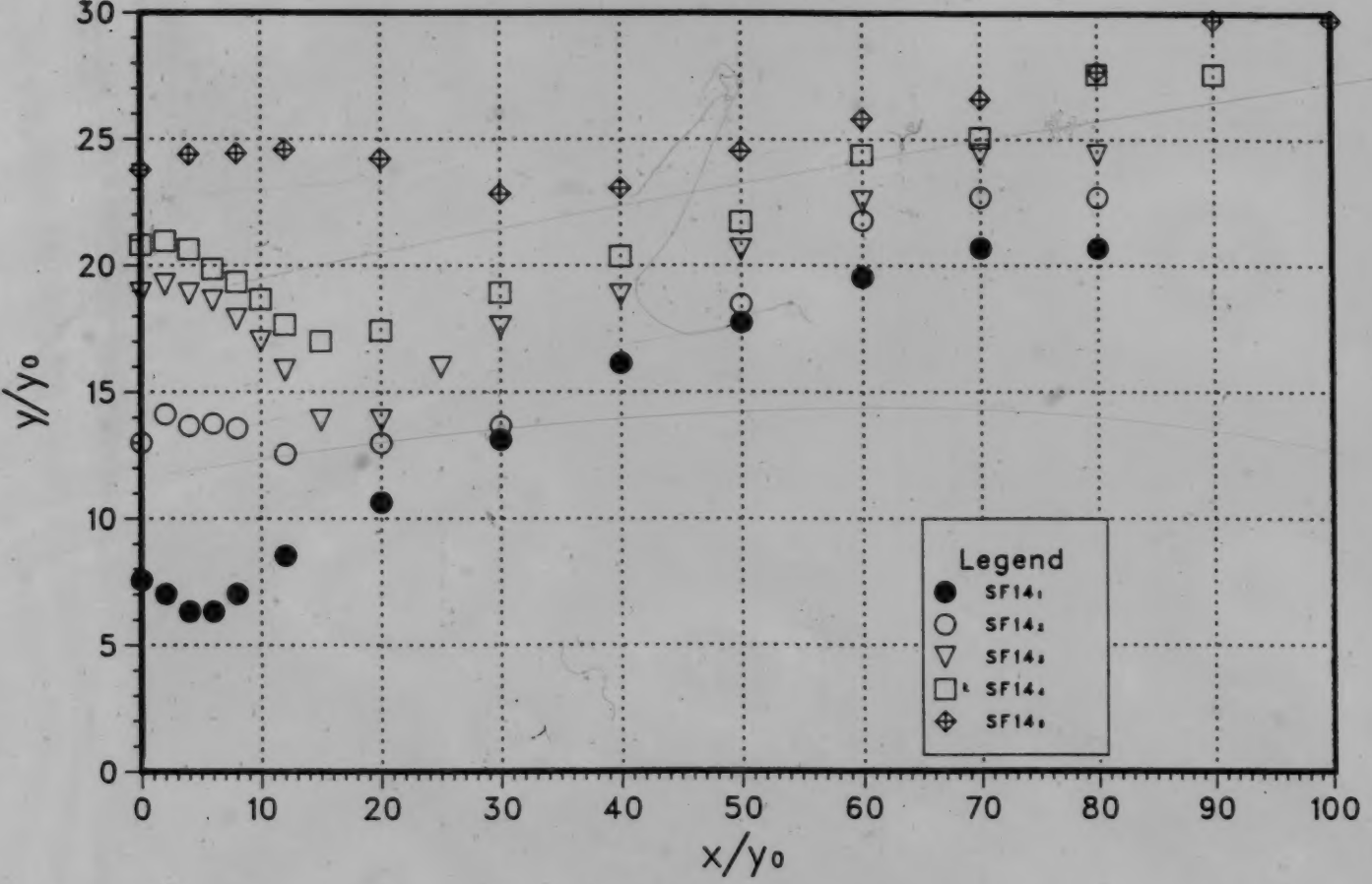

FIGURE 31
SUBMERGED INTERNAL JUMP
EXPERIMENTAL VS. THEORETICAL INLET DEPTH FACTOR – φ

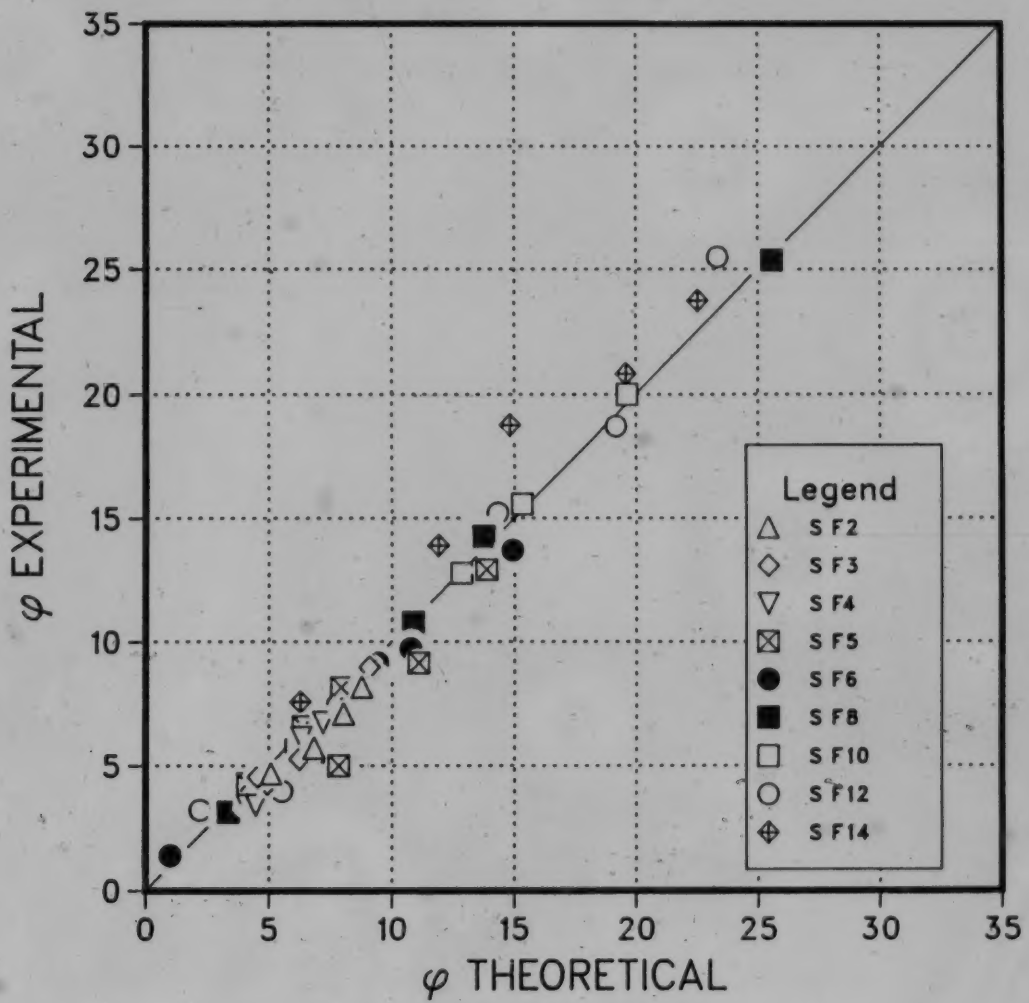

equation (46) provided a fairly accurate prediction of conditions as measured in the experiments.

The expression for energy loss in a submerged internal jump (equation (49)) was checked for validity in the same manner and the results appear in Figure 32. The agreement between equation (49) and the experimental data was also found to be quite good.

Measurements of the length of the roller in the submerged internal jump were made using the same method described in the discussion of the free internal jump. Figure 33 shows how the length of the roller increases with the level of submergence and the following empirical relation was derived from the data:

$$L_{RSJ}/y_2 = 2.70S + 2.94 \qquad (61)$$

It was found that measurements of the length of the submerged internal jump yielded much more consistent results than similar attempts to measure the length of the free internal jump, probably due to the highly stable nature of the submerged jump. Figure 34 shows how the length of the submerged internal jump varies with submergence in a manner similar to the submerged open channel jump. The following empirical relation provides a reasonably good fit to the data:

$$L_{SJ}/y_2 = 2.79S + 3.77 \qquad (62)$$

FIGURE 32
SUBMERGED INTERNAL JUMP
EXPERIMENTAL VS. THEORETICAL NONDIMENSIONAL ENERGY LOSS

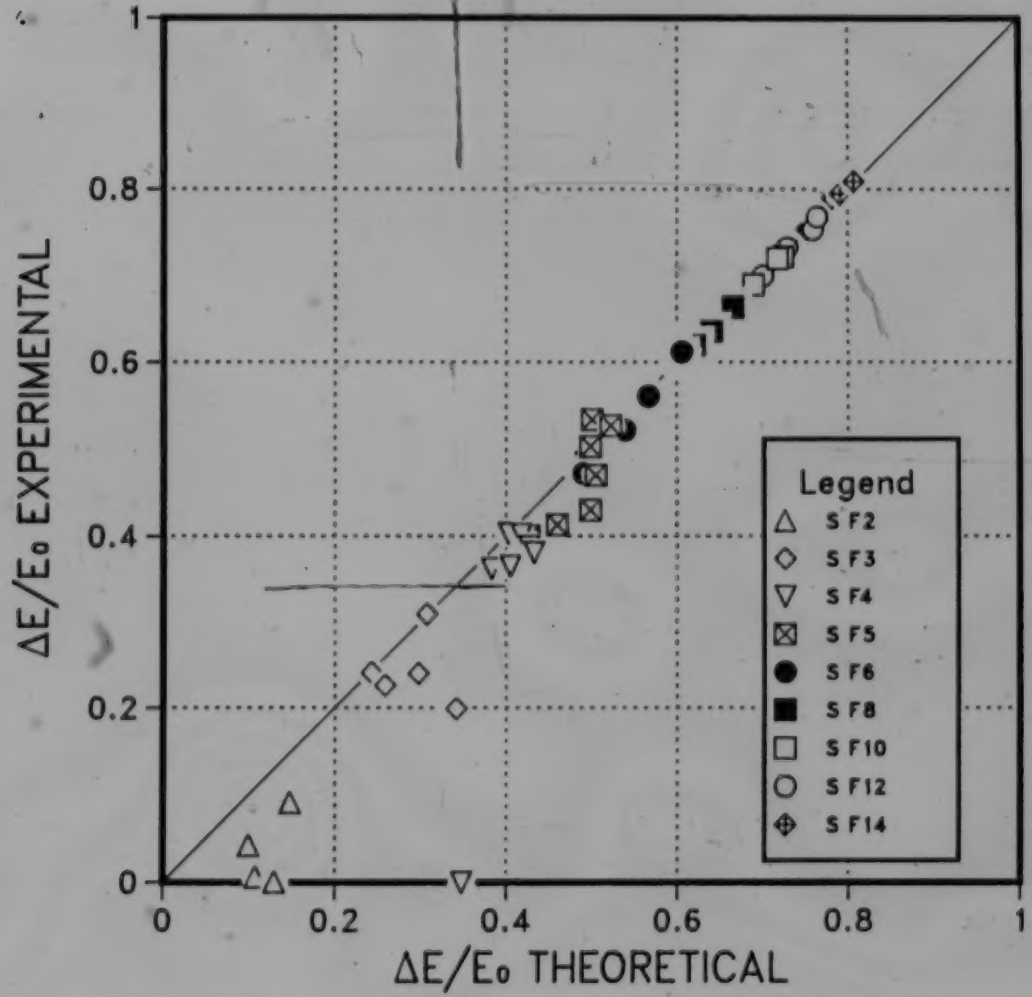

FIGURE 33
SUBMERGED INTERNAL JUMP
GROWTH OF ROLLER LENGTH WITH SUBMERGENCE

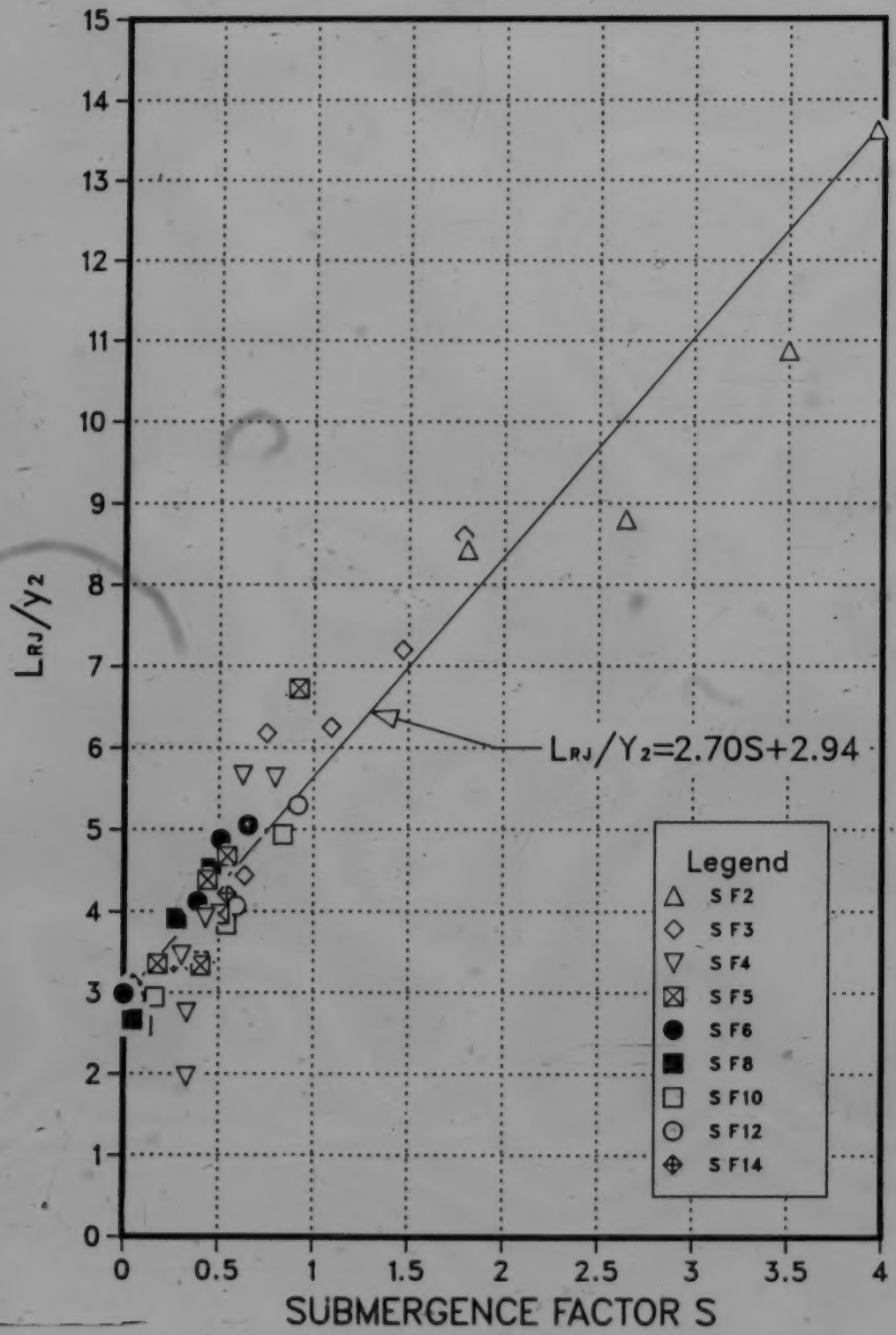

FIGURE 34
SUBMERGED INTERNAL JUMP
GROWTH OF JUMP LENGTH WITH SUBMERGENCE

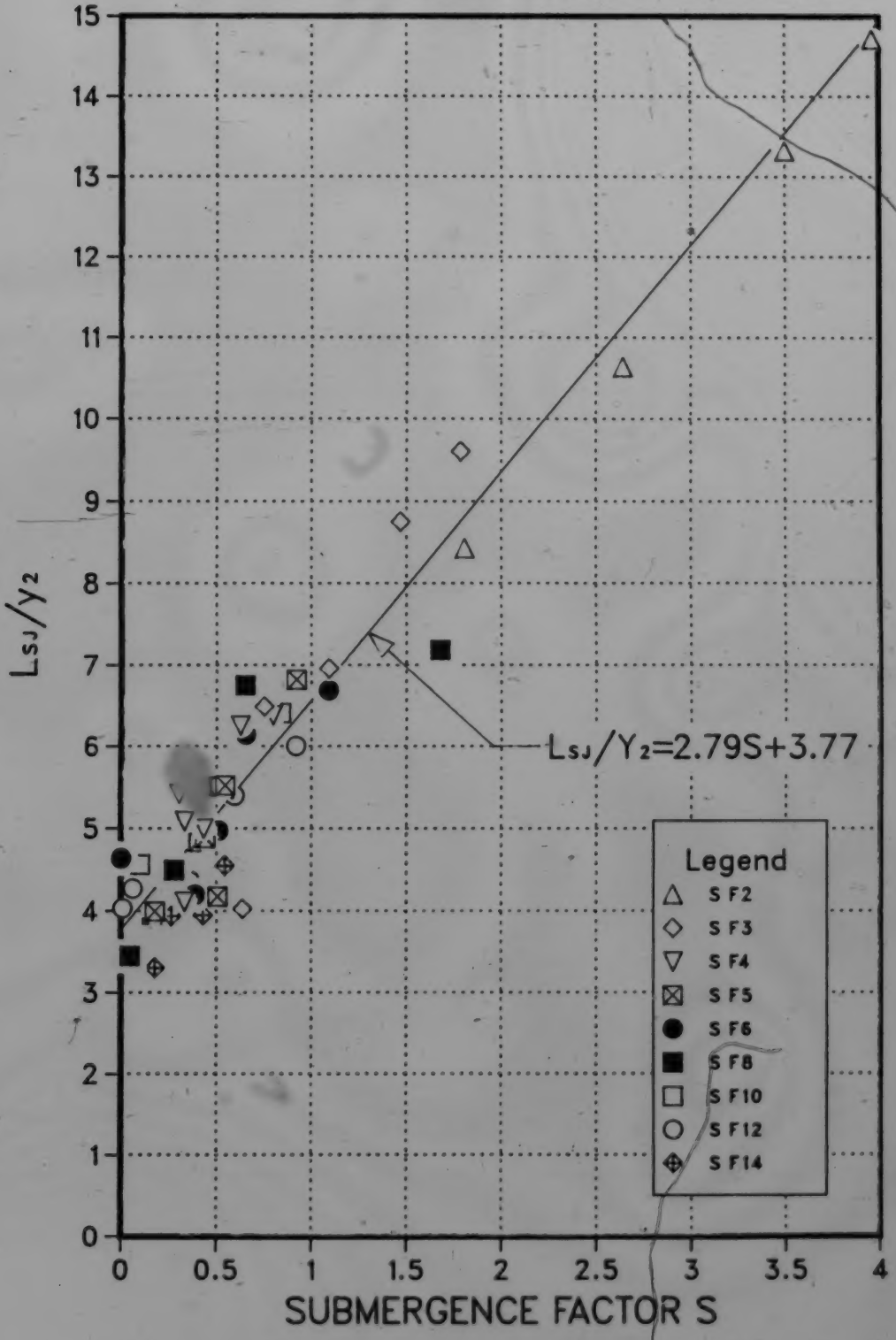

A study of submerged open channel jumps by Govinda Rao and Rajaratnam (1963) gives the folowing relationship between jump length and submergence:

$$L_{SJ}/y_2 = 4.9S + 6.1 \qquad (63)$$

Comparison of equations (62) and (63) indicates that a submerged internal jump tends to be shorter than a dynamically similar submerged open channel jump. It also appears that the rate of increase of jump length with submergence is higher for the open channel situation. The reason for this anomaly is not immediately apparent but it may be conjectured that shear along the density interface may be a contributing factor. Nevertheless, it is generally accepted that interfacial shear is not a significant quantity, especially over a short reach, and it most certainly does not entirely account for the large discrepancy between equations (62) and (63).

During the course of the experiments, a number of qualitative observations were made. As previously mentioned, the submerged internal jumps tended to be much more stable than the free internal jumps. While the submerged jumps displayed similar short term unsteadiness in the form of pulsations or bursts, the magnitude of the unsteadiness as observed in the roller and subcritical flow region downstream was much smaller than that observed in the free jumps.

An observation similar to the one made by Wilkinson and Wood (1971) may also be worthy of note. At low levels of submergence, it would be expected that if the depth of the flow downstream of the jump was lowered to some level below that required for the jump to form just at the gate, the jump would move downstream. While this action was observed to take place, the response to this lowering of the "tailwater" was delayed somewhat since the denser fluid overlying the jet had to be entrained or swept away before the new steady state could be achieved.

It is generally accepted that entrainment of the ambient fluid by a submerged internal jump is negligible and this notion was supported by observations made in the current series of experiments. Injection of dye near the interface provided a means of visually verifying this assumption. It was found that the dye in the ambient fluid merely diffused over time and very little passed across the density interface. Also, the flow in the jump was generally tranquil except at the higher densimetric Froude numbers and/or the lower levels of submergence. As a result, entrainment by breaking waves along the density interface of the roller was almost non-existent. Similar observations by other authors such as Wilkinson and Wood (1971), Stefan and Hayakawa (1972), Macagno and Macagno (1975), Chu and Vanvari (1976), Chu and Baddour (1977), and Baddour and Abbink (1983) support the assumption of the non-entraining roller. Also, the fact that the results of the present series of

experiments conform well to a theory which assumes no entrainment lends support to the assumption of no entrainment.

4.3 THE SLOPING INTERNAL JUMP

A number of experiments were conducted on sloping internal jumps using three different bed slopes and a variety of densimetric Froude numbers for each slope. The data obtained are listed in Table A3 of Appendix A, and Figures 35 through 37 are the dimensionless profiles of the sloping internal jumps.

To assess the validity of equation (56), the measured ratio of the denser layer downstream of the jump to the vertical depth at the nozzle was plotted against the same ratio calculated using equation (56) and measured values of F_{o_*} and α (Figure 38). Figure 39 provides a similar check by plotting measured values of (d_2/y_o) against G_{o_*} to see if they follow the predictions of equation (56). As with the study of the free internal jumps, it appears from Figures 38 and 39 that the theory tends to consistently underestimate the downstream depth required to form a jump just at the outlet nozzle. The suspected reason for this departure is that the flow entrained some ambient fluid prior to the formation of the jump via the same mechanisms described in the discussion of the Free Internal Jump.

The length of a sloping jump is not explicitly defined but is generally accepted to be the horizontal distance from

FIGURE 35
SLOPING INTERNAL JUMPS
DIMENSIONLESS PROFILES
BED SLOPE=1:18.5

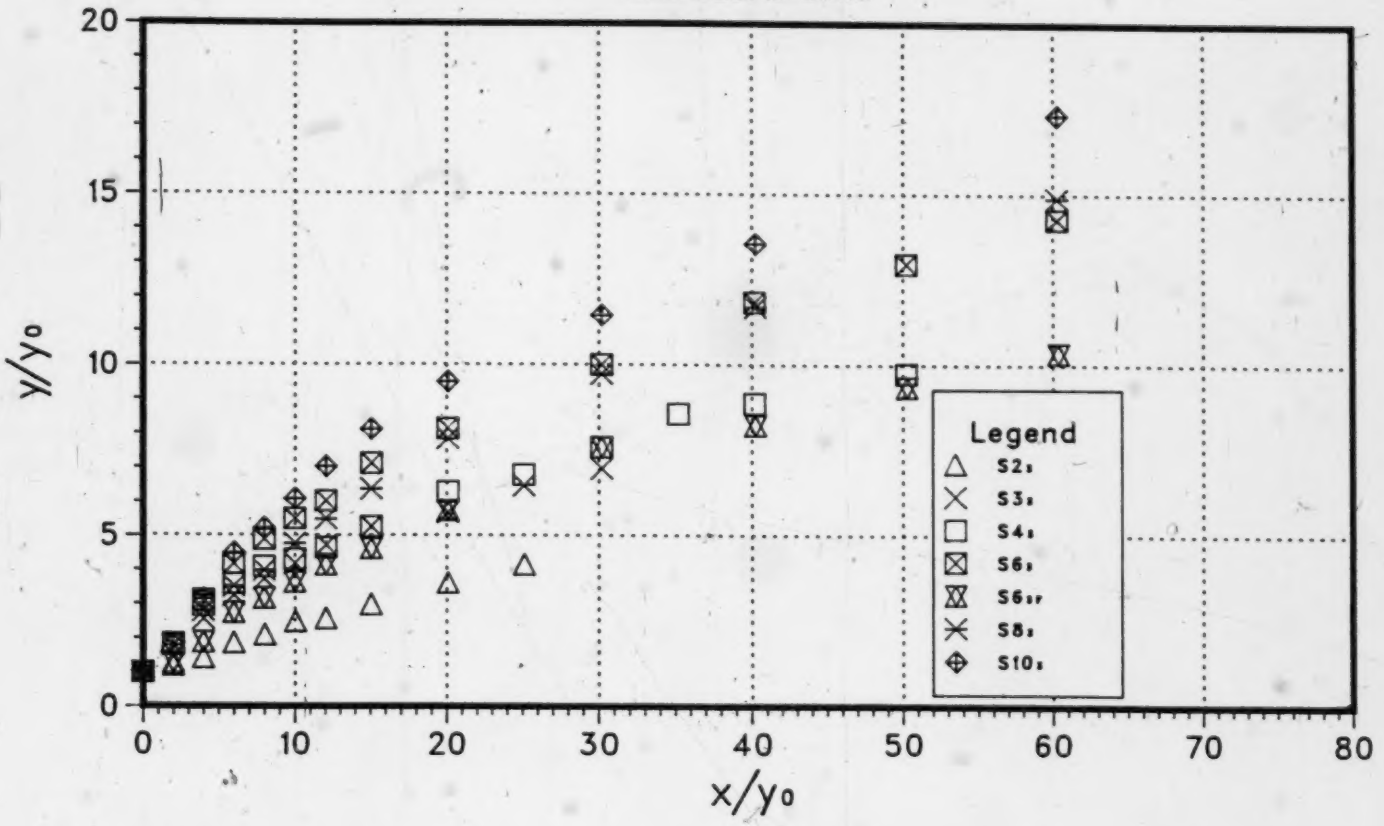

FIGURE 36
SLOPING INTERNAL JUMPS
DIMENSIONLESS PROFILES
BED SLOPE=1:10

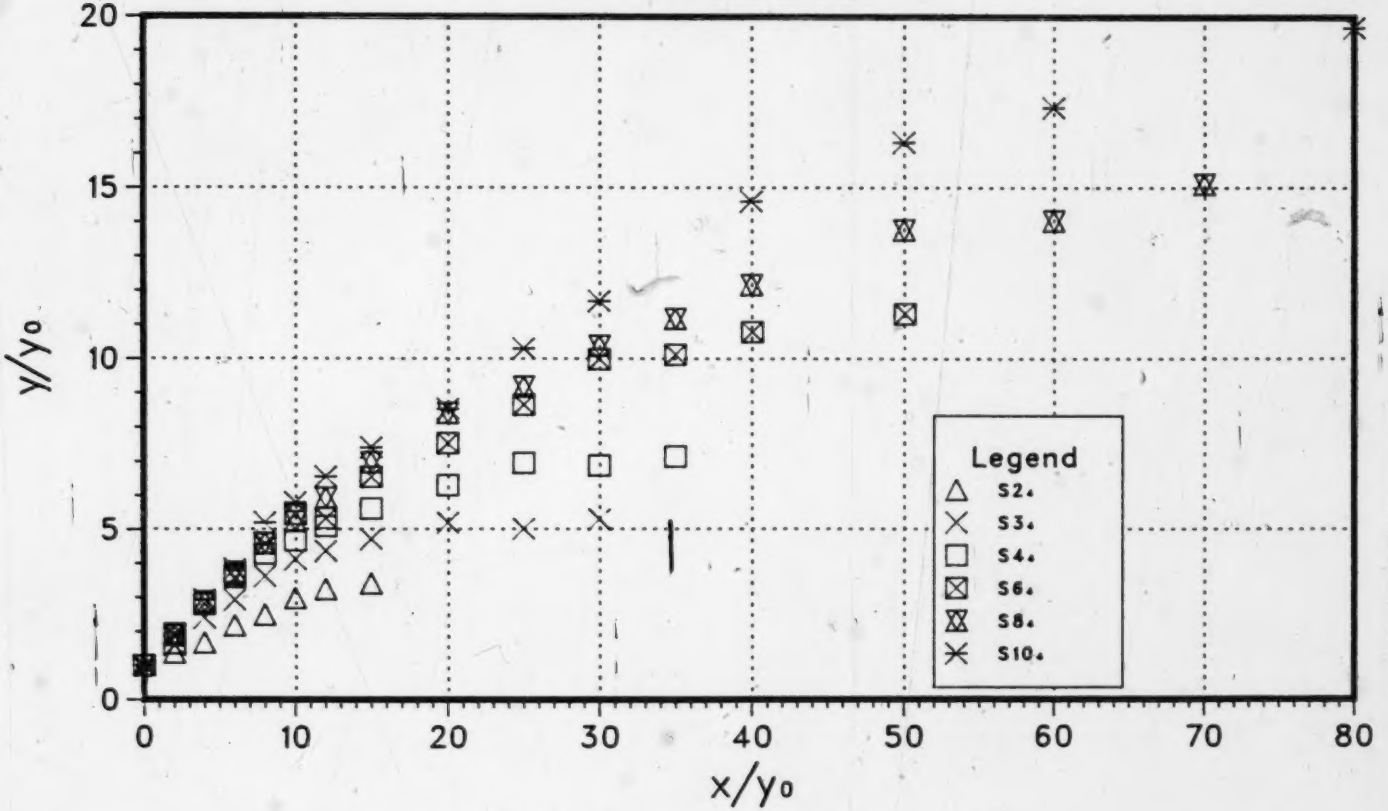

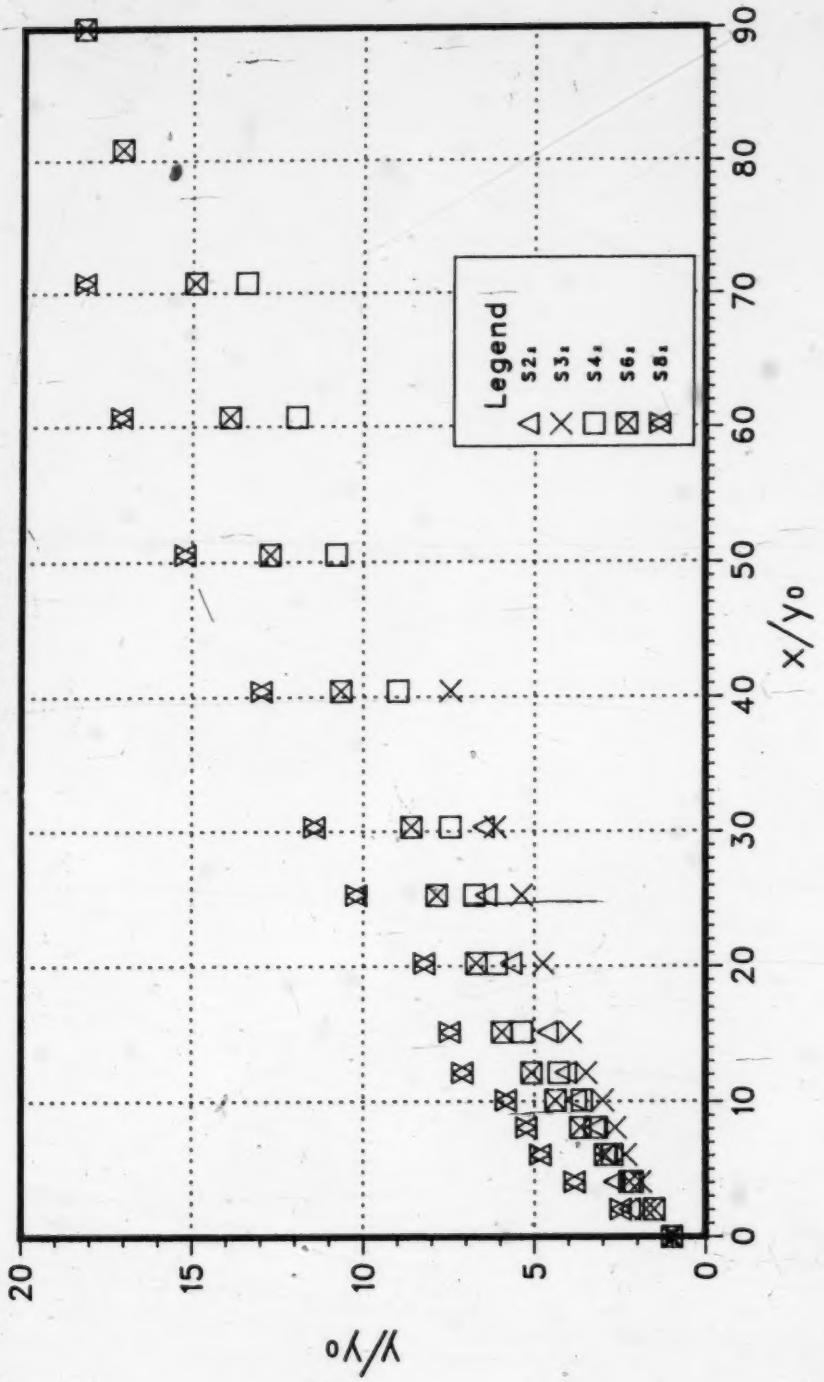

FIGURE 37
SLOPING INTERNAL JUMPS
DIMENSIONLESS PROFILES
BED SLOPE=1:6.67

FIGURE 38
SLOPING INTERNAL JUMP
THEORETICAL VS. EXPERIMENTAL SEQUENT DEPTH RATIO

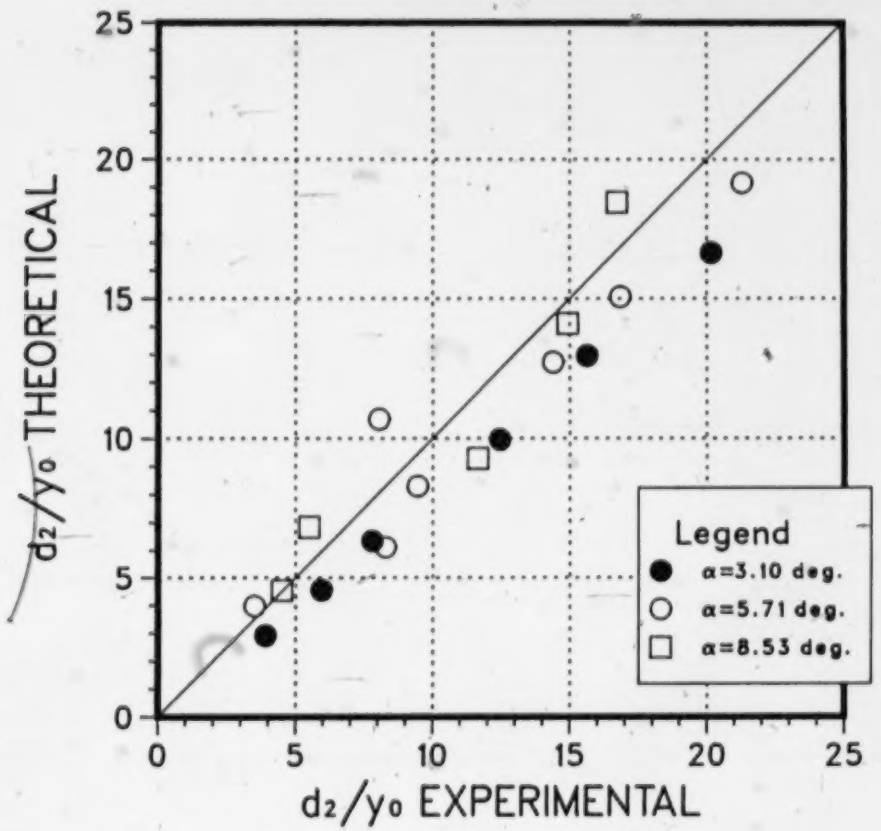

FIGURE 39
SLOPING INTERNAL JUMP
SEQUENT DEPTH RATIO VS. $G_{o\bullet}$

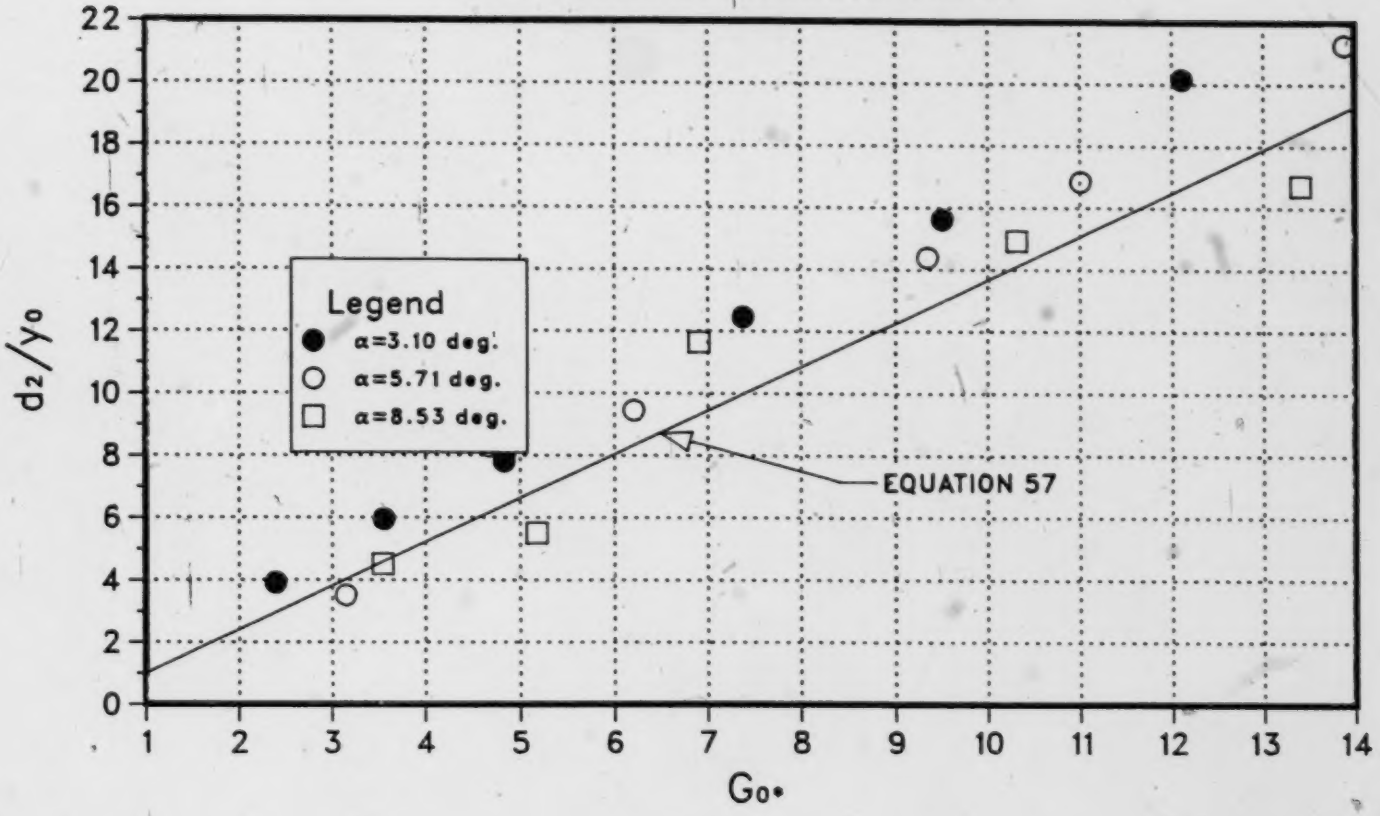

the toe of the jump to the end of the surface roller. Indeed, this dimension is the only dimension that can be fixed with any degree of accuracy or consistency. Consistent definition of a terminal point is especially important in any study of sloping jumps (especially D-type jumps) since the depth at the terminus is that used in the momentum analysis. Depending on the slope, the depth of flow will be significantly greater than the depth at the terminus even a relatively short distance downstream from the end of the jump. Since this study employed the empirical data derived from studies on sloping open channel jumps, it was felt that similar definitions of jump length and conjugate depth used for the open channel studies be used for the internal jump studies.

Rajaratnam (1966) included an empirically derived chart relating the length of a D-type sloping open channel jump to the Froude number of the supercritical flow upstream of the jump. The jump length was normalized by dividing by the corresponding depth at the end of the jump. Using this chart and the measured values of outlet densimetric Froude number and end depth, a "theoretical" jump length was calculated for each run. These values were plotted against measured values (Figure 40) and the agreement was found to be fairly good.

Figure 41 is a plot of the dimensionless energy loss based on calculated values of depth and velocity versus that based on measured values. The agreement is reasonably good

FIGURE 40
SLOPING INTERNAL JUMP
THEORETICAL VS. EXPERIMENTAL JUMP LENGTH

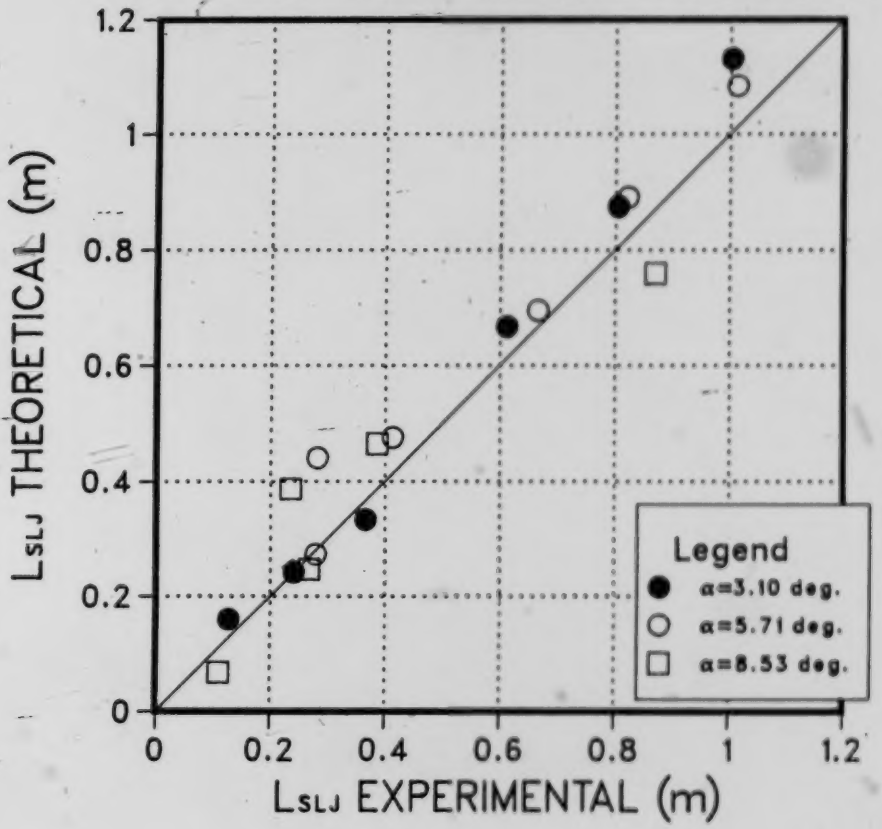

FIGURE 41
SLOPING INTERNAL JUMP
THEORETICAL VS. EXPERIMENTAL ENERGY LOSS

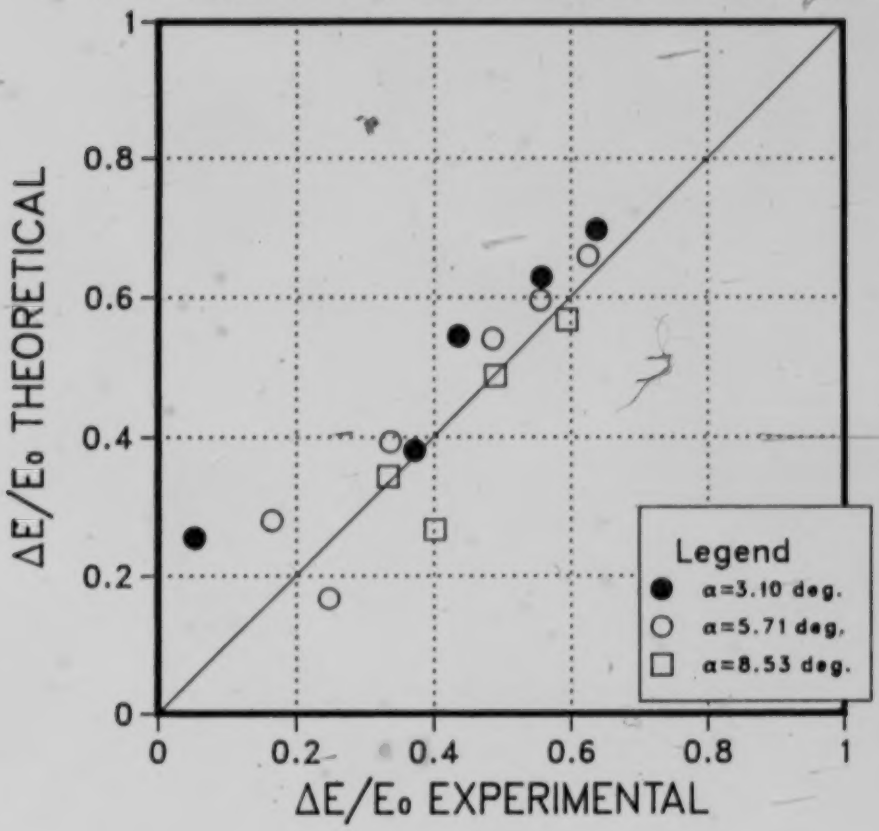

considering the highly empirical nature of the calculations and the fact that the empirical coefficients are those which are based on studies of a slightly different phenomenon.

It was thought that the profiles of the sloping internal jumps could be normalized in a manner similar to that employed in the analysis of the free internal jumps on a level floor. Instead of defining the jump length as the horizontal distance from the toe of the jump to the end of the roller, L'_{SLJ} was defined as the same distance measured along the bed. The distance from the bed to the density interface, as measured perpendicular to the bed, was used in defining the jump profile. Figure 42 is a definition sketch of the foregoing explanation.

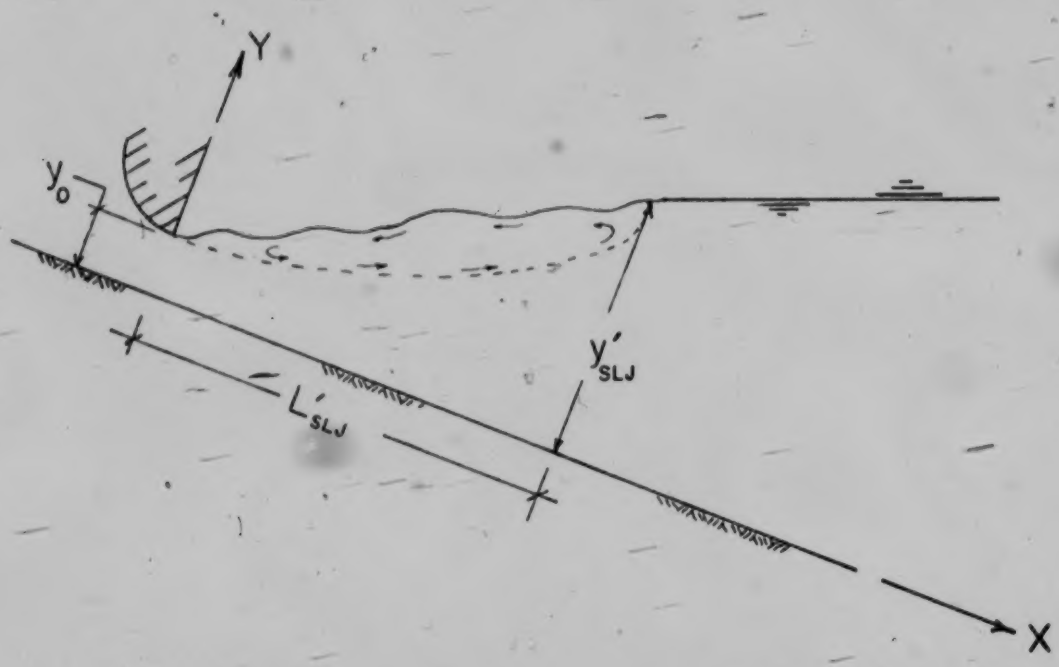

FIGURE 42 - COORDINATES AND LENGTH SCALES FOR NORMALIZATION OF SLOPING JUMP PROFILES

The normalized profiles appear in Figures 43 to 45, and Figure 46 is a plot of the non-dimensional profiles of the sloping jumps with a similar plot of the profile of the free internal jump on a level floor. It appears from Figure 46 that the effect of the sloping bed is to retard the initial growth rate of the jump.

As with the other series' of experiments, some qualitative observations were made on the sloping internal jump experiments. It was observed that the supercritical stream seemed to diffuse or expand much more slowly in a sloping jump than in a jump on a level floor and that the high velocity jet seemed to persist at higher slopes. This is likely due to the effect of gravity which would tend to continue to "drive" the flow down the slope despite the fact that the flow is being sheared or retarded by the slower moving overlying layers. These observations seem consistent with findings from studies of sloping open channel jumps by Rajaratnam and Murahari (1974).

FIGURE 43
SLOPING INTERNAL JUMP
NORMALIZED JUMP PROFILES α=3.10 deg.

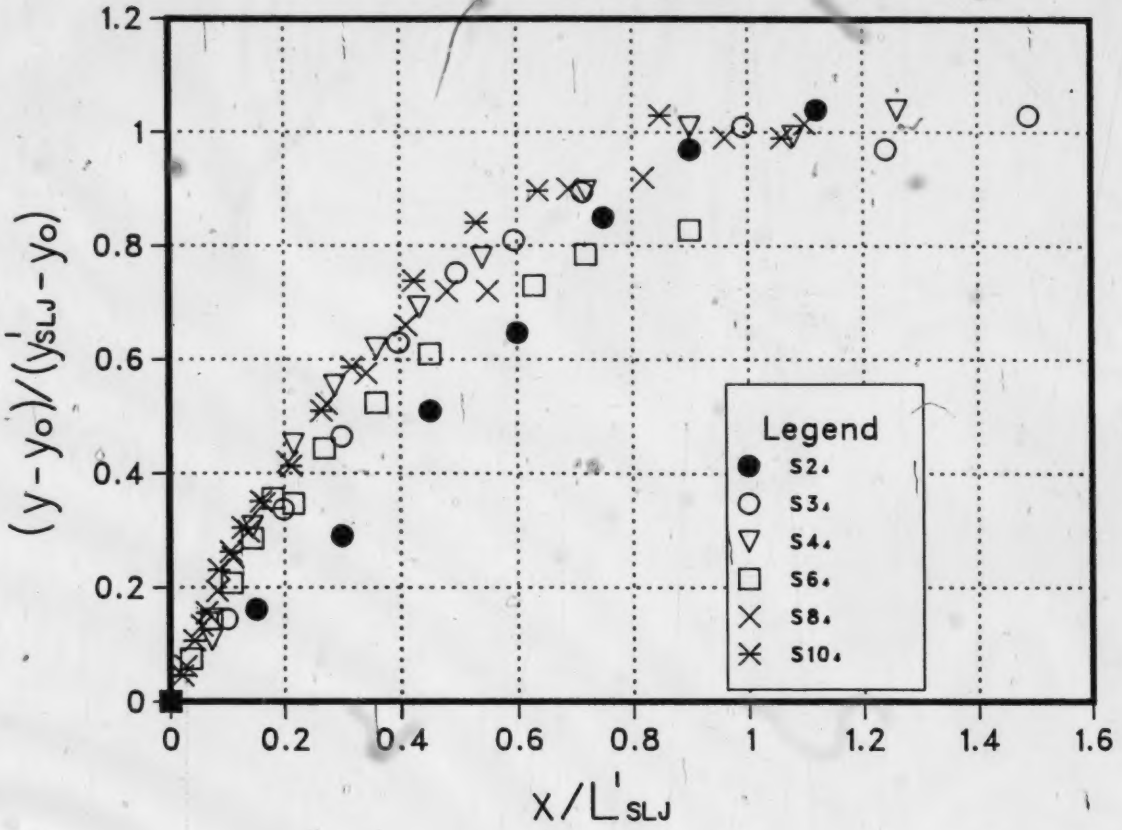

FIGURE 44
SLOPING INTERNAL JUMP
NORMALIZED JUMP PROFILES α=5.71 deg.

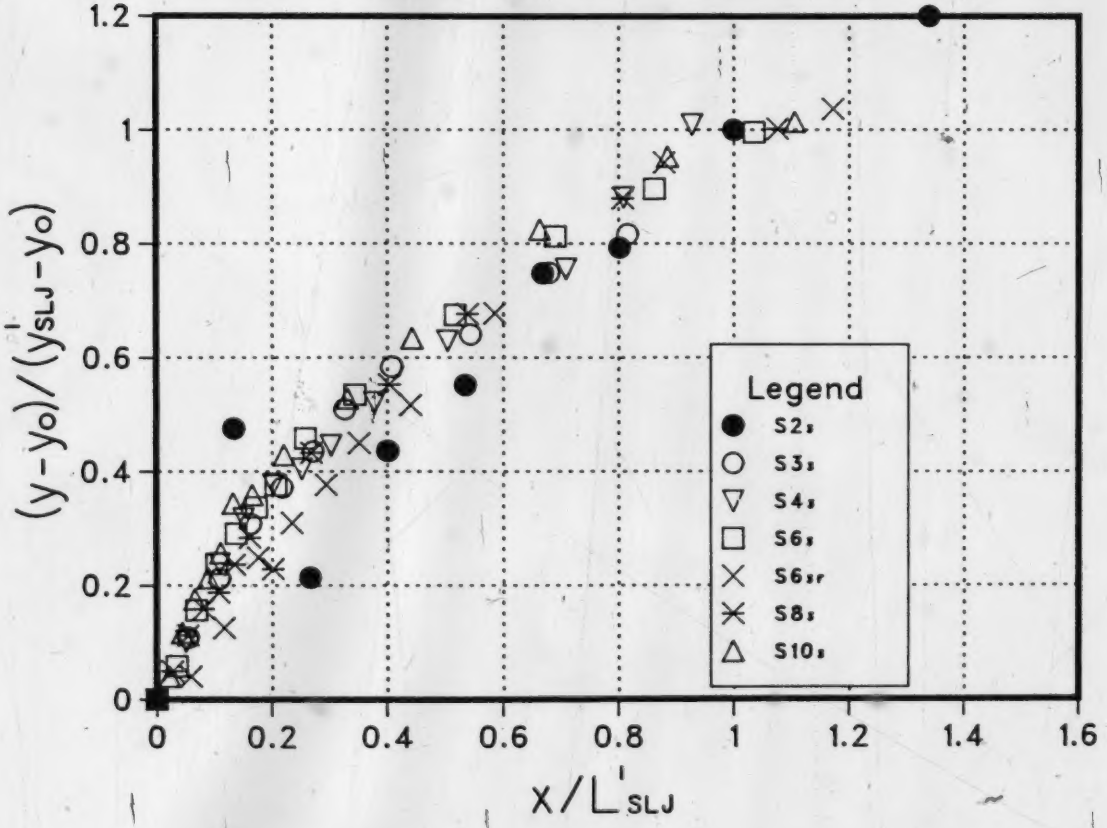

FIGURE 45
SLOPING INTERNAL JUMP
NORMALIZED JUMP PROFILES α=8.53 deg.

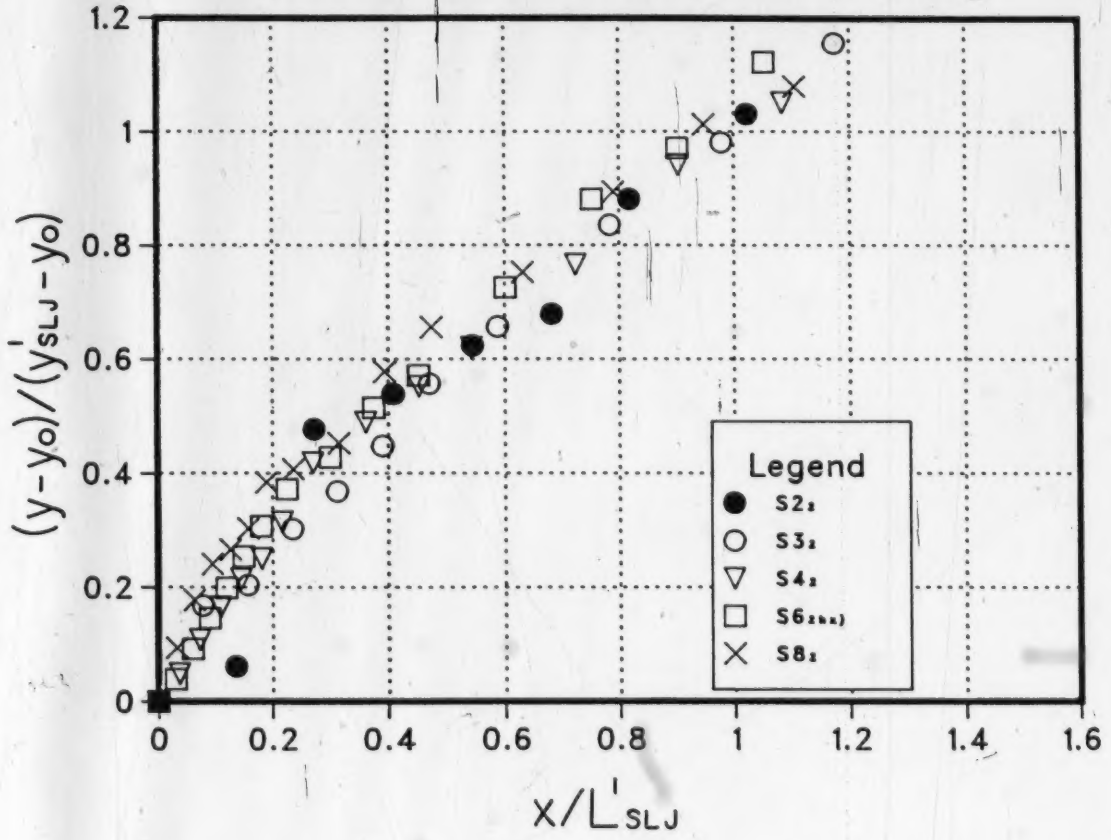

FIGURE 46
INTERNAL HYDRAULIC JUMP
NORMALIZED JUMP PROFILES

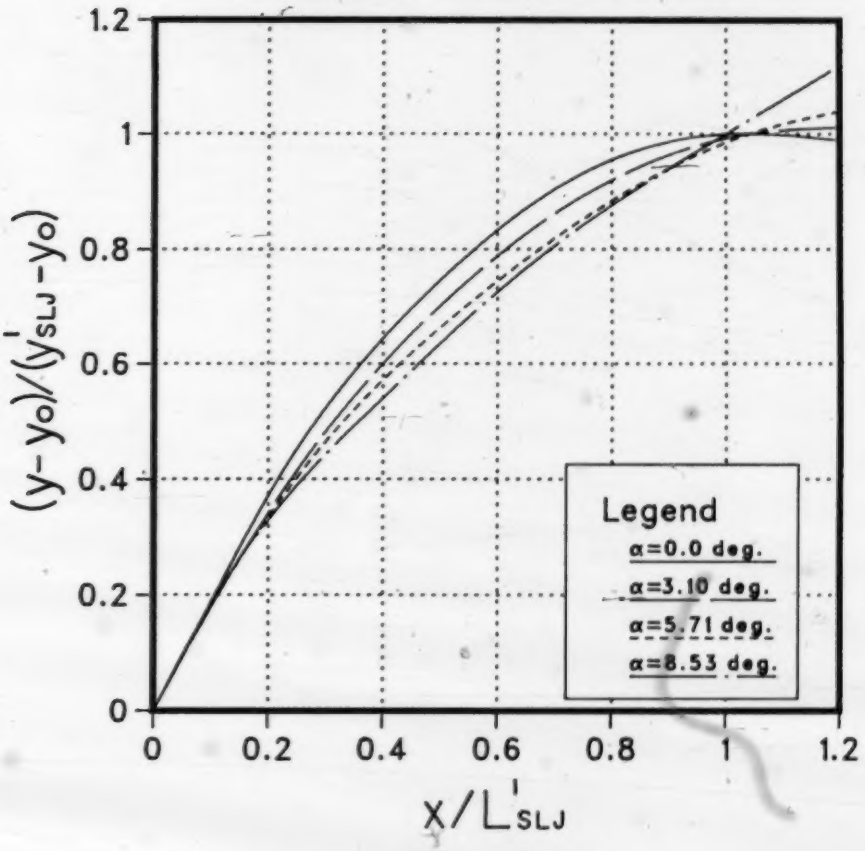

5. PART FIVE: CONCLUSIONS

5.1 THE FREE INTERNAL JUMP

For a non-entraining supercritical flow of a dense fluid in a deep quiescent ambient field of lighter fluid, the downstream depth required to form a stable jump is uniquely determined by a Belanger-type relation. For an internal jump in a miscible two-fluid field, the surface roller entrains little or no ambient fluid, but some entrainment occurs just prior to jump formation. The amount of this entrainment increases with densimetric Froude number and results in a greater sequent depth than that predicted by the Belanger-type relation. The profile and length of the free internal jump are similar to the length and profile of the open channel jump.

5.2 THE SUBMERGED INTERNAL JUMP

The global parameters of a submerged internal jump in a quiescent semi-infinite ambient can be predicted by a relation similar to that used for submerged open channel jumps. The fact that the aforementioned relation, based on the assumption of no entrainment, accurately predicts these parameters is indirect proof that the roller region of internal jumps entrains little or no ambient fluid. Empirical relations have been developed to predict the length of the roller and the ultimate length of the jump.

5.3 THE SLOPING INTERNAL JUMP

A relation similar to that used for sloping open channel jumps, including empirical parameters derived from open channel experiments, has been successfully used to predict the sequent depth of a sloping internal jump. As with the free internal jump on a horizontal bed, sloping internal jumps in a miscible two-fluid system entrain some ambient fluid just prior to jump formation; the amount of entrainment increases with densimetric Froude number. Normalized profiles of sloping internal jumps have been developed, and by comparing them to the normalized profile of the horizontal jump, it appears that the effect of a sloping bed is to retard the initial rate of jump development. The length of a sloping internal jump is similar to that of a dynamically similar sloping open channel jump.

5.4 LIMITATIONS OF THE PRESENT ANALYSIS

This study has shown that internal hydraulic jumps can be analysed with open channel flow theory as long as the supercritical stream does not entrain any ambient fluid prior to jump formation. It has also shown that entrainment is not a consideration in the analysis of submerged internal jumps. However, entrainment does occur in turbulent stratified flows involving miscible fluids. There are presently theories which address entraining internal jumps on horizontal beds (Wilkinson and Wood (1971), Stefan and

Hayakawa (1972), Macagno and Macagno (1975), Baddour and Abbink (1983), and Wood and Simpson (1984)). However, entraining jumps of different geometry have yet to be investigated.

The present study and the work of others have only analysed internal hydraulic jumps in a global manner. While some preliminary work has been carried out to investigate the internal flow structure in stratified jumps, much has yet to be done in this regard.

Turbulent entrainment in stratified flow has been investigated fairly thoroughly within the bounds of the present theory. However, it is suspected that entrainment in stratified flows results not only from the classical turbulent entrainment mechanism, but from modes such as breaking interfacial waves and other mechanisms which have yet to be described.

It is also recommended that research be conducted on the far field conditions which would produce the subcritical flow situations downstream of internal jumps.

6. REFERENCES

Baddour, R.E. and Abbink, H., "Turbulent Underflow in a Short Channel of Limited Depth", Journal of Hydraulic Engineering, American Society of Civil Engineers, Vol. 109, No. 5, 1983, pp. 723-740.

Christodolou, G.C., "Interfacial Mixing in Stratified Flows", Journal of Hydraulic Reasearch, Vol.24, 1986, No. 2, pp. 77-92.

Chu, V.H. and Baddour, R.E., "Surges, Waves and Mixing in a Two-Layer Density Stratified Flow", Proceedings of the XVIIth Congress, International Association for Hydraulic Reasearch, Baden-Baden, 1977, pp. 303-310.

Chu, V.H. and Vanvari, M.R., "Experimental Study of Turbulent Stratified Shearing Flow", Journal of the Hydraulics Division, Proceedings of the American Society of Civil Engineers, Vol. 102, No. HY6, 1976, pp. 691-706.

Ellison, T.H. and Turner, J.S., "Turbulent Entrainment in Stratified Flows", Journal of Fluid Mechanics, Vol.6, 1959, pp. 432-438.

Govinda Rao, N.S. and Rajaratnam, N., "The Submerged Hydraulic Jump", Journal of the Hydraulics Division,

Proceedings of the American Society of Civil Engineers, Vol. 89, No. HY1, 1963, pp. 139-162.

Harleman, D.R.F., "Stratified Flow", in Handbook of Fluid Dynamics, V.L. Streeter, ed., Section 26, McGraw-Hill Book Co., Inc., New York, N.Y., 1960.

Hayakawa, N., "Internal Hydraulic Jump in Co-current Stratified Flow", Journal of the Engineering Mechanics Division, Proceedings of the American Society of Civil Engineers, Vol. 96, No. EM5, 1970, pp. 797-800.

Jirka, G.H. and Harleman, D.R.F., "Stability and Mixing of a Plane Buoyant Jet in Confined Depth", Journal of Fluid Mechanics, Vol. 94, 1979, pp. 275-304.

Kindsvater, C.E., "The Hydraulic Jump in Sloping Channels", Transactions of the American Society of Civil Engineers, Vol. 109, Paper No. 2228, 1944, pp. 1107-1154.

Macagno, E.O. and Macagno, M.C., "Mixing in Interfacial Hydraulic Jumps", Proceedings of the XVIth Congress, International Association for Hydraulic Reasearch, Sao Paulo, 1975, pp. 373-380.

Mehrotra, S.C., "Limitations on the Existence of Shock

Solutions in a Two-Fluid System", Tellus, Vol. 25, 1973, pp. 169-173.

Mehrotra, S.C. and Kelly, R.E., "On the Non-uniqueness of Internal Jumps and Drops in a Two-Fluid System", Tellus, Vol. 25, 1973, pp. 560-567.

Peterka, A.J., "Hydraulic Design of Stilling Basins and Energy Dissipators", Water Resources Monograph No.25, United States Department of the Interior, Bureau of Reclamation, 1963.

Rajaratnam, N., "Submerged Hydraulic Jump", Journal of the Hydraulics Division, Proceedings of the American Society of Civil Engineers, Vol. 91, No. HY4, 1965, pp.71-76.

Rajaratnam, N., "Hydraulic Jumps in Sloping Channels", Journal of the Central Board of Irrigation and Power, New Delhi, India, 23, 1966, pp.137-149.

Rajaratnam, N., "Hydraulic Jumps" in Advances in Hydroscience, Vol. 4, V.T. Chow, ed., Academic Press, N.Y., 1967, pp. 197-280.

Rajaratnam, N. and Murahari, V., "Flow Characteristics of Sloping Open Channel Jumps", Journal of the Hydraulics

Division, Proceedings of the American Society of Civil Engineers, Vol. 100, No. HY6, 1974, pp.731-740.

Rajaratnam, N. and Subramanyam, S., "Plane Turbulent Denser Wall Jets and Jumps", under review for publication.

Schijf, J.B. and Schoenfeld, J.C., "Theoretical Considerations on the Motion of Salt and Fresh Water", Proceedings of the Minnesota International Hydraulics Convention, International Association for Hydraulic Research and American Society of Civil Engineers, 1953, pp. 321-333.

Stefan, H. and Hayakawa, N., "Mixing Induced by an Internal Hydraulic Jump", Water Resources Bulletin, American Water Works Association, Vol. 8, 1972, pp. 71-86.

Wilkinson, D.L. and Wood, I.R., "A Rapidly Varied Flow Phenomenon in a Two-layer Flow", Journal of Fluid Mechanics, Vol. 47, 1971, pp. 241-256.

Wood, I.R. and Simpson, J.E., "Jumps in Layered Miscible Fluids", Journal of Fluid Mechanics, Vol. 140, 1984, pp. 329-342.

Yih, C.H. and Guha, C.R., "Hydraulic Jumps in a Fluid System of Two Layers", Tellus, Vol. 7, 1955, pp. 358-366.

7. APPENDIX A

TABLE A1

Free Internal Jump Data

RUN	Y_o (m)	T_a (°C)	T_o (°C)	$T_{D/S}$ (°C)	Q_o (1/sec)	Y_2 (m)	L_{RJ} (m)
$S2_5$	0.012	25.94	4.47	6.63	0.263	0.0511	0.126
$S3_5$	"	25.71	4.10	6.20	0.295	0.0610	0.171
$S4_5$	"	25.79	4.02	6.59	0.390	0.0725	0.206
$S6_5$	"	13.13	4.76	6.56	0.269	0.1314	0.485
$S8_5$	"	13.16	4.50	6.36	0.339	0.1648	0.629
$S10_5$	"	13.42	3.80	6.80	0.422	0.1900	0.721
SR_2	0.0195	22.41	8.58	9.56	0.308	0.0657	0.168
SR_3	"	22.39	8.24	9.62	0.461	0.0938	0.291
SR_4	"	17.92	9.08	10.76	0.435	0.1248	0.385
SR_5	"	17.22	8.80	10.22	0.540	0.1647	0.543
SR_6	"	17.25	8.82	10.35	0.613	0.1927	0.775
$SR4_2$	0.007	34.20	11.00	13.80	0.199	0.0413	0.143
$SR5_2$	"	34.10	10.57	16.27	0.254	0.0499	0.152
$SR6_2$	"	33.86	10.39	16.01	0.305	0.0614	0.190
$SR8_2$	"	33.81	10.41	15.70	0.413	0.0877	0.286
$SR10_2$	"	31.35	10.37	14.85	0.473	0.1060	0.367
$SR12_2$	"	31.53	10.50	14.70	0.550	0.1273	0.500

TABLE A2
Submerged Internal Jump Data

RUN	T_a (°C)	T_o (°C)	Y_o (m)	O_o (1/sec)	Y_T (m)	Y_3 (m)	L_{SJ} (m)	L_{RSJ} (m)
$SF2_1$	41.2	5.5	0.0135	0.308	0.0750	0.0633	0.225	0.225
$SF2_2$	"	"	"	"	0.0973	0.0771	0.284	0.235
$SF2_3$	43.7	"	"	"	0.1124	0.0955	0.333	0.272
$SF2_4$	44.2	5.3	"	"	0.1219	0.1102	0.362	0.335
$SF3_1$	43.9	7.2	0.0135	0.532	0.0790	0.0615	0.194	0.214
$SF3_2$	44.5	6.0	"	"	0.0977	0.0712	0.325	0.292
$SF3_3$	44.3	6.5	"	"	0.0828	0.0577	0.307	0.292
$SF3_4$	"	"	"	"	0.1167	0.0985	0.414	0.340
$SF3_4$*	"	"	"	"	0.1318	0.1211	0.458	0.407
$SF4_1$	44.5	14.4	0.007	0.252	0.0480	0.0240	0.148	0.099
$SF4_1$*	44.0	10.4	"	0.245	0.0440	"	0.168	0.065
$SF4_2$	44.5	13.1	"	0.252	0.0460	"	0.191	0.122
$SF4_3$	44.2	12.3	"	"	0.0502	0.0330	0.175	0.137
$SF4_4$	"	"	"	"	0.0570	0.0430	0.219	0.198
$SF4_5$	43.8	10.3	"	"	0.0616	0.0472	"	0.193
$SF4_6$	43.5	9.0	"	"	0.0740	0.0610	0.276	0.261
$SF5_1$	43.3	10.4	0.007	0.334	0.0710	0.0350	0.197	0.187
$SF5_1$*	43.6	10.5	"	0.333	0.0550	0.0300	0.186	0.156
$SF5_2$	43.3	10.4	"	0.334	0.0680	0.0390	0.230	0.206
$SF5_2$*	44.1	10.3	"	0.333	0.0646	0.0460	0.222	0.153
$SF5_3$	42.7	10.4	"	0.334	0.0740	0.0570	0.264	0.223
$SF5_4$	"	"	"	"	0.0920	0.0640	0.326	0.321
$SF5_5$	"	"	"	"	0.1090	0.0905	0.394	0.379
$SF6_1$	44.1	16.9	0.007	0.404	0.0620	0.0097	0.293	0.189
$SF6_2$	43.9	11.0	"	"	0.0795	0.0520	0.240	0.235
$SF6_3$	43.1	11.5	"	"	0.0890	0.0640	0.293	0.287
$SF6_4$	43.5	11.0	"	"	0.0957	0.0680	0.355	0.292
$SF6_5$	43.3	10.2	"	"	0.1200	0.0960	0.384	0.359
$SF8_1$	44.5	10.3	0.007	0.517	0.1940	0.1776	0.566	-
$SF8_2$	43.8	10.5	"	"	0.1221	0.1000	0.499	0.378
$SF8_3$	44.8	10.6	"	"	0.1055	0.0755	0.398	0.326
$SF8_4$	45.3	11.1	"	"	0.0919	0.0530	0.323	0.281
$SF8_5$	45.0	12.5	"	"	0.0775	0.0220	0.255	0.197
$SF10_1$	44.9	9.1	0.007	0.654	0.1650	0.1400	0.575	0.443
$SF10_2$	45.0	10.9	"	"	0.1420	0.1090	0.505	0.353
$SF10_3$	"	11.6	"	"	0.1300	0.0895	0.464	0.315
$SF10_4$	"	12.0	"	"	0.1090	0.0570	0.370	0.276
$SF10_5$	"	"	"	"	0.1030	0.0394	0.427	0.242
$SF12_1$	26.25	7.14	0.007	0.473	0.1117	0.0225	0.447	0.341
$SF12_2$	26.60	6.70	"	"	0.1147	0.0279	0.461	0.315
$SF12_3$	26.45	6.90	"	"	0.1488	0.1065	0.476	0.369
$SF12_4$	26.50	6.80	"	"	0.1735	0.1311	0.587	0.442
$SF12_5$	"	6.90	"	"	-	-	-	-
$SF12_6$	"	"	"	"	0.2091	0.1785	0.654	0.577
$SF14_1$	26.25	6.90	0.007	0.589	0.1448	0.0529	0.483	0.429
$SF14_2$	26.75	"	"	"	0.1590	0.0973	0.446	0.448
$SF14_3$	26.76	6.94	"	"	0.1709	0.1324	0.532	0.500
$SF14_4$	"	"	"	"	0.1932	0.1457	0.534	0.445
$SF14_5$	26.78	6.90	"	"	0.2083	0.1664	0.614	0.569

TABLE A3

Sloping Internal Jump Data

RUN	SLOPE	Y_o (m)	T_a (^oC)	T_o (^oC)	$T_{D/S}$ (^oC)	O_o (1/sec)	Y_2 (m)	Y_T (m)	L_{SLJ} (m)
$S2_4$	1:18.5	0.1202	25.77	5.25	10.23	0.187	0.0471	0.1166	0.160
$S3_4$	"	"	25.64	4.40	8.73	0.282	0.0716	0.1299	0.242
$S4_4$	"	"	25.67	4.22	7.68	0.384	0.0939	0.1482	0.333
$S6_4$	"	"	15.81	4.59	7.77	0.333	0.1498	0.1865	0.667
$S8_4$	"	"	16.21	4.49	6.89	0.444	0.1879	0.2198	0.875
$S10_4$	"	"	16.22	4.42	7.09	0.569	0.2424	0.2538	1.131
$S2_3$	1:10	0.0182	27.35	8.11	12.53	0.207	0.0643	0.1575	0.273
$S3_3$	"	0.0120	27.27	7.59	11.37	0.311	0.1000	0.1754	0.441
$S4_3$	"	"	27.25	7.13	11.30	0.418	0.1140	0.1868	0.476
$S6_3$	"	"	27.51	7.72	11.61	0.626	0.1736	0.2256	0.695
$S6_3$*	"	0.0193	16.94	5.34	8.47	0.321	0.1569	0.2136	0.658
$S8_3$	"	0.0120	17.40	5.24	7.75	0.464	0.2032	0.2278	0.891
$S10_3$	"	"	17.57	5.28	7.81	0.584	0.2568	0.2568	1.084
$S2_2$	1:6.67	0.0075	40.11	7.58	15.00	0.133	0.0342	0.1314	0.068
$S3_2$	"	0.0105	40.38	7.00	13.92	0.196	0.0585	0.1446	0.247
$S4_2$	"	0.0070	40.40	6.65	17.00	0.263	0.0825	0.1509	0.387
$S6_2$	"	"	40.74	6.53	16.70	0.397	0.1058	0.1609	0.465
$S8_2$	"	0.0120	17.72	5.10	7.81	0.488	0.2030	0.2196	0.759